STOOP P M

THE CALCULATION OF ADSORPTION PARAMETERS

USING EMBEDDED ATOM METHODS

DPhil UP 1990

THE CALCULATION OF ADSORPTION PARAMETERS USING EMBEDDED ATOM METHODS

by

Paulina Maria Stoop

The calculation of adsorption parameters using embedded atom methods

by

Paulina Maria Stoop

Submitted in partial fulfilment of the requirements

for the degree

Doctor of Philosophy

in the Faculty of

Mathematical and Physical Sciences

University of Pretoria

PRETORIA

May, 1990

ACKNOWLEDGEMENTS

I wish to thank my promoter Prof. J.H. van der Merwe and my co-promoter Dr M.W.H. Braun for unfailing support and expert guidance. Generous financial assistance in the form of post-graduate bursaries from the Foundation for Research Development of the CSIR, and the University of Pretoria is gratefully acknowledged. Sincere appreciation is expressed towards Mrs N. Boullion for the careful typing of the manuscript under very difficult circumstances.

ABSTRACT

The calculation of adsorption parameters using embedded atom methods

by

Paulina Maria Stoop

PROMOTER: Prof. J.H. van der Merwe

CO-PROMOTER: Dr. M.W.H. Braun

DEPARTMENT: Physics

DEGREE: Ph.D.

A comparative investigation to assess the suitability of various embedded atom methods for the calculation of adsorption properties of systems consisting of homo- and heteronuclear bcc metals have been undertaken. Homonuclear systems consisting of a tungsten adatom and an infinite tungsten monolayer adsorbed on a tungsten {110} substrate, were considered. For heteronuclear systems, the case of a tantalum adatom adsorbed on a tungsten {110} surface was analysed. The embedded atom methods introduced by Gollisch, by Johnson and Oh, and by Finnis and Sinclair were applied to the homonuclear system. The latter two models were also applied to the heteronuclear system. For both systems the potential of Finnis and Sinclair have been extended for application to {110} tungsten surfaces, by

introducing an additional parameter fitted to the empirical value of the adatom-surface migration energy.

Appropriate definitions for the desorption energy and the adatom-surface migration energy in terms of N-body potentials, were formulated. In addition, the vibration frequencies and coefficients for a truncated Fourier representation of the adatom-surface interaction potential were also calculated numerically. The potential models were assessed on their ability to reproduce the experimental values of the adatom-surface migration energy and the desorption energy, as well as the presence of a double well in the potential surface at an adsorption site on tungsten {110} substrates.

The surface modified model of Finnis and Sinclair appeared to be the most suitable potential for application to the homonuclear system, whereas, for the heteronuclear system, no specific model could be identified as being the most appropriate. For the homonuclear system, all N-body potentials yielded more realistic values of the adatom-surface migration energy, the desorption energy and the adatom-substrate equilibrium height than the conventional Morse and Lennard-Jones pair potentials. The magnitude of optimized Fourier coefficients for truncated Fourier series representations of the adatom-substrate interaction potential were shown to decay rapidly with harmonic order. This justifies the implementation of Fourier series truncated at low harmonic order for the theoretical description of isolated adsorbates on crystal surfaces. The relative values of the normalized Fourier coefficients appeared to be largely determined by the symmetry of the substrate. The success of embedded atom methods in describing surface phenomena was attributed mainly to their ability to incorporate environmental effects on bonding; while requiring only slightly more computational effort than pair potentials.

SAMEVATTING

The calculation of adsorption parameters using embedded atom methods

deur

Paulina Maria Stoop

PROMOTOR: Prof. J.H. van der Merwe

MEDE-PROMOTOR: Dr. M.W.H. Braun

DEPARTEMENT: Fisika

GRAAD: Ph.D.

'n Vergelykende studie om die toepaslikheid van verskeie atoom-inbeddingsmetodes vir die berekening van die adsorpsie eienskappe van enkelsoortige en meersoortige stelsels van metale met 'n liggaamsgesentreerde kristalstruktuur te evalueer, is onderneem. Enkelsoortige stelsels bestaande uit 'n wolfram adatoom en 'n oneindige wolfram monolaag geadsorbeer op 'n wolfram {110} substraat, is beskou. Die meervoudige stelsel wat geannaliseer is, bestaan uit 'n tantalum adatoom geadsorbeer op 'n wolfram {110} oppervlak. Die atoom-inbeddingsmetodes van Gollisch, Johnson en Oh, en van Finnis en Sinclair is op die enkelsoortige stelsel toegepas. Laasgenoemde twee modelle is ook op die meersoortige stelsel toegepas. Vir albei stelsels is 'n aanpassing van die potentiaal van Finnis en Sinclair vir die toepassing by wolfram {110} oppervlakke voorgestel. Dit behels die invoe-

ring van 'n bykomende parameter, wat aan die eksperimentele waarde van die adatoom-oppervlak migrasie-energie gepas is.

Geskikte definisies van die desorpsie energie en die adatoom-oppervlak migrasie-energie in terme van N-liggaampotensiale, is geformuleer. Daarbenewens is die vibrasiefrekwensies en die koëffisiënte van afgeknotte Fourierreeks-voorstellings van die adatoom-oppervlak wisselwerkingspotensiaal ook numeries bereken. Die potensiaalmodelle is beoordeel aan die hand van hulle vermoë om die eksperimentele waardes te reproduseer van die adatoom-oppervlak migrasie-energie en die desorpsie energie, sowel as die aanwesigheid van 'n dubbele trog in die potensiaal oppervlak by 'n adsorpsiepunt op wolfram {110} substrate.

Die oppervlak aangepaste model van Finnis en Sinclair was klaarblyklik die mees geskikte potentiaal vir toepassing op die enkelsoortige stelsel, terwyl geen spesifieke model vir die meersoortige stelsel as die mees geskikte geïdentifiseer kon word nie. In die geval van die enkelsoortige stelsel het al die N-liggaampotensiale meer realistiese waardes van die adatoom-oppervlak migrasie-energie, die desorpsie energie en die adatoom-oppervlak ewewigshoogte gelewer as die konvensionele Morse en Lennard-Jones paar-potensiale. Die optimale waardes van die Fourierkoëffisiënte in die afgeknotte Fourierreeks-voorstellings van die adatoom-oppervlak wisselwerkingspotensiaal neem vinnig af met toenemende harmoniese orde. Die relatiewe waardes van die genormaliseerde Fourierkoëffisiënte word klaarblyklik grotendeels deur die simmetrie van die substraat bepaal. Die sukses van atoom-inbeddingsmetodes om oppervlakverskynsels te beskryf, is hoofsaaklik toe te skryf aan hulle vermoë om die effek van omgewingsfaktore op binding te inkorporeer.

CONTENTS

CHAPTER 1

INTRODUCTION

1.1 SCOPE OF THE STUDY

The problem of the adsorption of atoms and molecules on solid surfaces are amongst the most challenging and the least resolved problems in surface physics. The adsorption of an isolated atom upon a single-crystal substrate is basic to many kinds of processes ranging from catalysis to the epitaxial growth of thin films. However these phenomena are still poorly understood. Theoretical models of adsorption systems have been limited severely by a lack of suitable interatomic potentials capable of describing the complex processes taking place at surfaces. In the past various forms of pair potentials were the only form of interaction available for computer simulation of adsorption processes. With pair potentials it is however impossible to include the effect of the surrounding atoms on bonding. Recently a new generation of semi-empirical potentials, the so-called embedded atom methods (EAM's), have been developed. In these methods many-body effects are incorporated through the electron density determined by surrounding atoms. It is expected that these potentials will be capable of a more realistic description of defects like vacancies and surfaces where electron density variations are large.

The aim of this study is to give a quantitative description of certain adsorption phenomena by employing various embedded atom methods for bcc metals in computer simulations of homo- and heteronuclear systems. In the

case of homonuclear systems, the present work is limited to the study of a tungsten adatom or an infinite tungsten monolayer adsorbed on a tungsten {110} surface. For heteronuclear systems, consideration is given to the case where a tantalum adatom is adsorbed on a tungsten {110} surface. These two systems were chosen because sufficient experimental data are available for fitting and assessment of the success of the models. In this study small modifications to existing models will also be introduced to obtain more realistic adsorbate-substrate interaction potentials. The following quantities which relate to adsorption phenomena will be considered: the desorption energy, the activation energy for surface migration, vibration frequencies of adsorbed atoms and truncated Fourier representations of the effective adatom-substrate interaction. The desorption energy is defined as the energy required to completely remove an adatom from the adsorption site of the substrate surface, and the activation energy for surface migration is the amount of energy the adatom must acquire to surmount the lowest energy barrier, the one at the saddlepoint, to migrate to a neighbouring adsorption site. Apart from the calculations performed by Gollisch (1986b) for fcc metals such as platinum, silver and gold adsorbed on tungsten {110} surfaces, this study is also a first attempt to quantify the above-mentioned adsorption parameters for bcc metals by employing embedded atom methods.

An adatom near a crystal surface experiences an interaction potential which has the two-dimensional periodicity determined by the substrate lattice. This potential V may therefore be represented phenomenologically by a two-dimensional Fourier series (Steele 1973). Although the most important contributions to V originate from its dependence on the co-ordinates of the surface plane (x,y), the adatom also experiences small

vertical (surface normal z) undulations in order to minimize its energy. These undulations are too small to have a significant effect on the relevant surface phenomena but are clearly vital in analytical and numerical techniques to calculate V. While the role of z in calculating V and in the desorption process itself is recognized, this study will be mainly, but not exclusively, concerned with the lateral (x,y) dependence of V. It is usually assumed in applications that V is an acceptable approximation of the interaction of the atoms of an adsorbed monolayer with the substrate and that it is also a crude but adequate representation of the interaction of a multilayer with the substrate crystal. Calculations in this study indicate that the relative values of the Fourier coefficients seem to be primarily determined by the symmetry of the substrate, independent of whether the adatom is an isolated self-adsorbate or forms part of a monolayer. The bonding parameter that constitutes an overall scale factor may be significantly different. The importance of these quantities in monolayer epitaxy has been established by van der Merwe (1982) and by Braun (1987). The Fourier coefficients are equally important in describing registry-disregistry phase transitions in adsorbed layers (Coppersmith *et al.* 1982). The realization of a general objective to calculate coefficients for optimum Fourier truncations is initiated by calculating the desorption energy, the coefficients for the relevant truncated Fourier series and the force constants for atomic surface vibrations using various many-body potential models.

Numerical calculations of the coefficients in a truncated Fourier series have previously been carried out by Stoop and Snyman (1988) for an argon adatom on the surface of an argon crystal using Lennard-Jones pair potentials. Alternative analytical approaches for expressing Fourier

coefficients in terms of pair potentials have been used by Steele (1973) and by Bruch and Venables (1984).

1.2 ATOMIC INTERACTION

The fundamental starting point for all quantitative calculations of solid state properties is the Schrödinger equation. If a full quantum mechanical treatment could be carried out from first principles for a solid, all its properties could be calculated accurately. Such calculations of atomic and electronic properties in crystalline solids are however limited by the size and symmetry of the system considered. More powerful computers and numerical techniques have recently permitted more ambitious first principle calculations to be carried out. At present most calculations are still limited to about sixty independent atoms in the computational cell. To overcome this limitation a variety of empirical and semi-empirical procedures have been developed for the description of interatomic forces in solids. These less fundamental approaches which can deal with more complicated arrangements of atoms, are usually easier to interpret and accordingly generate more physical insight.

At one end of the spectrum of methods for deriving interatomic forces (and their associated interatomic potentials) are those methods attempting a proper quantum mechanical description of the electrons. Among these approaches the most fundamental ones are based on density functional theory. Included in this category are the standard band-structure methods such as the linear muffin-tin orbitals method, the linear augmented-plane-wave method, and the use of plane-wave basis sets with norm-conserving pseudopotentials. Less fundamental approaches include the tight-binding method, pseudopotential perturbation methods, the Gordon-Kim model and the

embedded atom method. At the other end of the spectrum are the empirical and semi-empirical methods which do not even infer a proper quantum mechanical basis. All pair potential methods and methods involving three- or higher-body interatomic potentials, fall into this category.

For many years pair potential models, e.g. Lennard-Jones (6-12) and Morse models have been used with some success in *ab initio* calculations of materials properties (Meada *et al.* 1982), including surface phenomena (Broughton and Gilmer 1983 and Stoop 1977a). The parameters in these empirical and semi-empirical potentials are determined by fitting them in such a way that the model adequately predicts various known properties of the material, e.g. elastic constants, lattice parameter, bulk modulus, vacancy formation energy, stacking fault energy, cohesive energy, phonon dispersion data and activation energy for self-diffusion. By incorporating more parameters in the fitting process, the more physical phenomena can satisfactorily be described by the potential.

Pair potentials, however, have two fundamental shortcomings: they do not properly account for (i) the Cauchy pressure and (ii) the vacancy formation energy. For example, unless the elastic constants in a cubic crystal satisfy the Cauchy relation $C_{12} = C_{44}$ (C_{ij} being cubic stiffness constants), which is seldom the case in real metals, an equilibrium pair-potential calculation cannot reproduce them. This problem is usually overcome by adding to the pair-potential energy, a large volume-dependent term representing the energy of the electron gas and the structure independent portion of the electron-ion interactions (Johnson 1972). The elastic constants can then be adjusted arbitrarily at equilibrium. The volume-dependent term supplies a fictitious external pressure to balance the so-called Cauchy pressure $\frac{1}{2}\ (C_{12}-C_{44})$. The introduction of such

volume-dependent terms results in the paradox that the bulk modulus, calculated by the method of long waves, differ from its value calculated in homogeneous deformation, unless the volume-dependent term is linear in the volume. It is also not clear how these volume-dependent contributions should be treated near extended defects and surfaces.

In pair potential models for the transition and noble metals, with the elastic constants satisfying the Cauchy relation $C_{12} = C_{44}$, and fitting the potential parameters to the cohesive energy, the vacancy formation energy is found to be much too large and of the same order as the cohesive energy. Experimentally the cohesive energy is of the order three or four times the vacancy formation energy (Johnson 1973).

In the atomistic modelling of transition metals with pair potentials, the free surface furthermore displays an outward relaxation, contrary to experiment. Serious problems are also encountered in adsorption processes at metal surfaces if the binding energy of an atom is described by means of an additive pair potential (Gollish 1986a). In fact, with pair potentials the investigation of many-body effects on the binding is impossible (Stoop 1983). This follows from the fact that the bond between two atoms contributes the same amount of energy to the total binding energy independent of the number and kind of neighbouring atoms. A further shortcoming is related to the fitting of the potential parameters. If the potential parameters are fitted to the experimental binding properties of a diatomic molecule, the binding energy of an atom at the surface or within the corresponding crystal is seriously overestimated. On the other hand, if these parameters are fitted to experimental bulk data, the binding energy of the molecule turns out to be much too small.

These shortcomings of pair potentials clearly indicate that a completely new approach is needed. The new generation of semi-empirical methods, the so-called "embedded atom methods", introducing terms which are essentially related to a measure of local volume dependence through electron charge density or core-overlap considerations, appear to offer a solution.

The embedded atom method (EAM), a new procedure for the construction of N-body potentials for simple metals, has recently been developed by Daw and Baskes (1984). By combining the density functional formalism with traditional pair potentials, the EAM eliminates the above-mentioned shortcomings of pair potentials. Finnis and Sinclair (1984) independently developed a model mathematically equivalent to the EAM based on a second moment approximation to the tight-binding method. Other models having equivalent mathematical forms are the "glue" model of Ercolessi *et al* (1986b) for gold, the model of Tománek and Benneman (1985) and the effective binding potentials of Gollisch (1986a).

It has been suggested that the EAM can better describe defects such as vacancies and surfaces where the density variations are large. This is done by incorporating many-body effects through the electron density determined by surrounding atoms.

1.3 THE BASIC EQUATIONS OF THE EMBEDDED ATOM METHOD

The basic equations of the EAM are

$$E_t = \sum_{\text{bonds}} \phi(r_b) + \sum_{\text{atoms}} F(\rho_a); \qquad (1.1)$$

$$\rho_i = \sum_{j \neq i} f(r_{ij}), \qquad (1.2)$$

where E_t is the total internal energy of a system of N atoms. Here ρ_i can be interpreted as the electron density at atom i due to all other atoms, or, as a measure of the local density of atomic states in which case f(r) could be seen as the sum of squares of overlap integrals. $F(\rho)$ is the "embedding energy", which is attractive, while $\phi(r_b)$ is a repulsive two-body potential between atoms separated by a bond length r_b.

There seems to be basically three different approaches to the derivation of the basic equations of the EAM:

(i) density functional theory via quasi-atom (Stott and Zaremba 1980) or effective medium theory (Nørskov 1982);
(ii) density functional theory via the tight-binding approximation (Finnis and Sinclair 1984, Gupta 1981, Gollisch 1986a and 1986b, and Tománek *et al.* 1983); and
(iii) a purely phenomenological approach (Ercolessi *et al.* 1986b).

In Chapter 1 the notation followed is that used by the authors in the original description of the various models. In Chapters 3 and 4 the general notation of the basic equations of the EAM, as given in eqns. (1.1) and (1.2), are used.

1.3.1 The quasi-atom approach

The embedded atom method for fcc metals as proposed by Daw and Baskes (1984) is based on density functional theory. According to this theory the total electronic energy for an arbitrary arrangement of nuclei can be expressed as a unique functional of the total electron density (Hohenberg and Kohn 1964). In the quasi-atom theory, derived from density functional theory, the energy E to embed an impurity in a host is determined by the electron density of the host before the impurity was added:

$$E = \mathcal{F}_{Z,R_i}[\rho_h(R_i)].$$

Here $\rho_h(R_i)$ is the electron density at the site of atom i (independent of the source of the electron density), and Z and R_i are the type and position of the impurity. The approximation is made that the atom experiences a locally uniform electron density ρ_i (the uniform density approximation of Stott and Zaremba (1980)), mainly emanating from neighbouring atoms. The universal function $\mathcal{F}$ is approximated by a function F of the electron density at the position of the impurity. The embedding energy is supplemented by a short-range two-body purely repulsive pair interaction ϕ_{ij} to account for core-core repulsion. As each atom in the solid can in turn be viewed as an impurity embedded in a host consisting of all the other atoms, Daw and Baskes (1984) defined the total energy of the system as follows:

$$E_{tot} = \sum_i F_i(\rho_i(R_{ij})) + \frac{1}{2} \sum_{\substack{i,j \\ (i \neq j)}} \phi_{ij}(R_{ij}). \qquad (1.3)$$

Here ρ_i, the electron density at atom i due to all the other atoms, can be closely approximated by a superposition of atomic charge densities:

$$\rho_i = \sum_{j(\neq i)} f_j(R_{ij}), \qquad (1.4)$$

where f_j is the electron density distribution of a free atom, derived from Hartree-Fock calculations. With the further approximation of a radial density distribution around each atom in a metal, f_j only depends on the distance R_{ij} between atoms i and j. The functions ϕ and $F(\rho)$, respectively representing the repulsive pair potential and the embedding energy, are determined empirically by fitting them as cubic splines to the lattice constant, elastic constants, vacancy formation energy and sublimation energy in fcc and bcc phases, bearing in mind (Foiles *et al.* 1986) that

(i) the embedding energy F must tend to the free atom energy at zero electron density;

(ii) F must have a negative slope and a positive curvature for the background electron densities found in metals; and

(iii) the pair potential must be purely repulsive.

The short range nature of the charge distributions is taken into account by introducing cutoff distances between the first and second nearest neighbours.

Information about $F(\rho)$ for densities well away from the equilibrium density can be obtained through the equation of state of expanded or compressed metals. Rose *et al.* (1984) have shown that the binding energy of most metals, as a function of lattice constant, can be scaled to a simple function

$$E(r_1) = -E_{sub}(1 + a^*) \exp(-a^*), \tag{1.5}$$

where r_1 is a length scale of the system and a^* is a measure of the deviation from equilibrium. a^* is a function of the bulk modulus B and the atomic volume Ω through the relations

$$a^* = \alpha(r_1/r_{1e} - 1) \tag{1.6}$$

with

$$\alpha = 3[B\Omega/E_{sub}]^{1/2}. \tag{1.7}$$

E_{sub} is the absolute value of the sublimation energy at zero temperature and pressure. By requiring that the total energy per atom E of the solid

agrees with the universal equation of state (eqn. 1.5), the embedding function can be calculated from

$$F(\rho_i(r_1)) = E(r_1) - \frac{1}{2} \sum_m \phi(R_m), \qquad (1.8)$$

where R_m is the distance to the m-th neighbour of atom i. However to obtain F as a function of ρ, the functional dependence between a suitable length scale r_1 and ρ must be known, so that it can be inverted to give r_1 as a function of ρ. Here ϕ represents the pair potential.

Johnson (1988a) proposed an analytic nearest neighbour model for fcc metals based on equations (1.3) and (1.4). The interpretation of the various terms in the basic equations is the same as that of Daw and Baskes (1984). It is assumed that the host electron density at atom i, ρ_i, is a linear superposition of the contributions from individual atoms, which in turn is assumed to be spherically symmetric. The embedding energy is assumed to be independent of the electron distribution or gradients. To implement any EAM scheme in lattice model calculations, the functions f and F must be specified for each atomic species and ϕ for each possible combination of species. It was found that the Hartree-Fock spherically averaged free-atom electron density calculated by Clementi and Roetti (1974) may be adequately approximated by a single exponential term in the range of distances of interest in EAM calculations. Thus the single atom electron density function in the analytic model was taken as

$$f(r) = f_e \exp[-\beta(r/r_{1e} - 1)], \quad r \leq r_c, \qquad (1.9)$$

where r_c is a cutoff parameter taken between first and second nearest neighbours and r_{1e} is the first nearest neighbour distance at equilibrium electron density f_e. For analytical convenience the two-body potential is taken as a Born-Mayer repulsion:

$$\phi(r) = \phi_e \exp[-\gamma(r/r_{1e} - 1)], \quad r \leq r_c. \tag{1.10}$$

The embedding function F is determined by means of the equation of state derived by Rose *et al.* (1984) and was found to be

$$F(\rho) = -E_c\left[1 - \frac{\alpha}{\beta} \ell n\left[\frac{\rho}{\rho_e}\right]\right]\left[\frac{\rho}{\rho_e}\right]^{\alpha/\beta} - 6\phi_e\left[\frac{\rho}{\rho_e}\right]^{\gamma/\beta}. \tag{1.11}$$

The fitting parameters, f_e cancels and r_e does not play a significant role, while β is determined from atomic wave function calculations. The average shear modulus G_e gives a relationship involving all three parameters β, γ and ϕ_e. The cohesive energy, compressibility and lattice parameter are other inputs, while the shear anisotropy ratio was constrained to a value of 2. Johnson showed that the embedding functions in the models of Daw and Baskes, Finnis and Sinclair and the analytic fcc model were not uniquely determined – they differed only by terms linear in the electron density. It was also found that G_e plays a dominant role in determining the unrelaxed vacancy formation energy, di-vacancy binding energy and the surface energy of low index planes. This is due to the fact that the slope of the embedding function at equilibrium electron density is linear in G_e.

Johnson (1988b) applied his analytic fcc model to investigate the relationships between defect energies and the various EAM physical input parameters. He found that

(i) the cohesive energy has a negligible effect on defect energies;

(ii) the bulk modulus has a minor effect;

(iii) the variation of the defect energies with G_e is approximately linear;

(iv) there is little variation in defect energies with β and γ if their average is held constant;

(v) the attractive or repulsive nature of the two-body potential has little effect on defect energies; and

(vi) vacancy formation energies are decreased and interstitial energies increased by increasing the average of β and γ.

Oh and Johnson (1988) also devised a procedure for developing atomistic models needed in computer simulation calculations for fcc and hcp metals. The procedure was based on the analytic fcc model. A hardening parameter m was introduced to ensure that the second derivative of $F(\rho)$ was greater than zero for all ρ. The model was developed for any choice of cutoff distance. The predicted elastic constants were in satisfactory agreement with experimental values although only two elastic moduli were used in the fitting procedure. Generally the models yielded satisfactory results.

The bcc model of Johnson and Oh will be discussed in Section 1.4.

1.3.2 The tight-binding approach

The tight-binding model for transition metals proposed by Friedel (1969) has been the starting point for the models of both Gupta (1981) and Tománek *et al.* (1983). Accepting the second moment approximation for the cohesive energy (the density of states is approximated by a rectangular

step function) determined by the electrons in atomic d-levels at near equilibrium separations, and assuming that the corresponding hopping and transfer integrals decay exponentially with the interatomic distances r_{ij}, Gupta (1981) derived the following result for the total energy E per atom of a system of N atoms:

$$E = -a\left[\sum_{j\neq i}^{N} e^{-2qr_{ij}}\right]^{1/2} + b\sum_{j\neq i}^{N} e^{-pr_{ij}} . \qquad (1.12)$$

The short range repulsive interaction in eqn. (1.12), required for lattice stability, is generated by the compression of the free electron gas. In transition metals the repulsive component of the potential is due to the s-electrons (competition between attractive intra-atomic and repulsive inter-atomic s-band contributions). This differs from the core-core repulsion to be discussed below. With this model Gupta predicted multilayer contraction for the (100), (110) and (111) surfaces of a fcc transition metal, a result in agreement with experiment. The effective binding potentials of Gollisch (1986a and 1986b) to be discussed in Section 1.5 is a further refinement of this model.

Using an expression similar to eqn. (1.12) the interaction energy per atom, also derived within the tight-binding formalism, Tománek *et al.* (1983) calculated various fundamental properties of small clusters of transition metal atoms, as well as surface energies, multilayer relaxation and reconstruction trends at both fcc and bcc metal surfaces. The results showed good agreement with experiment (Tománek and Bennemann 1985).

An important objective of the simple empirical N-body potential for bcc metals, proposed by Finnis and Sinclair (1984), hereafter referred to as the FS model, was to incorporate in a simple model the essential band

character of metallic cohesion. In their model the energy per atom E is given by:

$$E = -A \sum_i (\rho_i)^{1/2} + \frac{1}{2} \sum_{\substack{i,j=1 \\ (j \neq i)}}^{N} V_{ij}, \qquad (1.13)$$

where

$$\rho_i = \sum_j \phi(r_{ij}). \qquad (1.14)$$

The square-root function in the band energy $-A \Sigma (\rho_i)^{1/2}$ has been motivated by the tight-binding theory of cohesion, where the cohesive energy per atom varies as $\sqrt{z}$, z being the atomic coordination. Here A is a constant which can be interpreted as a positive bonding parameter and ρ was identified with the second moment of the density of states. For transition metals tight-binding theory shows that the second moment is proportional to

$$\sum_{j,m} ddm(r_{ij})^2, \qquad (1.15)$$

where the parameters ddm are hopping integrals between five orbitals labelled m (Ackland *et al.* 1987). Thus $\phi(r_{ij})$ can be interpreted as the sum of squares of overlap integrals. By assuming that the atoms keep the same charge in all environments, it can be shown that the square root functional form is appropriate for all band fillings and not only for half-filled bands (Ackland *et al.* 1988). In the FS model for bcc transition metals the second moment is modelled empirically and ρ_i is taken as the sum of simple quadratic functions ϕ_{ij} tending to zero between the second and third nearest neighbour distances.

The difference between the approach of Daw and Baskes (1984), and Finnis and Sinclair (1984) as regards the implementation of the basic equations of the EAM is the following: Daw and Baskes specified ρ_i as an atomic charge density obtained from Hartree-Fock calculations for the free atom and then obtained $F(\rho_i)$ by empirical fitting. Finnis and Sinclair on the other hand, assumed a square root form for F and chose to represent the second moment empirically, where ρ_i is taken as the sum of simple quadratic functions ϕ_j tending to zero between the second and third nearest neighbour distances. The parameters of ϕ_j are then determined by fitting them to experimental data.

V_{ij} is a pairwise repulsive contribution representing a core-core repulsion, and is expressed as a cubic polynomial also tending to zero outside the second shell of neighbours. The parameters in ϕ_{ij} and V_{ij} are fitted to experimental atomic volumes, cohesive energies and elastic constants.

This model has been used to calculate unrelaxed vacancy formation energies, as well as surface energies. The former yielded results in reasonable agreement with experimental values, and the latter, results in fair agreement with tight-binding calculations.

Ackland and Thetford (1987) proposed an improved version of the FS potentials, hereafter referred to as the FS-AT model, to avoid problems of stability which arise in situations where the lattice is compressed. Their modified potentials yielded more realistic pressure-volume relationships. The formation energies of various interstitial configurations were also calculated.

Recently Ackland *et al.* (1987) proposed a simple N-body potential for the noble metals and for nickel. The physical interpretation of ρ and V

differed from the interpretation given to the corresponding terms in the potential for transition metals. The noble metals have a full d-band which can only contribute minimally to the bonding term. Their cohesion arises from the half-filled band of sp-states and the lowering of the energy of the d-orbitals and occupied sp-orbitals due to sp-d hybridization. These are volume effects that have to be counteracted by a pairwise repulsion due to d-orbitals. This in turn is related to the upward shift in energy of the entire d-band due to the Pauli repulsion of overlapping d-states. This model was used to study point defects, surface energies and stresses, surface relaxations, surface reconstructions and grain boundaries, yielding results in good agreement with empirical data.

Eridon and Rao (1989) proposed a method for deriving the form of pair potentials needed to described both the long- and short-wave length behaviour of bcc metals within the framework of the FS potential model. The fitting parameters in the pairwise and non-central components of the FS potential are matched to the three elastic constants and six measured values of the phonon frequency. The cutoff is taken between fifth and sixth nearest neighbours. The method was applied to niobium yielding an accurate value for the Debye frequency and a much improved static defect Green function. The electron density function was approximated by a polynomial going monotonically to zero at a cutoff radius. A further improved model (Eridon and Rao 1988) with a more complex form of the electron density function, was used in calculations pertaining to defect behaviour in bcc niobium. In this parameterization the electron density function had zeros at both the cutoff r_c = 4.0Å and the position of a minimum r_{min} = 3.1Å. The more complex form is indicative of the mixing of d-bands. This modification was needed because the polynomial of the FS

model produced a description that predicted a body centred tetragonal structure that was more stable than the bcc structure.

1.3.3 The phenomenological approach

The "glue" model of Ercolessi *et al* (1986b) for gold represents the most phenomenological approach to the motivation of the EAM. The failure of pair potentials, when applied to bulk noble metals, is due basically to their inability to account for the strongly non-local electronic cohesion. In noble metals electronic cohesion is due partly to outer s-electrons, but largely to very broad filled d-bands. This part should be spherical symmetrical since the same d-bandwidth can be produced either by several distant neighbours or by fewer close-by ones. A potential for gold (and similar metals) should contain many-body forces, capable of incorporating atomic coordination. In the "glue" model the total energy of a system of N particles is written as

$$E_{tot} = \frac{1}{2} \sum_{\substack{i,j \\ (j\neq i)}}^{N} \phi(r_{ij}) + \sum_{i}^{N} U(n_i), \qquad (1.16)$$

where

$$n_i = \sum_{\substack{j \\ (j\neq i)}}^{N} \rho(r_{ij}). \qquad (1.17)$$

Suitable functions $\phi(r_{ij})$, $U(n_i)$ and $\rho(r_{ij})$ are constructed empirically. $\phi(r_{ij})$ is a standard short-range two-body potential, repulsive at small distances, and n_i is a "generalised coordination" of atom i. The latter is calculated as the sum of the contributions $\rho(r_{ij})$ from neighbouring atoms. The function $\rho(r_{ij})$ is a positive monotonically decaying short-range

function. The "glue function" $U(n_i)$ associates an energy with a particular coordination, on the basis that $n_0 = 12$, the number of nearest neighbours of an atom in a perfect fcc lattice. The functions ϕ, U and ρ are approximated by polinomial splines, and are fitted to the lattice parameter, the cohesive energy, the surface energy, the bulk modulus and the transverse phonon frequency and, indirectly, by a trial- and error approach, to the thermal expansion coefficient and the melting temperature. Both $\phi(r_{ij})$ and $\rho(r_{ij})$ extend only to first neighbours. The "glue" model yielded a good description of both bulk and surface properties of gold such as the reconstruction of the Au(100) (Ercolessi *et al.* 1986a) and the Au(110) surfaces (Garofalo *et al.* 1987), as well as the surface melting behaviour of Au(111) (Carnevali *et al.* 1987).

1.3.4 General features of EAM models

In all EAM models the total internal energy of an assembly of atoms is written as the sum of a cohesive component E_N and a conventional central pair potential E_p effecting lattice stability. E_p may or may not be purely repulsive. E_N, often referred to as the embedding energy, is the N-body term in the potential. It is dominant and effects cohesion. Through its dependence on the local electron density or the local density of atomic states, environmental effects are incorporated in the potential. The exact "universal" form of the embedding function F has not yet been determined. Johnson and Oh (1988) and Gollisch (1986b) have shown, however, that their expressions for F are equivalent to other models under certain conditions.

It follows from the quasi-atom theory (Stott and Zaremba 1980) that the embedding energy curves of the different elements should fall into two main categories. Chemically inert elements should have energy curves

linear in electron density, whereas the curves of the reactive elements will tend to show a minimum at low densities becoming positive with a linear increase at high enough densities. The latter feature reflects the increasing repulsion associated with the increase in kinetic energy due to orthogonalization or the exclusion from the occupied core states (Puska *et al* 1981). In the region where the embedding energy rises linearly with density, the interaction energy of an atom with its environment is a linear function of the density. If the total density is taken as a superposition of atomic charge densities, the linearity of the embedding function indicates that the total energy of interaction of an atom with the surrounding atoms is also obtained as the superposition of the interaction energies. This means that the interaction can be described by a well-defined pair potential. Consequently all EAM models are invariant with respect to the transformation

$$\begin{cases} F(\rho) \rightarrow \hat{F}(\rho) = F(\rho) \mp \lambda\rho(r) \\ \phi(r) \rightarrow \hat{\phi}(r) = \phi(r) \pm 2\lambda\rho(r) \end{cases} \tag{1.18}$$

where λ is an arbitrary constant (Johnson 1988a). The two-body potential then becomes the effective two-body potential (Johnson and Oh 1989) when this transformation is made such that the slope of the embedding function is zero when evaluated at the equilibrium electron density for the perfect crystal. This is referred to as the normalized form for EAM models. In such a model the deviation from the perfect crystal energy is then dominated by the effective two-body potential for any arrangement of atoms in which the electron density at atom sites are not significantly altered. This is the case with defect configurations in close-packed metal crystals.

It also explains why the embedding function in such a model, makes only a small contribution to the defect energies, while contributing a major part to the cohesive energy.

1.4 EXISTING BCC MODELS

In this section a brief summary is given of the main features of three of the existing bcc models, *viz.* the "effective binding potential" model of Gollisch (1986b), the simple empirical N-body potential model of Finnis and Sinclair (1984) and finally the analytic EAM model for bcc metals developed by Johnson and Oh (1989). These potentials are semi-empirical and their parameters are fitted, for example, to cohesive energies, lattice parameters and bulk elastic constants.

1.4.1 Model of Gollisch

In order to describe the adsorbate-substrate interaction, Gollisch (1986a and 1986b) used tight-binding theory to develop an "effective binding potential", whose repulsive part was a two-body (pair) potential of the Morse type and whose attractive part was an N-body potential depending on all atoms of the N-atom system – the crystal in this case. He expressed the interaction of atom i as an effective interaction energy

$$U_i = \sum_{i\neq j}^{N} b_{ij}[\Phi_{ij}(r_{ij})]^{\mu S_{ij}\lambda_{ij}} - \left\{ \sum_{i\neq j}^{N} a_{ij}[\Phi_{ij}(r_{ij})]^{\lambda_{ij}} \right\}^{\mu}, \quad (1.19)$$

where λ_{ij}, a_{ij} and b_{ij} are adjustable parameters depending on the type of atoms at i and j respectively. The function $\Phi_{ij}(r_{ij})$, which represents the overlap between the electronic densities of atoms i and j, defines the dependence of the interaction of atoms i and j on their separation r_{ij}. By

comparing the predictions of eqn. (1.19) with empirical values of the binding energy for a variety of diatomic molecules, Gollisch concluded that optimum values for the exponent μ and the anharmonicity factor S_{ij} are approximately given by

$$\mu = 0.6, \quad S_{ij} = 2/\mu \tag{1.20}$$

for all kinds of atoms at i and j. For a homonuclear system, the indices i and j can be dropped from the parameters b_{ij}, a_{ij} and λ_{ij}, as well as from the function Φ_{ij}. Furthermore, the interaction function Φ could adequately be expressed as

$$\Phi(r) = c_1\exp(-p_1 r) + c_2\exp(-p_2 r), \tag{1.21}$$

for suitable adjustable parameters c_i and p_i. These parameters were fitted to empirical values of the cohesive energy, the lattice parameter and the bulk modulus.

An attractive feature of the work of Gollisch is that his results for homonuclear systems have been extended for application to heteronuclear systems as would be needed in considerations of epitaxy, for example.

1.4.2 Model of Finnis and Sinclair

The Finnis and Sinclair (1984) N-body potential, which is also based on the embedded atom method (EAM), was specifically designed to overcome the shortcomings of pair potentials. In the FS potential the total energy U of an assembly of N atoms is written as the sum $U = U_P + U_N$ of a core-core repulsive pair potential

$$U_P = \frac{1}{2} \sum_{i,j} V(r_{ij}), \tag{1.22}$$

and a cohesive N-body potential

$$U_N = -A \sum_i \rho_i^{1/2}, \quad \rho_i = \sum_i \phi(r_{ij}). \tag{1.23}$$

The function $\rho_i^{1/2}$ is justified on the basis of tight-binding theory, where ρ_i can be interpreted in terms of the squares of overlap integrals, or more appropriately, as the charge density at atom i as obtained by a linear superposition of the electronic charge densities, ϕ, of all the other atoms.

Within the tight-binding assumptions, Finnis and Sinclair assumed that both V(r) and $\phi(r)$ are of short range and introduced the cutoff distances d and c such that

$$\phi(r) = \begin{cases} (r-d)^2 , & r \leq d \\ 0 , & r > d, \end{cases} \tag{1.24a}$$

$$V(r) = \begin{cases} (r-c)^2(c_0 + c_1 r + c_2 r^2) , & r \leq c \\ 0 , & r > c \end{cases} \tag{1.24b}$$

$$a < d < c < \sqrt{2}a , \tag{1.24c}$$

where a and $\sqrt{2}a$ are the second and third nearest neighbour distances. Whereas values of c and d are selected from an array of feasible pairs, the adjustable parameters A, c_0, c_1 and c_2 are obtained by fitting to the cohesive energy, the equilibrium volume and the three elastic moduli of the

particular bcc transition metal. Feasibility requires that the values of c and d be chosen so that they should yield a value of the unrelaxed vacancy formation energy between 0.3 and 0.5 times the total energy per atom.

When applying the FS model, Ackland and Thetford (1987) found that the values of the parameters thus obtained gave unphysical values for properties involving small separations. They overcame this difficulty by adding a short-range core-core repulsive term

$$\Delta V(r) = B(b_0-r)^3\exp(-\alpha r) \quad , \quad r < b_0 \qquad (1.25)$$

where b_0 is the nearest neighbour distance. This potential will be referred to as the FS-AT potential.

1.4.3 Model of Johnson and Oh

Johnson and Oh (1989) have independently developed an analytic EAM model for bcc transition metals. Their starting point was Johnson's analytic EAM model for fcc metals (Johnson 1988a) discussed in Section 1.3.1. The extension of this model to bcc metals at constant atomic volume was unsuccessful, however, because of the difficulty in matching the anisotropy ratio $A_r = C/C'$ ($C = C_{44}$ and $C' = (C_{11} - C_{12})/2$) with the monotonically decreasing exponential form of the two-body interaction $\phi(r)$ used in the fcc model (Oh and Johnson 1988). In order to explain this problem, the fcc model is assumed to be transformed to its normalized form, i.e. the pair potential is the effective pair potential which has the form of a Morse potential. The shear elastic modulus will then only depend on the two-body potential and the crystallographic direction. (The bulk modulus only include terms involving the curvature of the embedding function at

equilibrium electron density.) First nearest neighbour atoms only contribute to C and not C', while second nearest neighbour atoms only contribute to C', and not to C. With the exponentially decreasing functions, the curvature of the two-body potential is much less at the second nearest neighbour distance than at the first nearest neighbour distance. A greater contribution is thus made to C than to C' by the curvature. The negative slope at the first neighbour distance decreases C'. The result is a very large value for C and a very small one for C'. A reshaping of the two-body potential was therefore necessary to match the anisotropy ratio in bcc metals. This was achieved by modelling the pair potentials in terms of a cubic polinomial.

In the bcc model, the energy of an atom i in an assembly of atoms (crystal) is written as a sum $E_i = E_{P_i} + E_{N_i}$ of a repulsive two-body central pair potential

$$E_{P_i} = \frac{1}{2} \sum_{j \neq i} \phi_{ij}(r_{ij}), \tag{1.26a}$$

where the function ϕ_{ij} depends on the type of atom at i and j a distance r_{ij} apart and a cohesive (binding) embedding function

$$E_{N_i} = F_i(\rho_i); \quad \rho_i = \sum_{j \neq i} f_j(r_{ij}). \tag{1.26b}$$

In eqn. (1.26b) ρ_i is the total electron density at atom i due to all other atoms each of which contributes an amount $f_j(r_{ij})$ to ρ_i. Here $F_i(\rho_i)$ is the energy to embed atom i into the electron density ρ_i.

For application to bcc transition metals, Johnson and Oh (Johnson 1988a) employed the invariance of the EAM to terms linear in the electron

density and transformed eqn. (1.26) to a *normalized* form by adding a term linear in the electron density to $F_i(\rho_i)$ in such a way that its slope vanishes at the equilibrium electron density ρ_e. This term is again subtracted from the pair potential contribution.

The short range nature of the atomic forces is again accounted for by introducing a cutoff distance r_c for $\phi_{ij}(r)$ lying between second and third nearest neighbour distances. Accordingly first and second nearest neighbour distances, r_{1e} and r_{2e}, enter into the results.

For homonuclear systems, the subscripts on F_i, f_j and ϕ_{ij} can again be dropped. The two-body potential is then written as a cubic equation

$$\phi(r) = K_3\left[\frac{r}{r_{1e}} - 1\right]^3 + K_2\left[\frac{r}{r_{1e}} - 1\right]^2 + K_1\left[\frac{r}{r_{1e}} - 1\right] + K_o, \qquad (1.27)$$

where the coefficients in the normalized model are uniquely determined by fitting to the unrelaxed vacancy formation energy E_{1V}^{UF}, the atomic volume Ω, the Voigts average shear modulus G and the anisotropy ratio A_r.

Johnson and Oh proposed a general analytic form for $F(\rho)$ containing parameters F_o,F_1, m and n. By assigning appropriate values to these parameters, the models of Finnis and Sinclair (1984), of Baskes (1987), and of Banerjea and Smith (1988) could be reproduced. The power law form

$$f(r) = f_e\left[\frac{r_{1e}}{r}\right]^{\beta}, \qquad (1.28)$$

was adopted for f(r). The authors showed that the parameter f_e cancels for all monatomic models and that there is little loss of generality if m and n are taken equal. Either β or n, which satisfy the relation

$$n^2\beta^2 = \frac{9\,\Omega B - 15\,\Omega G}{E_c - E_{1V}^{UF}}, \qquad (1.29)$$

B being the bulk modulus, could be used as adjustable parameter. The generalized analytic form of the embedding function then reduced to

$$F(\rho) = -(E_c - E_{1V}^{UF})[1 - \ell n(\frac{\rho}{\rho_e})^n](\frac{\rho}{\rho_e})^n \ . \qquad (1.30)$$

In order to ensure that the functions $f(r)$ and $\phi(r)$ satisfy a cutoff between second and third nearest neighbour distances and smoothly become zero at the cutoff, the distances r_s and $r_c > r_s$ are defined by fractions k_s and k_c ($r_i = r_2 + k_i(r_3 - r_2)$) such that a cubic polynomial with the same value and slope at $r = r_s$ and zero value and slope at $r = r_c$ can be fitted to $f(r)$. The same procedure may then be applied to $\phi(r)$.

When comparing their results with a universal Rydberg function proposed by Rose *et al.* (1984), the authors concluded that their analytic representation needed to be adjusted to give a "harder" total energy curve at distances below $r = r_{1_e}$, analogous to the short range core-core repulsion in eqn. (1.25). The authors accomplished their goal by stiffening the two-body potential according to

$$\phi_a(r) = \phi(r) + K_a[\phi(r) - \phi(r_{1e})](\frac{r}{r_{1e}} - 1)^2 \ ; \quad r < r_{1e} \ , \qquad (1.31a)$$

$$K_a = 4.5 \ (1 + \frac{4}{A_r - 0.1}). \qquad (1.31b)$$

1.5 OVERVIEW

The purpose of this study is to assess the validity of EAM models for bcc metals with respect to the calculation of the following adsorption parameters: desorption energy, activation energy for adatom surface

migration, vibration frequencies of adsorbed atoms, and a truncated Fourier series representation of the adatom substrate interaction.

In Chapter 2 a brief and simplified qualitative discussion of the adsorption of an isolated atom on a single crystal surface is presented. Elementary definitions of the various adsorption parameters in terms of N-body potential models are given and computational procedures for quantifying the adsorption parameters are described.

In Chapter 3 the suitability of the EAM models introduced by Gollisch, Finnis and Sinclair, and by Johnson and Oh for calculating self-adsorption parameters is examined for a homonuclear system consisting of a tungsten adatom adsorbed on a W{110} surface. A minor modification to the Finnis and Sinclair potentials to improve the fundamental form of these potentials for application to isolated adsorbed atoms, is introduced. The Finnis and Sinclair potential is also applied to an infinite adsorbed monolayer as is relevant to epitaxy.

Chapter 4 presents an overview of existing alloy models and some of the practical problems associated with the application of EAM potentials in the computational modelling of heterogeneous systems. The adsorption parameters for a heterogeneous system consisting of a tantalum adatom adsorbed on a W{110} surface, are also calculated using the models of Finnis and Sinclair, and of Johnson and Oh.

In Chapter 5 the main results of the study are summarised and the conclusions to be drawn from them are presented.

CHAPTER 2

DEFINITIONS RELEVANT TO ADSORPTION

2.1 INTRODUCTION

Adsorption is of fundamental importance in a wide variety of processes ranging from catalysis to vacuum technology. For this study the main importance of adsoption lies in the fact that it is the first stage in the formation of an oriented or epitaxial overgrowth on a single crystal substrate. The adsorption of a single adatom on a metal crystal substrate is a very complex phenomenon characterized by the large gradient of electron density near the surface of the substrate and the relaxation of the ion cores due to asymmetrical bonding. The quantitative understanding of the phenomenon is still far from satisfactory.

A wide variety of events are possible when an atom collides with a crystal surface (Prutton 1975). The atom could be reflected or diffracted without any loss of energy. Alternatively some of its energy may be transferred to the substrate atoms by exciting lattice phonons in the substrate. If the atom loses only a small amount of its energy it may still be reflected, inelastically though. If sufficient energy is transferred to the cystal it may become effectively bound to the surface. The strength of the bond depends upon the particular kinds of atoms involved. The atom is then said to be accommodated by the surface, i.e. it acquires an energy determined by the temperature T_S of the crystal surface. It has become adsorbed and is referred to as an adatom.

The adatom is captured in a wide potential well that extends over the entire substrate surface. To leave the surface the adatom must acquire an amount of energy (desorption energy E_{des}) at least equal to the depth of the potential well. With a weak bond (adsorption energy of the order of 0.25 eV) the process is called physisorption. In this case binding is due to van der Waals interactions and the desorption energy is equal to the adsorption energy. On the other hand, very strong bonds are associated with charge transfer and ionic bonds are formed. Usually the wavefunctions of the valence electrons of the adatom combine with the valence electrons of the substrate atoms to form a new wavefunction. The electrons responsible for bonding are to be found in orbitals between the substrate and the adatom giving rise to covalent bonding. Chemisorption is said to have taken place. In this case the desorption energy is slightly higher than the adsorption energy. The adsorption energies for chemisorption range between 0.43 eV for nitrogen on nickel to about 8.4 eV for oxygen on tungsten.

A physi- or chemisorbed atom finds itself in the three-dimensional potential described above (Gomer 1983). Perpendicular to the surface for a fixed position (x,y) in the surface plane, the potential has a characteristic shape similar to that of a Morse or Lennard-Jones (6-12) potential, describing the binding of the adsorbate to the substrate. Parallel to the surface the potential is corrugated with the atomic periodicity of the substrate. These corrugations are important in surface diffusion. At a small enough surface temperature the adatom remains in a position of minimum energy, usually the adsorption site, and vibrates with a certain frequency. The adatom may experience a thermal fluctuation induced by the heat bath, *viz.* the lattice vibrations of the substrate. This fluctuation

may provide the adatom with sufficient energy to surmount the lowest energy barrier (the one at the saddle point) to a neighbouring position of minimum potential energy. This represents the basic mechanism for diffusion of an adatom across a perfect crystal surface.

Should the temperature of the substrate be raised still further, a point will be reached where the adatom can acquire enough energy from the thermal fluctuations to overcome the energy barrier equal to the depth of the potential well. It can then break free to join other gas atoms in the space above the surface. The adatom has been desorbed. If the temperature of the substrate is raised still further, the atomic vibrations of the surface atoms will become stronger and stronger until a temperature is reached where the crystallographic order is lost and the atoms are in a disordered conglomeration. This order-disorder transition is called surface melting. There is an intermediate temperature range between the temperatures at which surface diffusion starts and desorption begins, where the adatom moves relatively freely across the surface simulating a molecule in a two-dimensional gas.

An adatom, adsorbed on a crystal surface of which the temperature is such that the atom remains localized on the surface in a position of minimum potential energy, may be joined by other atoms. Up to now the adatom-substrate interaction potential has been the important parameter. However, the presence of other atoms on the surface brings into play another important parameter, *viz.* the adatom-adatom interaction potential that usually has the tendency to arrange the atoms in a structure close to that of the corresponding bulk. The adatoms are now subjected to two competing periodicities. An important effect of the competition is the realization of a crystallographic order that may be the beginnings of

epitaxial growth. The binding energy of an adatom on a substrate is usually diminished by the presence of other atoms at neighbouring adsorption sites (Bauer 1984).

In the following section elementary definitions of the adsorption parameters are given to facilitate the comparison of the various EAM models with respect to their applicability in quantitative studies of adsorption phenomena.

2.2 ADSORPTION PARAMETERS

2.2.1 Adatom-substrate interaction potential (ASIP)

In the modelling of adsorption phenomena on the {110} plane of tungsten, the substrate surface is assumed to be a rigid planar array of exposed atoms, having the same stoichiometry, lattice spacing and lattice symmetry as the bulk. Multilayer relaxation and surface reconstruction are neglected. This assumption is supported by results of Constant-Moment-Transfer Averaging of LEED intensities from the W {110} substrate surface. According to Buchholz *et al.* (1975) the clean surface is unrelaxed to a resolution of less than 0.06 Å. Van Hove and Tong (1976) found the relaxation on the W {110} surface to be ~ 0%. These results also agree with the suggestion of Finnis and Heine (1974) that "smoothing" of the surface electronic density is a mechanism for driving the inward displacement of the outermost atomic layer. As the {110} surface is a close-packed surface in a bcc crystal, the surface electronic density is relatively constant and little or no relaxation will occur (Jiang *et al.* 1986).

In the adsorption of single adatoms on a crystal surface, the single most important parameter is the adatom-substrate interaction potential

(ASIP). *Ab initio* calculations of the ASIP is still very much an intractable problem due to the complexity of the analysis. The interaction potential of the adatom with the atoms of the substrate has been approximated in various ways, for example

(i) Fourier series representations;

(ii) additive pair potentials; and

(iii) N-body potentials.

A Fourier series constitutes a purely phenomenological approach to the adatom-substrate interaction based on the periodicity of the substrate and it contains unknown coefficients that can be estimated using additive pair potentials or N-body potentials. The converse is, however, not true. Of the three types of approximations, the N-body approximations are considered to be the most fundamental. In their derivations attempts have been made towards simulations of a quantum mechanical approach to the electrons. Due to the short-comings of pair potentials, discussed in Chapter 1, and particularly their inadequacy in handling environment effects on bonding, this study will mainly be limited to N-body potentials. The Fourier series representation of the ASIP is tailored to reproduce the periodicity and symmetry of the Bravais lattice of the underlying substrate surface. Two Fourier series representations of the ASIP of an adatom on a bcc {110} surface, one in skew and one in Cartesian axes, are presented here. The appropriate full Fourier series representation of the ASIP, taking into account the lattice symmetry, is derived naturally within the reciprocal lattice formalism. The Fourier series for the adatom-substrate interaction potential, expressed in skew axes $x^{(1)}$, $x^{(2)}$ (see Fig. 2.1) with the origin at an adsorption site (AS), and truncated at the n-th harmonic order (Stoop *et al.* 1988), is

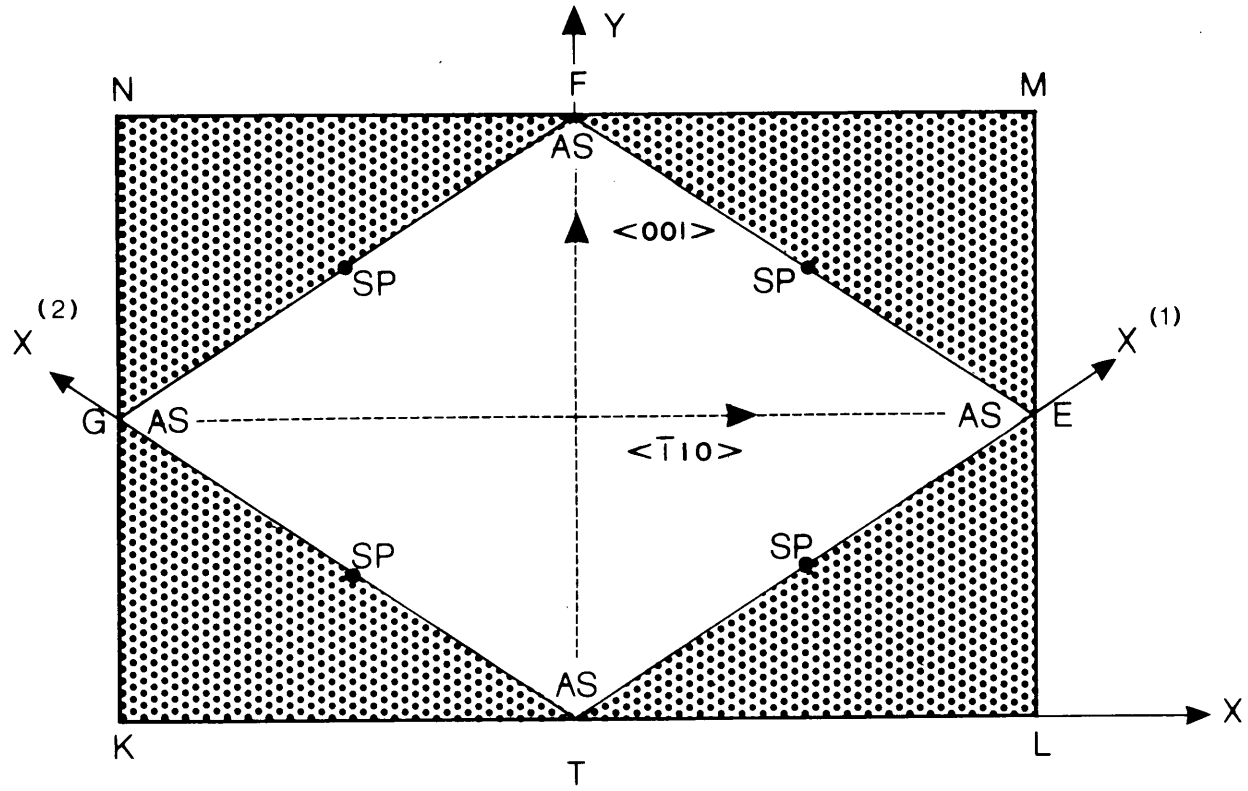

Figure 2.1 Diagram of {110} bcc surface unit cell showing (i) Cartesian (x,y) and skew ($x^{(1)}$,$x^{(2)}$) axes and (ii) adsorption sites AS and saddlepoints SP. Data obtained for points within the rhombic unit cell TEFG (TE = $\sqrt{3}a/2$) has been used to calculate the Fourier coefficients and data for the rectangular unit cell KLMN (KN = a_y = a ≡ nearest neighbour distance, KL = a_x = $\sqrt{2}a$) to construct the three-dimensional diagrams.

$$F_s^n(\xi,\eta) = A_{oo} + \sum_{h=1}^{n} 2A_{ho}\cos 2\pi h\xi + \sum_{k=1}^{n} 2A_{ok}\cos 2\pi k\eta$$

$$+ \sum_{h,k=1}^{n=h+k} [2A_{hk}\cos 2\pi(h\xi + k\eta) + 2A_{h,-k}\cos 2\pi(h\xi - k\eta)], \qquad (2.1)$$

where $\xi = x^{(1)}/b$, $\eta = x^{(2)}/b$; b being the nearest neighbour distance. The summation in the last line of eqn. (2.1) implies that the sum of the integers h and k should not exceed the order n. The Fourier representation in Cartesian axes (van der Merwe 1984), with the origin at a minimum, is given by

$$F_c^{(n)}(\xi,\eta) = \sum_{\substack{h,k=0 \\ (h+k)\ \text{even}}}^{n} A_{hk}\{\cos[2\pi(h\xi + k\eta)] + \cos[2\pi(h\xi - k\eta)]\}, \qquad (2.2)$$

where $\xi = x/a_x$, $\eta = y/a_y$, $a_x = \sqrt{2}a$ and $a_y = a$; a being the cubic lattice parameter and a_x and a_y the diagonal lengths of the rhombic surface unit cell in Fig. 2.1.

The optimum Fourier coefficients for a Fourier representation truncated at relatively low order harmonics are calculated using analytically derived expressions (see Appendices A and B).

2.2.2 Desorption energy E_{des} and activation energy for surface migration Q

It should be noted that there are certain subtleties involved in the definition of the desorption energy E_{des} in terms of a many-body potential. The desorption energy is defined as the difference between the total energy of the adatom/substrate system before and after the atom has been adsorbed (Plummer and Rhodin 1968). Within the many-body framework, both the substrate surface with the adatom and the substrate surface without the adatom are considered to be defects. Thus E_{des} is actually the difference between

two defect energies. The defect energy in turn is calculated by summing both the electron density function and the two-body repulsive contribution over those atoms within the range of the defect, and to subtract the corresponding perfect lattice terms (Finnis and Sinclair 1984). For the bcc models considered in this study, the atoms within the range of the defect are those whose first and second nearest neighbour coordination is changed by the presence of the defect.

In this study the following approach has been adopted in the calculation of E_{des}: At each position (x,y) within the surface unit cell the adatom is allowed to relax to its equilibrium height h_e above the surface. The basic principles of the calculation are displayed schematically in the energy diagram in Fig. 2.2. In region I the curve represents the adatom surface migration of the adatom with activation energy Q and in region II it represents the desorption of the adatom with desorption energy E_{des} (= − adsorption energy E_{ads}). With the adatom B at an arbitrary point P(x,y) within the unit cell at a height h (about one interplanar spacing) above the surface atomic plane S, there will be a number, say n, of atoms (including B) that fall within the cutoff distances for B. E^* represents the energy of the array of n atoms as compared to their energy when they are at their normal positions within the crystal. The adatom B is now taken to infinity, i.e. desorbed. The same n atoms will now have an energy E_∞ relative to the energy of the n atoms at normal crystal positions. The difference

$$E^*_{des}(h,P) = E_\infty(n) - E^*(h,n,P) = -E^*_{ads}(h,P) \qquad (2.3)$$

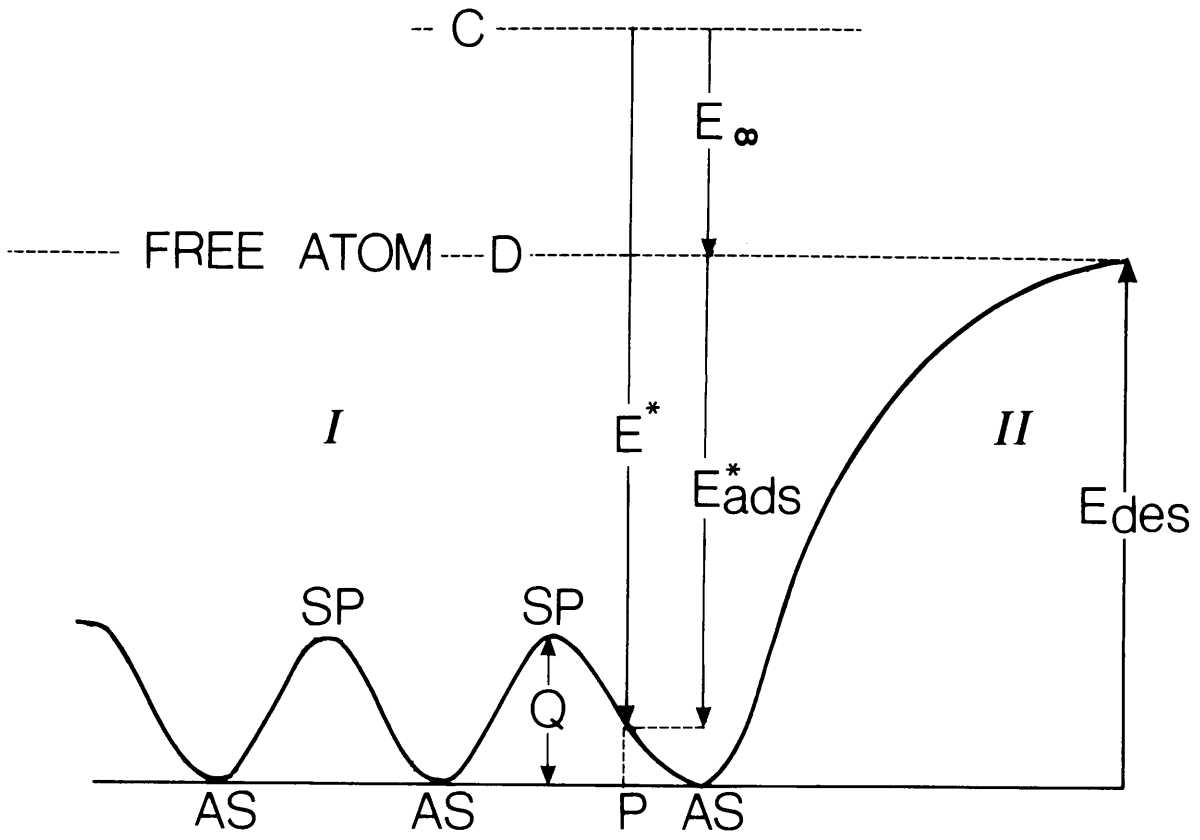

Figure 2.2 A diagram illustrating the physical principles involved in the calculation of (i) the adsorption energy E^*_{ads} in eqn. (2.5d) of an adatom at an arbitrary point P(x,y) within the unit cell on the crystal surface, (ii) the activation energy of surface migration Q (region I) through the saddle point SP and (iii) the desorption energy E_{des} (region II) from the adsorption site AS.

then represents the work needed to desorb B from the position P(x,y). The equilibrium height $h = h_e$ of B above the surface plane S and the corresponding "desorption" energy may be obtained by minimizing either E^* or E^*_{ads} to yield the equation

$$E^e_{des}(h_e,P) = E_\infty(n) - E^e(h_e,n,P). \qquad (2.4)$$

When P coincides with an adsorption site AS in Fig. 2.1, then $E^e_{des}(h_e,AS) \equiv E_{des}$ which corresponds to the absolute minimum of E^*. It is important to note that, whereas E_∞, E^* and E^e all depend on n, E^e_{des} and E^e_{ads} do not depend on n. $E^e_{des} = -E^e_{ads}$ is simply the work needed to desorb the single atom B.

The desorption energy E_{des} from an adsorption site AS, the desorption energy E^{sad}_{des} from a saddle point SP, the activation energy Q through a saddle point SP and the adatom substrate interaction energy E(P) at P may now respectively be written as

$$E_{des} = E_\infty(n_1) - E^e(h_e,n_1,AS) = -E_{ads}, \qquad (2.5a)$$

$$E^{sad}_{des} = E_\infty(n_2) - E^e(h_e,n_2,SP) = -E^{sad}_{ads}, \qquad (2.5b)$$

$$Q = E_{des} - E^{sad}_{des}, \qquad (2.5c)$$

$$E(P) = E^*_{ads}(h_e,n,P) = E^*(h_e,n,P) - E_\infty(n), \qquad (2.5d)$$

where n_1 and n_2 are the values of n at AS and SP, respectively.

2.2.3 Vibration frequencies and force constants

Within the framework of the harmonic oscillator simulation the vibration frequencies are given by

$$\nu = \left[k_i/4\pi^2 m\right]^{1/2}, \qquad (2.6)$$

where m is the adatom mass and k_i the relevant force constant.

Force constants are usually calculated directly by taking the second derivative of the ASIP at a minimum. In the case where the ASIP is expressed in terms of an N-body potential, this results in rather complicated expressions for the force constants. In this study the force constants are numerically approximated by a second order difference at the potential minimum. The force constant k_z, for example, is most simply calculated from a second order difference as

$$k_z^{(f)} = \frac{\partial^2 V}{\partial z^2} \approx \frac{E(z_e+\bar{\delta}) + E(z_e-\bar{\delta}) - 2E(z_e)}{\bar{\delta}^2} \qquad (2.7)$$

where $\bar{\delta}$ defines some small "vertical" displacement from the position of the potential energy minimum, and the superscript (f) pertains to the finite difference technique used in the calculation. The lateral force constants k_x and k_y can alternatively be calculated as the second derivative of the n-th order Fourier truncation (eqn. 2.2) of the ASIP with respect to the coordinates x and y respectively, i.e.

$$k_x^{(n)} = \frac{\partial^2 F_c^{(n)}}{\partial(a_x\xi)^2} = \frac{1}{a_x^2}\frac{\partial^2 F_c^{(n)}}{\partial\xi^2} \qquad (2.8a)$$

and

$$k_y^{(n)} = \frac{\partial^2 F_c^{(n)}}{\partial (a_y \eta)^2} = \frac{1}{a_y^2} \frac{\partial^2 F_c^{(n)}}{\partial \eta^2} , \qquad (2.8b)$$

where $a_x = \sqrt{2}a$ is the repeat period in the <$\bar{1}$10>-direction and $a_y = a$ is the repeat period in the <001>-direction. The dependence of $k_y^{(n)}$ and $k_x^{(n)}$ on the order n of truncation is investigated where appropriate.

Some of the potentials under consideration display a double well in the adatom potential energy surface. Two very shallow local minima (of depth < 0.055 eV) are situated along the <$\bar{1}$10>-direction (taken as the x-direction) a short distance (< 0.3Å) on either side of the hollow site. This double well has interesting implications for the force constants k and corresponding adatom vibration frequencies ν. When the surface temperature T_S is small enough, i.e. $k_B T_S << 0.055$ eV (k_B is Boltzman's constant) the adatom will perform small amplitude vibrations (frequency ν_{x1}) and practically stay put in one of the minima. An observation such as that of Bauer (1984) will then locate the adatom asymmetrically with respect to the hollow site. If T_S is increased, a value T_{S1} will be reached where thermal fluctuations can carry the adatom across the barrier between the two minima and the adatom spends more or less equal time intervals in each of them. At an appreciably higher temperature T_{S2} the adatom will "see" little of the double well, vibrate with frequencies ν_x and ν_y and thermal fluctuations may carry it across the saddle point to a neighbouring hollow site. This is where adatom surface migration sets in. The vibration frquency ν_z normal to the surface, is present at all temperatures and begin to play a role when T_S is high enough to effect desorption.

2.3 NUMERICAL PROCEDURE

A golden section search technique (Brent 1973) is employed in the computation of the equilibrium ASIP energy E(P) in eqn. (2.5d) at point P. Data for optimizing the Fourier coefficients are obtained by calculating the energy E(P) for each point on the surface mesh of gridpoints $P(x_i^{(1)}, x_j^{(2)})$ within the unit cell TEFG (see Fig. 2.1) using the many-body potentials under consideration. The discrete set of values $\{E_{ij} = E(x_i^{(1)}, x_j^{(2)}, h_e);\ i,j = 1,\ldots,40\}$, one for each gridpoint, are used to calculate the optimum coefficients of the two-dimensional truncated Fourier series representations of the ASIP in skew (eqn. (2.1)) and in Cartesian axes (eqn. (2.2)). The standard error, $\delta^{(n)}$, pertaining to a truncated Fourier series representation $F^{(n)}$, for the set of data, is defined as

$$\delta^{(n)} = \frac{1}{N}\left[\sum_{\ell=1}^{N} \{E^{e}_{ads}(\sigma_\ell) - F^{(n)}(\sigma_\ell)\}^2\right]^{1/2} \qquad (2.9)$$

where N is the number of data points σ_ℓ. $\delta^{(n)}$ provides a meaningful overall measure of the accuracy of the n-th order Fourier truncation.

2.4 CONCLUDING REMARKS

In this chapter the following has been given: (i) an elementary description of the temperature dependent behavior of an isolated atom adsorbed on a crystal surface and (ii) the definitions needed for calculating adsorption parameters. The magnitudes of the binding energies of a tungsten and a tantalum adatom respectively on a W{110} substrate, calculated in Chapters 3 and 4 respectively, are reminiscent of the process

of chemisorption. As the complexities of chemisorption have as yet not been fully analysed, no attempt has been made to incorporate them explicitly in the simple definitions of the adsorption parameters given in Section 2.2. In Chapter 3 the suitability of EAM models - designed for bcc metals - to calculate adsorption parameters is assessed by calculating the self-adsorption parameters of a tungsten adatom on a W{110} surface. Adequate reproduction of the empirical values of the desorption energy and the activation energy for surface migration is considered to render a potential suitable for surface calculations.

CHAPTER 3

APPLICATION TO HOMONUCLEAR SYSTEMS: TUNGSTEN ON W{110} SUBSTRATES

3.1 INTRODUCTION

In this chapter the suitability of the EAM's for bcc metals, introduced by Gollisch (G), by Finnis and Sinclair (FS) and by Johnson and Oh (JO), for application to self-adsorbates on W{110} surfaces is investigated (i) by calculating and comparing the self-adsorption parameters (*viz.* desorption energy, activation energy of adatom surface migration and vibration frequencies of adsorbed atoms) with one another and with empirical data, and (ii) by calculating the optimum truncated Fourier representations of the adatom-substrate interaction. EAM's employ expressions qualitatively justified by physical theory but contain adjustable parameters obtained by fitting to the relevant data, e.g. cohesive energy and elastic constants. In all three cases, the fitting parameters determined by the authors for bulk crystals are used. In the case of the FS potential small modifications will be introduced in this chapter to obtain a more realistic adsorbate-substrate interaction potential.

3.2 THE FITTING PARAMETERS

The convention is adopted that no indices will be attached to the quantities E, ρ, F, ϕ and f if they refer to a pure metal. Thus the basic equations of the EAM, eqns. (1.1) and (1.2), for a homonuclear system consisting of N atoms can be written as

$$E_t = NE \tag{3.1}$$

$$E = F(\rho) + \frac{1}{2}\sum_m \phi(r^m) \tag{3.2}$$

$$\rho = \sum_m f(r^m), \tag{3.3}$$

where E is the energy per atom and r^m the mth neighbour distance to some particular atom. In order to apply any EAM, the functional forms f, ϕ and F must be given.

For a homonuclear system, such as a W adatom on a W{110} substrate, the functional forms of f, ϕ and F in the effective binding potential (eqn. (1.19)) of Gollisch (1986b) reduce to

$$\phi(r) = b[c_1\exp(-p_1 r) + c_2\exp(-p_2 r)]^{S\mu\lambda}, \tag{3.4}$$

$$f(r) = a[c_1\exp(-p_1 r) + c_2\exp(-p_2 r)]^{\lambda}, \tag{3.5}$$

$$F(\rho) = -\rho^{\mu}; \quad \mu = 0.6; \; S = 2/\mu. \tag{3.6}$$

By fitting the parameters to empirical data for W, Gollisch obtained the values of 120.0, 1.37, 16.0 and 2.00 for the parameters c_1, p_1, c_2 and p_2 respectively, and 0.82400 Ry, 0.39104 $Ry^{5/3}$ and 0.70747 for the parameters b, a and λ. The lattice parameter a_W for tungsten was taken to be 3.15918669 Å.

The parameterized forms for ϕ, f and F introduced by Johnson and Oh (1989) are

$$\phi(r) = K_3\left[\frac{r}{r_{1e}} - 1\right]^3 + K_2\left[\frac{r}{r_{1e}} - 1\right]^2 + K_1\left[\frac{r}{r_{1e}} - 1\right] + K_o, \tag{3.7}$$

$$f(r) = f_e\left[\frac{r_{1e}}{r}\right]^{\beta}, \tag{3.8}$$

$$F(\rho) = -(E_c - E_{1V}^{UF})[1 - \ell n(\frac{\rho}{\rho_e})^n](\frac{\rho}{\rho_e})^n; \quad n = 1/\sqrt{8}. \tag{3.9}$$

Like others the authors also introduced a hard-core modification

$$\phi_a(r) \rightarrow \phi(r) + K_a[\phi(r) - \phi(r_{1e})](\frac{r}{r_{1e}} - 1)^2 \quad \text{for} \quad r < r_{1e} \tag{3.10}$$

to improve the modelling of the atomic interaction at small separations. Fitting the parameters to empirical data yielded the values of −0.43531 eV, −1.06484 eV Å^{-1}, 9.87819 eV Å^{-2}, −10.61219 eV Å^{-3}, 6 and 24.28022 for K_0, K_1, K_2, K_3, β and K_a, respectively. Johnson and Oh used a value of 3.16475 Å for the lattice parameter a_W of tungsten. Although the fitting procedure in the JO model is independent of the cutoff distance, the latter does have a profound effect on the value of the activation energy Q for surface migration. The cutoffs r_c = 4.3996 Å and r_s = 3.2958 Å, with r_c very close to the third neighbour distance, yield the best value of Q. With these values of r_s and r_c the repulsive two-body potential ϕ has a very small positive maximum while approaching r_c.

Finnis and Sinclair (1984) adopted the following parameterization:

$$\phi(r) = \begin{cases} (r-c)^2(c_0+c_1r+c_2r^2) & , \quad r \leq c \\ 0 & , \quad r > c \end{cases}; \tag{3.11}$$

$$f(r) = \begin{cases} (r-d)^2 & , \quad r \leq d \\ & \\ 0 & , \quad r > d \end{cases} ; \qquad (3.12)$$

$$F(\rho) = -A\rho^{1/2}. \qquad (3.13)$$

The fitting procedure to bulk data for W, described in Section 1.4.2, yielded values of 3.25 Å, 47.1346499 eV $Å^{-2}$, -33.7665655 eV $Å^{-3}$, 6.2541999 eV $Å^{-4}$ for c, c_0, c_1 and c_2, when ϕ and r are measured in eV and Å respectively, as well as values of 4.400224 Å and 1.896373 eV for d and A respectively. Ackland and Thetford (1987) introduced the hard-core modification

$$\phi_{tot} = \phi + B(r_{1e} - r)^3 \exp(-\alpha r) \quad \text{for} \quad r < r_{1e} \qquad (3.14)$$

for the repulsive two-body component. Fitting the parameters to electron gas calculations on dimers, yielded values of 90.3 eV $Å^{-3}$ and 1.2 $Å^{-1}$ for the parameters B and α in the core function. In this model (the so-called FS-AT model) the lattice parameter is taken to be a_W = 3.1652 Å.

3.3 TRADITIONAL PAIR POTENTIALS VERSUS EAM MODELS

In the atomistic modelling of transition metals, the traditional Morse and Lennard-Jones (6-12) pair potentials, contrary to experiment, always predict an expansion of the outermost layer of the crystal (see Table 3.1). The various EAM models under discussion all predict a slight contraction of the W{110} surface, which suggests that in this respect they are superior to pair potentials for application at surfaces.

TABLE 3.1. Desorption energy E_{des}, relaxation z_0 and activation energy Q for surface migration of a W-adatom on a W{110} substrate. Here z_0 is the deviation of the equilibrium height of the adsorbate from the surface (atomic) lattice plane.

Model	E_{des}[eV]	z_0[Å]	Q[eV]
Lennard-Jones (6-12)	5.5900	+0.0285	0.6916
Morse	5.8895	+0.0774	0.5031
Gollisch	9.1897	−0.5490	0.9529
Johnson and Oh	6.6682	−0.0807	0.8852
Finnis and Sinclair	6.4648	−0.1344	0.6301
FS-AT	6.4565	−0.1206	0.6464
Surf. mod. FS-AT	8.2366	−0.2084	0.8724
Experimental	8.2*	negative	0.86 − 0.92**

* Plummer and Rhodin (1968).

** Tsong and Cowan (1979).

The values of the desorption energy E_{des} predicted by the G-, JO- and FS-AT models do not compare favourably with the empirical value. In fact they deviate by more than 12%, 18% and 21% respectively, from the measured value of E_{des} for tungsten. In the case of Q, the JO potential is the only one which yields a value lying within the experimental limits. The G, JO and FS-AT potentials are clearly not adequate for a quantitative description of adsorption phenomena.

The modification of the EAM model by fitting the parameters to specific surface properties in order to improve its performance as a surface potential presents interesting possibilities. Because of its simple analytical form, the FS-AT potential may be the most suitable candidate for such a modification.

The FS-AT model yields values of 6.4565 eV and 0.6464 eV for E_{des} and Q respectively. If these values are compared to the experimental value of E_{des} which was found to be about 8.2 eV, and that of Q, ranging between 0.86 eV and 0.92 eV (see Table 3.1), the calculated values of E_{des} and Q are clearly too low. In fact, the calculated value of E_{des} using this potential, do not differ much (less than 10% or 0.6 eV) from that predicted by Morse and Lennard-Jones pair potential models. As can be seen from Table 3.1, the Lennard-Jones value of Q is about 0.04 eV higher than that predicted by the FS and FS-AT models. A potential suitable for calculations of adsorption phenomena, should yield values of E_{des} and Q closer to experiment. The work function of the W{110} substrate surface (Plummer and Rhodin 1968, and Ehrlich and Kirk 1968) is an important input parameter in the determination of the experimental value of E_{des}. Because of the uncertainty in the value of this input parameter, the modification of the FS-AT potential to reproduce an average empirical value of Q is pursued further.

3.4 THE SURFACE MODIFIED FS-AT POTENTIAL

It is assumed that the FS-AT model describes bulk and surface properties (Ackland and Thetford 1987) satisfactorily but that adjustments are needed for the adatom which is in an entirely different electronic environment. The assumption is made that the repulsive pairwise component U_p of the interaction potential between two substrate atoms has the same functional form as the interaction potential between a substrate atom and the adatom. This assumption is justified on the grounds that, within the framework of the tight-binding description of bonding, U_p comes mainly from the interaction of "rigid" superimposed free atomic charge densities (Sutton *et al.* 1988). For the repulsive interaction U_p between all atoms (including the adatom), the FS-AT model (eqn. (3.14)) is adopted. The "origin" of the contributions towards the cohesive component of the energy U_N, fall into two categories. The first category (i) consists of the contribution from charge densities emanating from the substrate atoms: f_{ss} at the other substrate atoms and f_{as} at the adatom. The second category (ii) consists of the charge densities generated by the adatom and which is denoted by f_{sa}. It is assumed (a) that f_{sa} is functionally different from f_{as} and f_{ss} and (b) that this can adequately be taken into account by appropriately adjusting the value of f_{sa}. This assumption is justified on the basis that the electron distribution carried by the adatom will be distorted due to polarization effects which occur when the adatom comes into close proximity of the metal surface (Al-Rawi and Jones 1983, Jones and Roberts 1977, and Knowles and Suhl 1977). A modified fitting parameter λ with

$$A^* = \lambda A \tag{3.15}$$

has accordingly been introduced for the interaction of the adatom with the substrate atoms. This procedure also has the practical advantage that the fitting parameters for the bulk, specifically for f_{ss} and f_{as} need no readjustment.

The corresponding values of Q and E_{des} for different values of λ were calculated using the FS-AT model. Fig. 3.1 shows the relationship between Q, as well as E_{des}, and λ is approximately linear. If λ is conveniently taken as 1.4, the corresponding value of Q is then 0.8724 eV, which is within 2% of the average of the experimental values quoted by Tsong and Cowan (1979). This value of λ then yields a value of E_{des} = 8.2366 eV (see Table 3.1) in excellent agreement with empirical data. The dependence on λ of the deviation z_o of the equilibrium height h_e from the bulk interlayer spacing, was also calculated for both the adsorption site (AS) and the saddle point (SP). Fig. 3.2 shows that the deviation z_o is also closely linear in λ in both cases.

It is concluded that the extended FS-AT model with the adatom-substrate interaction adjusted according to the relation $A^* = \lambda A$, with $\lambda = 1.4$ to fit the activation energy Q for surface migration (hereafter referred to as the surface modified FS-AT model) is suitable for application to self-adsorption phenomena on a W{110} surface. It yields a value of E_{des} deviating by less than 0.5% (or 0.0366 eV) from the experimental value.

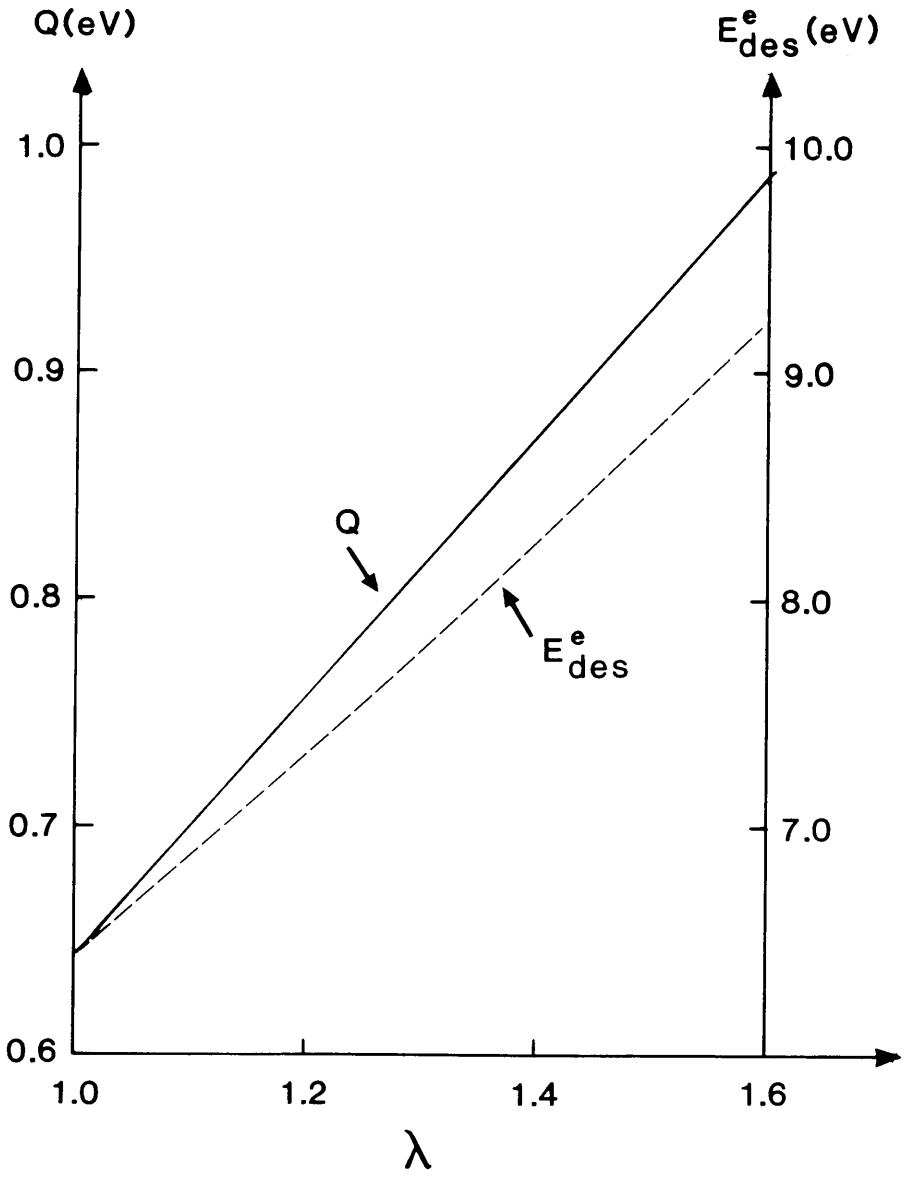

Figure 3.1 Dependences of the surface migration activation energy Q (solid line) and the desorption energy E_{des} (broken line) on $\lambda = A^*/A$, the surface modified fitting parameter adjusting the cohesive adatom-substrate interaction for the tungsten on W {110} system.

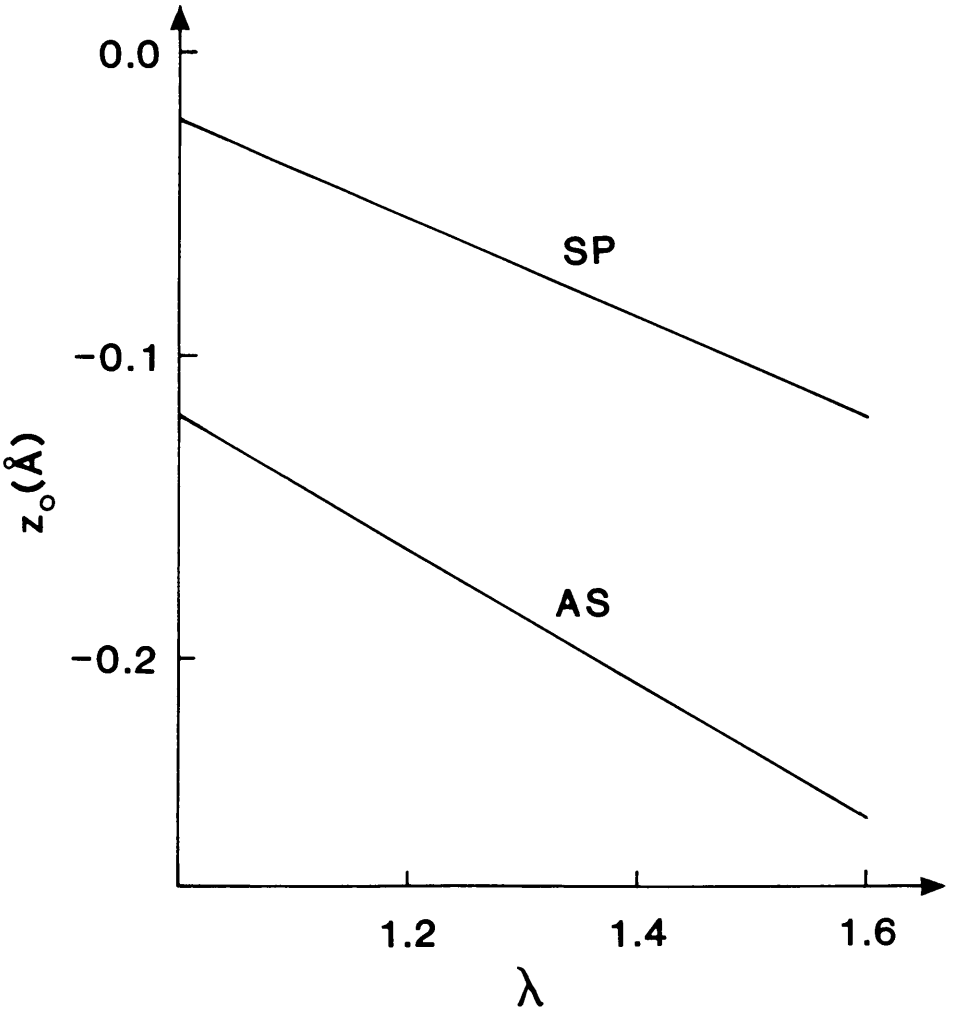

Figure 3.2 Dependence, on the surface modifying fitting parameter λ, of the deviation z_0 of the equilibrium height h_e from the bulk interlayer spacing for an adsorption site (AS) and a saddle point (SP) determined for the tungsten on W {110} system.

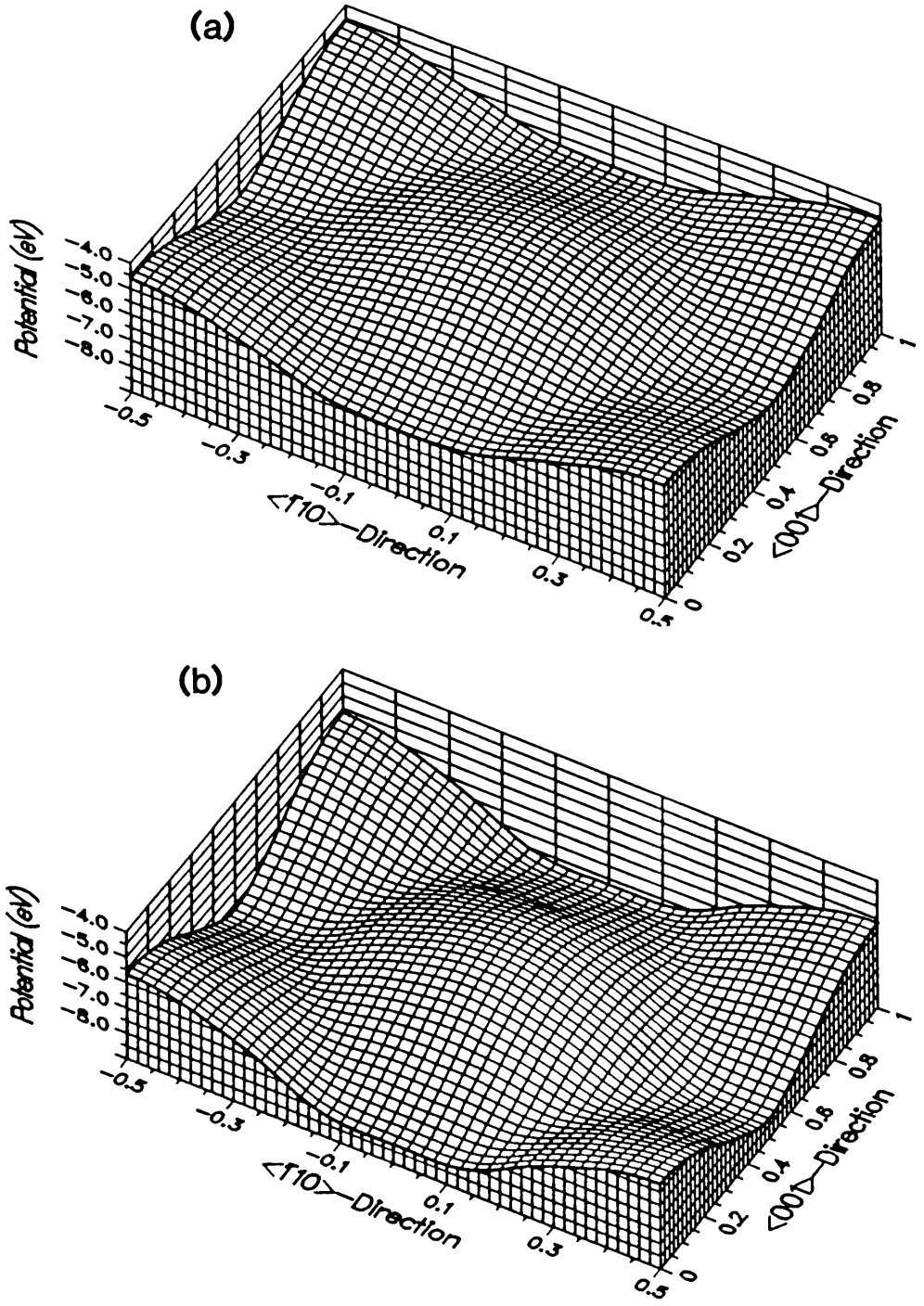

Figure 3.3 Three-dimensional representations of the potential surface E(P) in eqn. (2.5d) for migration of a tungsten adatom on a W {110} substrate: (a) the FS-AT model and (b) the surface modified FS-AT model with λ = 1.4. (The representation for the FS potential is indistinguishable from that of the FS-AT potential.) Positions are expressed in terms of normalized rectangular unit cell sidelengths (Fig. 2.1).

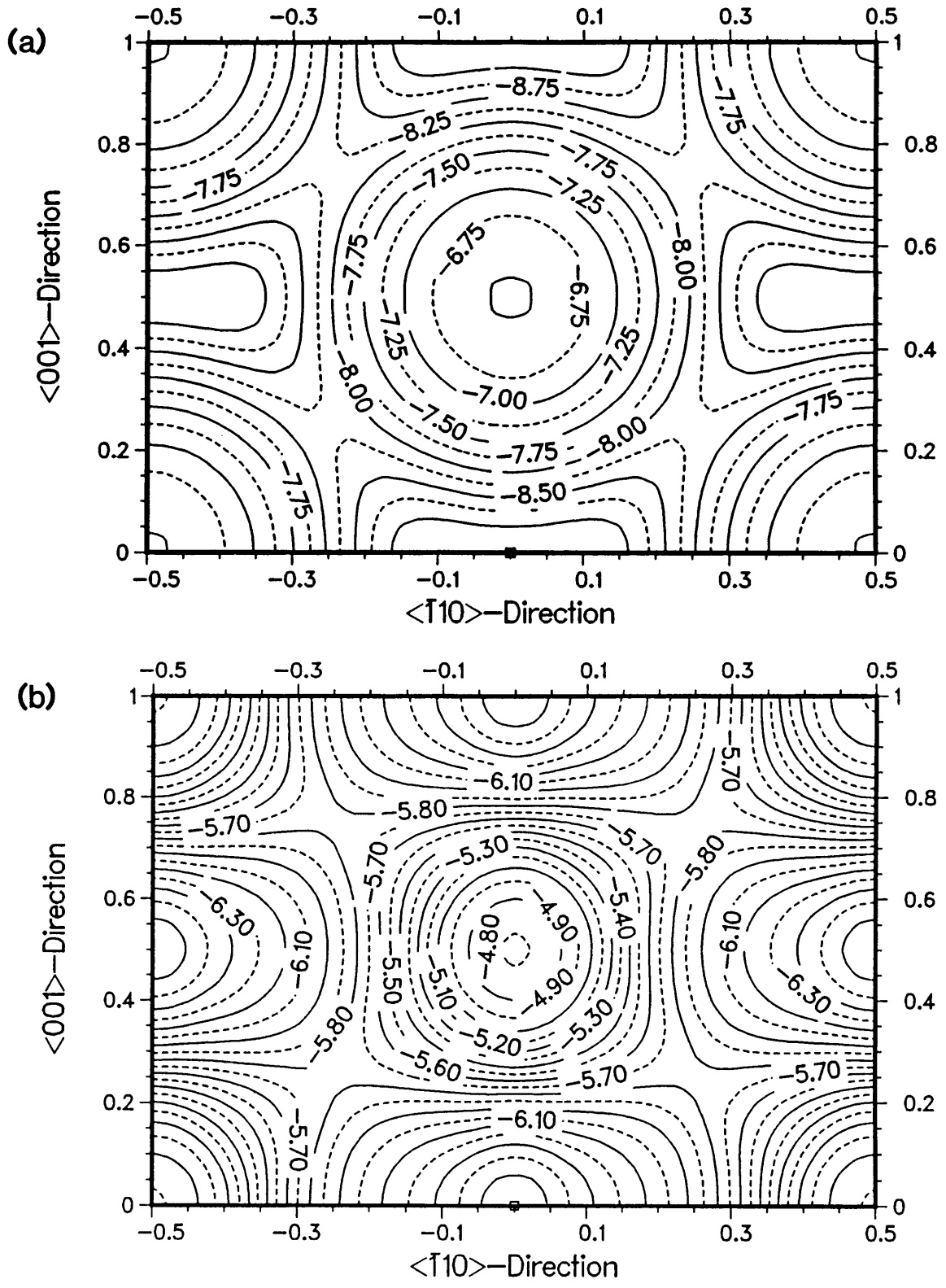

Figure 3.4 Contour plots of the self-adsorption energy E^*_{ads}(eV) (eqn. (2.5d)) of a tungsten adatom on a W {110} surface as calculated using the models of (a) Gollisch, (b) Johnson and Oh, (c) Finnis and Sinclair with Ackland and Thetford hard-core modification (FS-AT) and (d) the surface modified FS-AT model. Positions are expressed in terms of normalized rectangular unit cell sidelengths (Fig. 2.1).

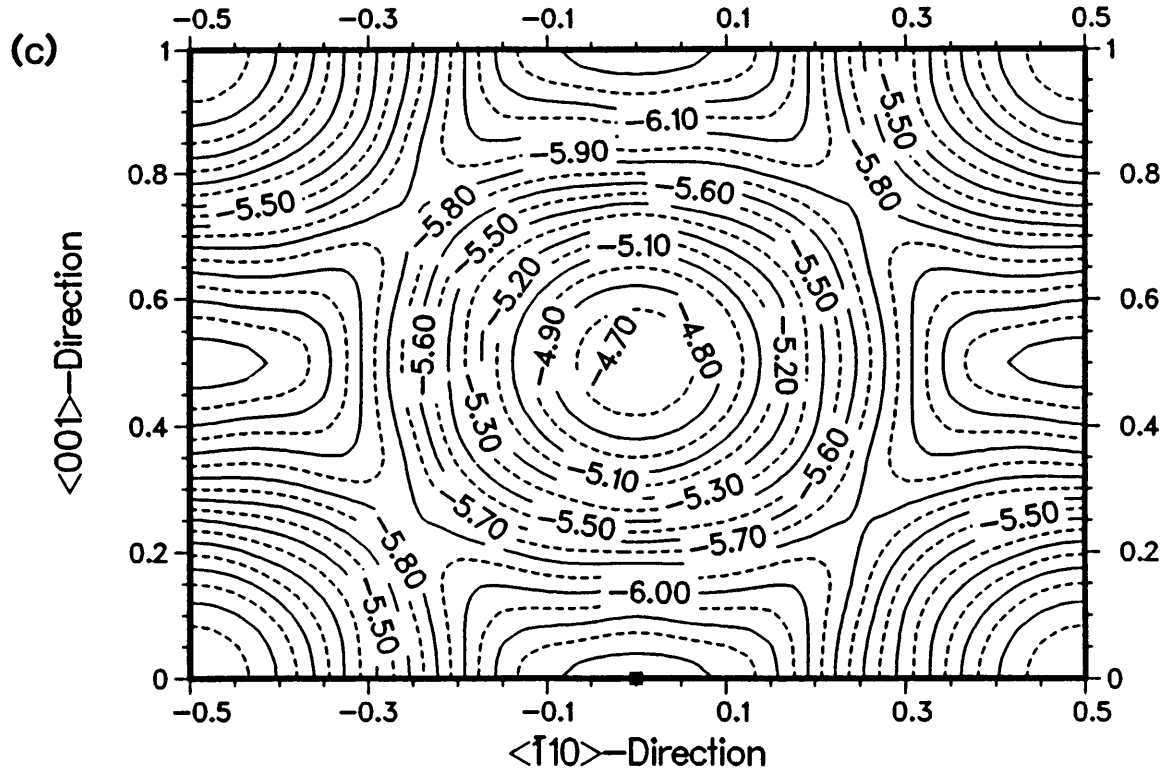

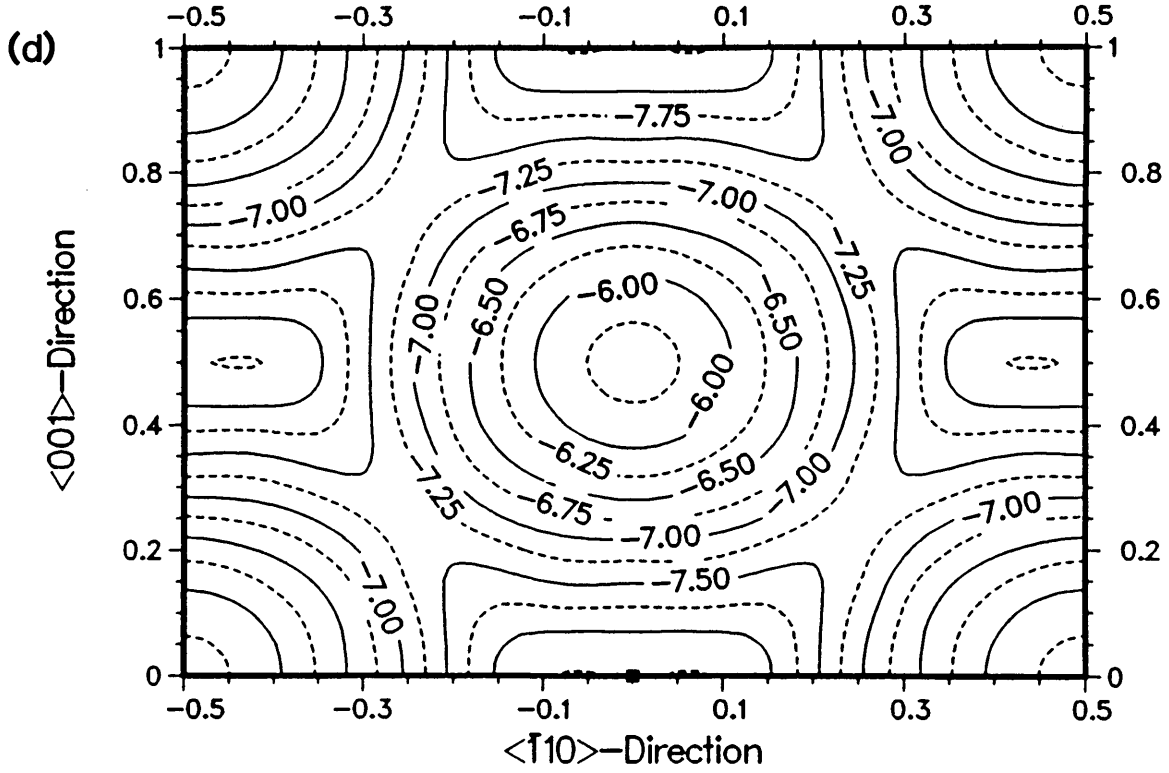

3.5 RESULTS

3.5.1 Potential surface $E(x,y,h_e)$

Three-dimensional representations of the adatom-substrate interaction potential (eqn. (2.5d)) – within the cell KLMN of Fig. 2.1 – for the FS-AT and surface modified FS-AT models respectively, are displayed in Figs. 3.3a and 3.3b.

Contour plots of the potential surfaces generated by the Gollisch (Fig. 3.4a) and surface modified FS-AT models (Fig. 3.4d) reveal two equivalent shallow local minima at sites ($\pm \Delta x,0$) (or equivalent positions) on either side of the adsorption site (AS) with $\Delta x \approx 0.09a_x$ and $0.0625a_x$ for the Gollisch and surface modified FS-AT potentials respectively. The depths of the local minima are 0.054 eV and 0.027 eV respectively. The FS-AT potential (Fig. 3.4c) and the potentials of Finnis and Sinclair and of Johnson and Oh (Fig. 3.4b) yield a single minimum at the adsorption site. It is interesting to note that a double well also appears in calculations with Lennard-Jones (6-12) pair potentials (Stoop 1977, and Neustadter and Bacigalupi 1967), but that the Morse potential displays a single minimum at the adsorption site.

Bauer (1984) has concluded from experiments that the absolute energy minimum on a W{110} surface is slightly displaced from the hollow site along the $\langle\bar{1}10\rangle$ direction. The double well phenomenon in the potential surfaces of the Gollisch and the surface modified FS-AT models thus supports the applicability of these models to W{110} surfaces.

3.5.2 Desorption and activation energies

Calculated values of the self-desorption energy E_{des}, the surface relaxation z_o and the activation energy Q for surface migration for the potential models under consideration are summarized in Table 3.1. The values of E_{des} and Q obtained from the pair potential models (Lennard-Jones and Morse) deviate by more than 20% from the experimental values of 8.2 eV (Plummer and Rhodin 1968) for E_{des} and from the average value of 0.89 eV (Tsong and Cowan 1979) for Q. For these pair potentials, the positive values of z_o indicate an outward relaxation of the top layer of the W {110} substrate surface, which is contrary to experiment (Jona 1978). As regards the N-body potentials, the Gollisch and the surface modified FS-AT models yield values of E_{des} within 12% of the empirical value. The values of Q calculated with the models of Gollisch and of Johnson and Oh, as well as the surface modified FS-AT potential, differ by less than 8% from the average experimental value of Q. For all the N-body potentials considered, the equilibrium binding distance of the tungsten adatom is therefore smaller than the interlayer spacing of the unrelaxed W {110} surface. In view of these results, N-body potentials constitute a definite improvement over pair potentials in the modelling of adsorption phenomena.

It is particularly encouraging that the surface modified fitting parameter A*, obtained by fitting to the empirical value of the activation energy Q for surface migration, also yields a value of the calculated desorption energy E_{des} which almost matches the empirical value (see Table 3.1). This is seen as evidence of the reliability of the approach and therefore also of its applicability to modelling adsorption phenomena.

3.5.3 Truncated Fourier representations

The adatom-substrate interaction potential (ASIP) data, needed for calculating the optimized Fourier coefficients in skew, as well as Cartesian axes, are obtained from eqn. (2.5d) with 1600 data points within the unit cell TEFG (see Fig. 2.1) for each of the G, JO, FS-AT and surface modified FS-AT models respectively.

The truncated Fourier series representation for the ASIP expressed in skew axes $x^{(1)}$, $x^{(2)}$ (see Fig. 2.1), with the origin at an adsorption site AS, is given by eqn. (2.1). The coefficients A_{hk} calculated from the data generated by the potential models under consideration are listed in Table 3.2. It is clear that $A_{hk} = A_{kh}$ and that $A_{h,-k} = A_{k,-h}$ in accordance with symmetry requirements and that the Fourier coefficients tend to zero with increasing harmonic order. As can be seen from the histograms in Fig. 3.5 the standard error $\delta_s^{(n)}$ (eqn. (2.9)), which provides a meaningful overall measure of the accuracy of the n-th order Fourier truncation, is reduced by more than 90%, 83% and 75% for the G, JO and surface modified FS-AT models respectively, when using a third order instead of a first order truncation.

The truncated Fourier series representation of the ASIP for bcc {110} symmetry expressed in Cartesian axes x,y (see Fig. 2.1), with the origin at an adsorption site AS is given by eqn. (2.2). The coefficients A_{hk} for the G, JO, FS-AT and surface modified FS-AT potentials are listed in Table 3.3. The coefficients tend rapidly to zero with increasing harmonic order, as is to be expected. The standard error $\delta_c^{(n)}$ as defined in eqn. (2.9), decreases by more than 94%, 83%, 80%, for the G, JO and surface modified FS-AT models respectively when using a sixth instead of a second order truncation (see Fig. 3.6). This is equivalent to using a third rather than a first order truncation in skew axes.

TABLE 3.2. Calculated Fourier coefficients A_{hk}[eV] in skew axes (eqn. 2.1)) showing the dependence on harmonic order n = |h| + |k|.

n	h,k	Gollisch	Johnson and Oh	FS-AT	Surface modified FS-AT
0	0,0	−7.81993	−5.73331	−5.58298	−7.0150
1	1,0	−0.35865	−0.23912	−0.23456	−0.33191
	0,1	−0.35865	−0.23912	−0.23456	−0.33191
2	2,0	−0.04690	0.00423	−0.01678	−0.03055
	1,1	−0.07455	−0.02690	−0.00596	−0.01785
	1,−1	0.16000	0.06840	0.06818	0.09961
	0,2	−0.04690	0.00423	−0.01678	−0.03055
3	3,0	−0.00527	−0.00004	−0.00515	−0.00689
	2,1	−0.01653	0.00852	−0.00078	−0.00661
	1,2	−0.01653	0.00852	−0.00078	−0.00661
	2,−1	0.04478	−0.01631	0.01150	0.02667
	1,−2	0.04478	−0.01631	0.01150	0.02667
	0,3	−0.00527	−0.00004	−0.00515	−0.00689
4	4,0	−0.00071	−0.00057	−0.00011	0.00053
	1,3	−0.00386	−0.00031	−0.00244	−0.00413
	3,1	−0.00386	−0.00031	−0.00244	−0.00413
	3,−1	0.01128	−0.00638	0.00663	0.01484
	1,−3	0.01128	−0.00638	0.00663	0.01484
	2,2	−0.00590	0.00337	−0.00230	−0.00729
	2,−2	−0.00063	0.00650	−0.00095	0.00113
	0,4	−0.00071	−0.00057	−0.00011	0.00053

TABLE 3.3. Calculated Fourier coefficients A_{hk}[eV] in Cartesian axes (eqn. 2.2)) showing the dependence on harmonic order n = |h| + |k|. The Fourier coefficients A_{hk}[eV] calculated with the FS-AT model for a tungsten adatom forming part of a monolayer adsorbed on a W {110} substrate are listed in the last column.

n	h,k	Gollisch	Johnson and Oh	FS-AT	Surf. mod. FS-AT	FS-AT (monolayer)
0	0,0	-3.90997	-2.86666	-2.79149	-3.50752	-1.01945
2	2,0	0.16000	0.06839	0.06818	0.09961	0.03708
	1,1	-0.71731	-0.47825	-0.46912	-0.66382	-0.29807
	0,2	-0.07455	-0.02690	-0.00596	-0.01785	-0.00235
4	4,0	-0.00063	-0.00650	-0.00095	0.00113	-0.00145
	3,1	0.08954	-0.03262	0.02300	0.05335	0.00087
	2,2	-0.09381	-0.00847	-0.03356	-0.06109	-0.01287
	1,3	-0.03306	0.01704	-0.00155	-0.01323	0.00569
	0,4	-0.00590	0.00337	-0.00230	-0.00729	0.00180
6	6,0	-0.00107	-0.00186	-0.00186	-0.00194	-0.00131
	5,1	-0.00556	-0.00280	-0.00790	-0.00948	-0.00475
	4,2	0.02255	-0.01276	0.01325	0.02969	-0.00206
	3,3	-0.01055	-0.00009	-0.01029	-0.01378	-0.00571
	2,4	-0.00772	-0.00062	-0.00488	-0.00826	-0.00133
	1,5	-0.00337	-0.00289	-0.00568	-0.00851	-0.00221
	0,6	-0.00027	-0.00093	-0.00252	-0.00230	-0.00212
8	8,0	0.00010	-0.00057	-0.00066	-0.00068	-0.00045
	7,1	-0.00024	-0.00142	-0.00116	-0.00094	-0.00076
	6,2	-0.00372	-0.00312	-0.00643	-0.00705	-0.00435
	5,3	0.00586	0.00518	0.01170	0.01520	0.00643
	4,4	-0.00142	-0.00113	-0.00022	0.00106	-0.00172
	3,5	-0.00141	-0.00066	-0.00042	-0.00007	-0.00115
	2,6	-0.00071	0.00004	-0.00094	-0.00080	-0.00113
	1,7	-0.00484	0.00095	-0.00030	0.00027	-0.00116
	0,8	-0.00018	0.00037	0.00061	0.00059	0.00015

TABLE 3.4. Normalized Fourier coefficients A_i in a truncated representation of the interaction potential of a tungsten adatom on W {110} as given by eqn. (3.16). V(0,0) is the value of the potential at the origin as calculated with eqn. (3.16). W_0 is the bonding parameter, constituting an overall scale factor in eqn. (3.16). The normalized Fourier coefficients in a truncated representation of the interaction potential of a tungsten atom in a monolayer adsorbed on W {110}, as calculated with the FS-AT model, are listed in the last row.

Model	A_1	A_2	A_3	A_4	V(0,0) [eV]	W_0 [eV]
Van der Merwe	−0.4	−0.4	−0.12	−0.08	0	–
Gollisch	−0.5237	−0.5237	0.2336	−0.1089	0.1060	1.36976
Johnson and Oh	−0.5116	−0.5116	0.1463	−0.0576	0.0614	0.93488
FS-AT	−0.5371	−0.5371	0.1561	−0.0137	0.0597	0.87352
Surface modified FS-AT	−0.5434	−0.5434	0.1631	−0.0292	0.0574	1.22156
FS-AT (Monolayer)	−0.5078	−0.5078	0.1263	−0.0080	0.0602	0.5869

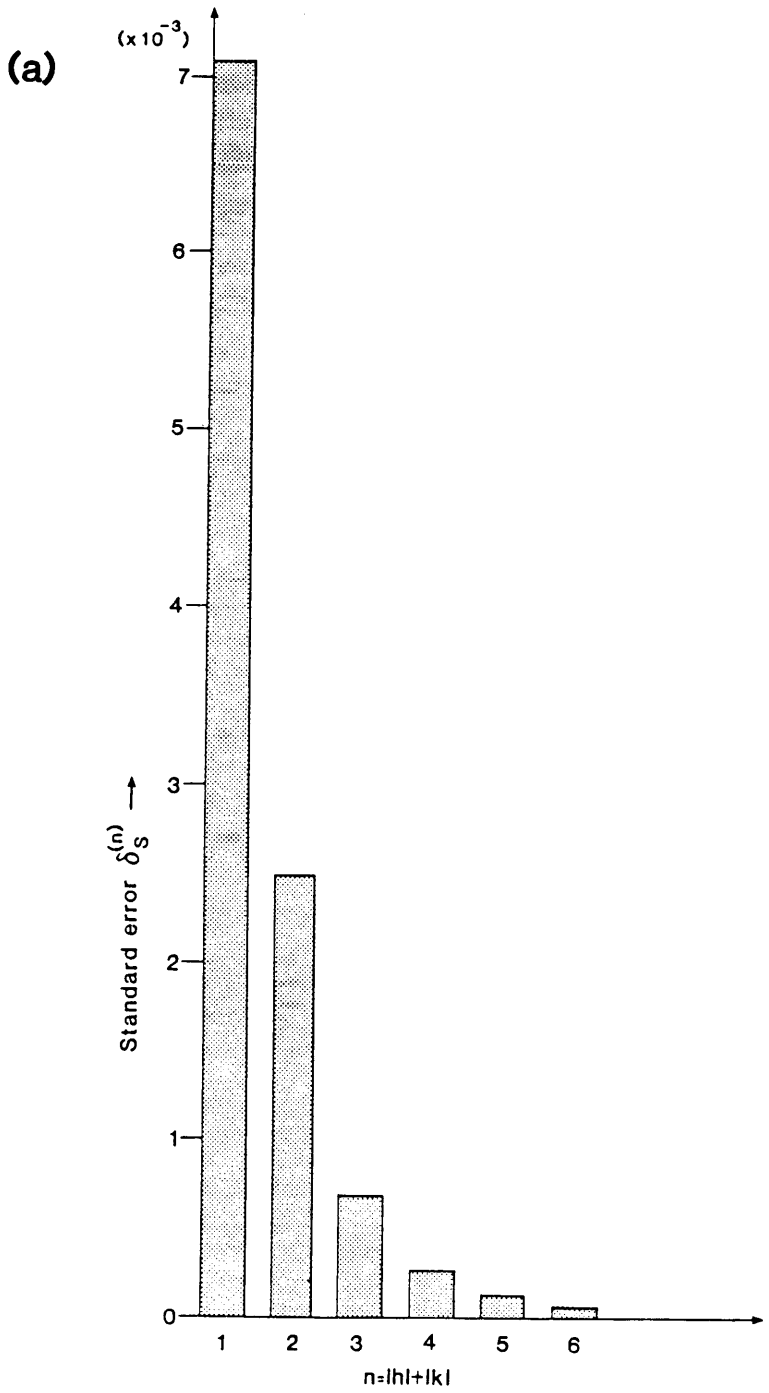

Figure 3.5 Histograms displaying the dependence of the standard error $\delta_S^{(n)}$ (eqn. (2.9)) on the order n of Fourier truncation of the adatom-substrate interaction potential expressed in skew axes for (a) the Gollisch, (b) the Johnson and Oh, and (c) the surface modified FS-AT potential models.

(b)

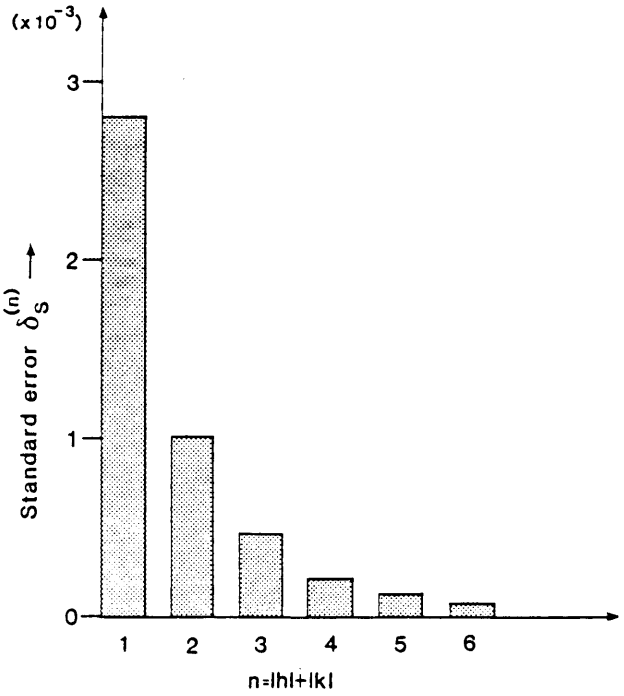

(c)

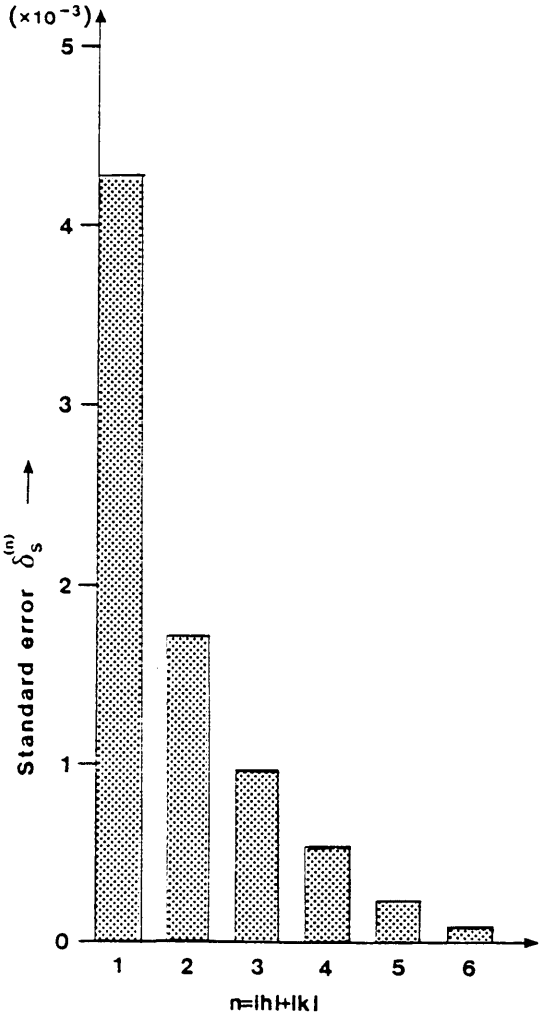

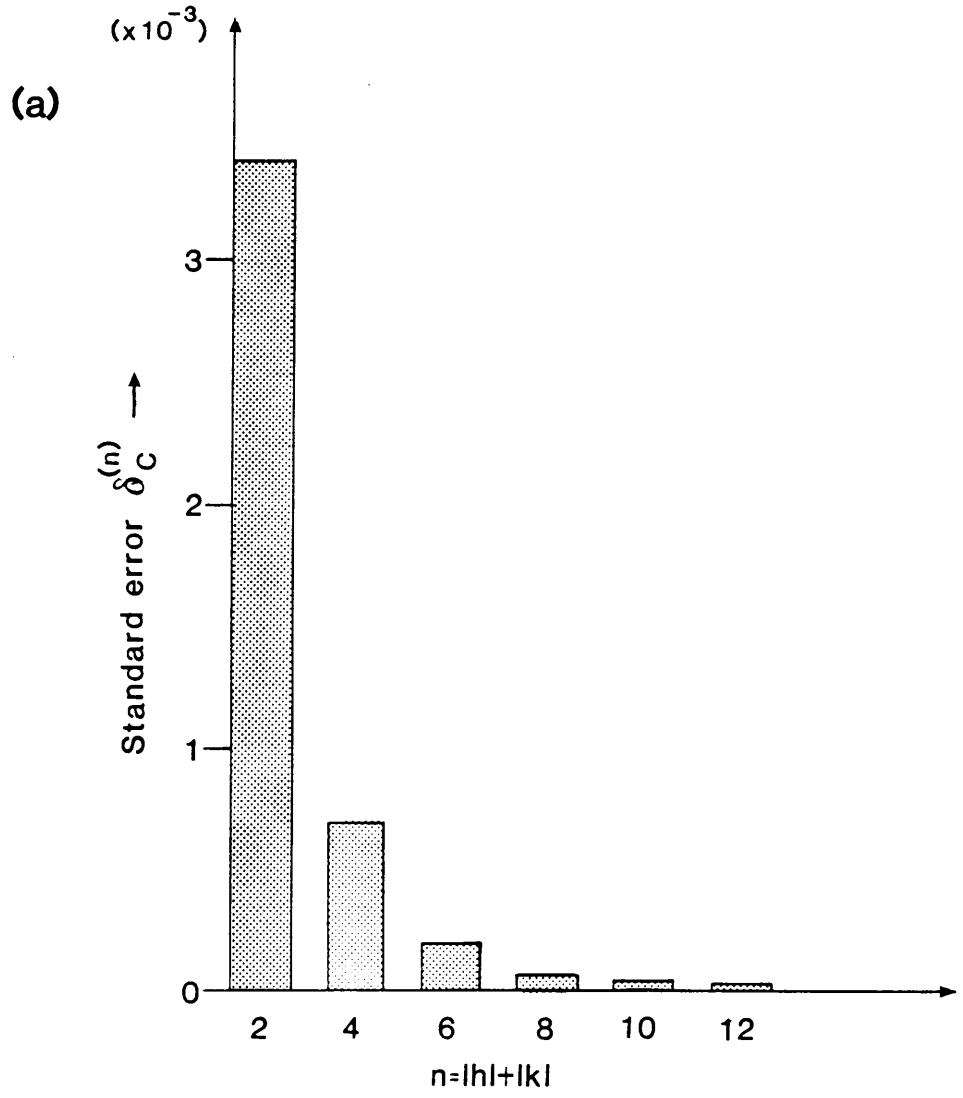

Figure 3.6 Histograms displaying the dependence of the standard error δ_C^n (eqn. (2.9)) on the order n of truncation of the Fourier series representation of the adatom-substrate interaction potential expressed in Cartesian axes for (a) the Gollish, (b) the Johnson and Oh, and (c) the surface modified FS-AT potential models.

(b)

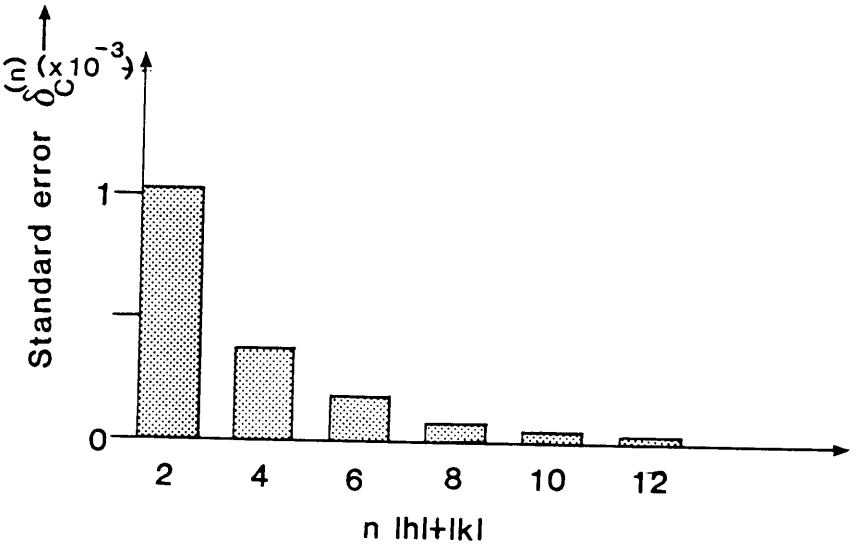

(c)

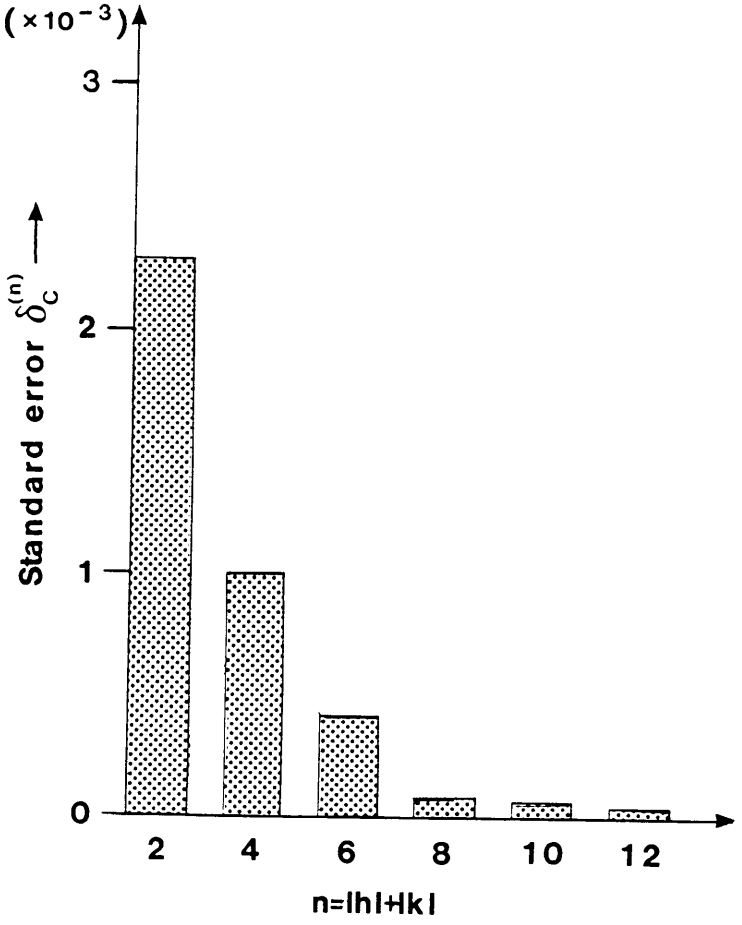

In Table 3.4 the normalized values of the coefficients, as previously determined by van der Merwe (1984) on a qualitative basis are compared with those obtained using the N-body potentials. Here the potential energy at an adsorption site is taken as zero. The truncated Fourier series representation suggested by van der Merwe is given by

$$V(x,y) = W_0\{1 + A_1\cos[2\pi(\frac{x}{a_x} + \frac{y}{a_y})] + A_2\cos[2\pi(-\frac{x}{a_x} + \frac{y}{a_y})]$$

$$+ A_3\cos(4\pi\frac{x}{a_x}) + A_4\cos(4\pi\frac{y}{a_y})\}. \qquad (3.16)$$

W_0 is an overall scale factor, or bonding parameter, which is approximately proportional to the self-desorption energy for bcc {110} surfaces. There is reasonable agreement between the calculated values of the Fourier coefficients and the proposed values of van der Merwe. The coefficients obtained by using the JO and the surface modified FS-AT potential data, give the best approximation to the zero potential energy at an adsorption site.

3.5.4 Force constants

The double well in the adatom potential energy surface of both the Gollisch and the surface modified FS-AT models has interesting implications for the force constants k and corresponding adatom vibration frquencies ν. It is significant in the case of these potentials that the two minima are respectively only 0.054 eV and 0.027 eV deep as compared to the saddle point heights of respectively 0.9529 eV and 0.8724 eV. The minima are situated along the x-direction about 0.4049Å and 0.2798Å respectively on either side of the hollow site. Different force constants feature in different substrate temperature (T_s) regions, as determined by the Arrhenius relationship between energy barrier heights and T_s.

With T_s low enough, i.e. $k_B T_{s1}$ much smaller than the depth of the local minima, the adatom performs small amplitude vibrations (frequency ν_{x1}) and practically stays localized in one of the minima. At this stage the value of the force constant is determined by the curvature of the minimum and the force constants $k_x^{(f)}$ and $k_y^{(f)}$, calculated with finite difference techniques (e.g. eqn. (2.7)), apply in this temperature range. For the FS-AT and the J0 potentials, the force constants $k_x^{(f)(0,0)}$ and $k_y^{(f)(0,0)}$ are calculated at the adsorption or hollow site. Due to the presence of the double well in their respective potential surfaces, $k_x^{(f)(0,0)}$ cannot be calculated likewise for the G- and surface modified FS-AT models. A force constant $k_x^{(f)min}$ at the approximate position of the local minimum can however be calculated. The shape of the potential surfaces permits $k_y^{(f)(0,0)}$ to be calculated for all the potential models under consideration. For the calculation of $k_x^{(f)(0,0)}$ and $k_x^{(f)min}$ $\bar{\delta}$ was taken as $0.0125a_x$ in all cases, except in the case of the G potential where $\bar{\delta}$ was taken to be $0.009375a_x$ due to the flatness of the potential curve at the minimum. For all potentials under consideration, $\bar{\delta} = 0.0125a_y$ was taken in the calculation of $k_y^{(f)(0,0)}$ and $k_y^{(f)min}$.

If T_s is increased, a value T_{s2} will be reached where the thermal fluctuations will carry the adatom across the barrier between the two minima and the adatom will spend more or less equal time intervals in each of them. An observation such as that of Bauer (1984) will then position the adatom asymmetrically with respect to the hollow site. At a much higher temperature T_{s3}, the adatom will "see" little of the double well, vibrate with frequencies ν_{x3} and ν_{y3}, and thermal fluctuations may carry it across the saddle point to a neighbouring hollow site. This is where adatom surface migration sets in. It is suggested that if a parabola is

fitted to the lower half of the potential energy curve around an adsorption site AS, it will yield a fair representation of the vibration frequencies ν_{x3} and ν_{y3} operating at these higher temperatures. In the case of potentials with a double minimum, as well as those with a single minimum at the AS, "effective" force constants $k_x^{(p)}$ and $k_y^{(p)}$ were calculated from parabolas fitted to the trace of cuts through the energy surface by a "vertical" plane along the $\langle\bar{1}10\rangle$- and $\langle 001\rangle$ directions respectively.

The vibrations normal to the surface with frequency ν_z, are present at all temperatures and become significant when T_s is high enough to effect desorption. The force constant $k_z^{(f)(0,0)}$ at the hollow site was calculated for all potentials under consideration, using the finite difference method of eqn. (2.7). For the potentials exhibiting the double well phenomenon, an additional force constant $k_z^{(f)min}$ was calculated at the approximate position of the local minimum. Here $\bar{\delta}$ was taken as 0.0025Å, except in the case of the G potential where it was taken as 0.005Å due to the flatness of the curve. With $\bar{\delta}$ = 0.005Å, the JO and FS potential models, yield values of 12.2070 eV/Å^2 and 12.2074 eV/Å^2 respectively for $k_z^{(f)(0,0)}$. In the case of the G potential it was found that $k_z^{(f)(0,0)}$ = 19.531 eV/Å^2. The corresponding values obtained using the surface modified FS-AT data are 19.53 eV/Å^2 and 21.97 eV/Å^2, respectively. This corresponds to values of between $4.02 \times 10^{10} s^{-1}$ and $4.27 \times 10^{10} s^{-1}$ for the vibration frquency as given by eqn. (2.6). All the calculated force constants and vibration frequencies are listed in Table 3.5.

It should be noted that the cutoff scheme in the JO potential does not seem to have an influence on the values of the force constants. Calculations with a cutoff scheme where r_s = 3.230294Å and r_c = 4.375000Å, yielded values of $k_x^{(f)(0,0)}$, $k_y^{(f)(0,0)}$ and $k_z^{(f)(0,0)}$ equal to those tabulated for

TABLE 3.5. Force constants $k_i[eV/Å^2]$ and corresponding vibration frequencies $\nu_i[s^{-1}]$ for lateral and normal vibrations of the adsorbed atom. The super scripts (f)(0,0), (f)min and (p) pertain to force constants calculated at the origin with a finite difference technique, calculated at the position of the absolute minimum with a finite difference technique and calculated by fitting a parabola over the lower half of the potential energy curve respectively.

Model	Gollisch	Johnson and Oh	FS	FS-AT	Surface modified FS-AT
$k_x^{(f)(0,0)}$	–	3.09	0.58	0.86	–
ν_{x1}	–	1.60×10^{10}	0.69×10^{10}	0.84×10^{10}	–
$k_x^{(f)min}$	2.366	–	–	–	2.37
ν_{x1}	1.40×10^{10}	–	–	–	1.40×10^{10}
$k_x^{(p)}$	1.825	1.07	1.31	1.36	1.98
ν_{x3}	1.23×10^{10}	0.94×10^{10}	1.04×10^{10}	1.06×10^{10}	1.28×10^{10}
$k_y^{(f)(0,0)}$	15.656	3.71	6.28	7.82	10.31
ν_{y1}	3.60×10^{10}	1.75×10^{10}	2.28×10^{10}	2.55×10^{10}	2.92×10^{10}
$k_y^{(f)min}$	13.151	–	–	–	12.48
ν_{y1}	3.30×10^{10}	–	–	–	3.22×10^{10}
$k_y^{(p)}$	6.457	3.64	3.14	3.41	4.83
ν_{y3}	2.31×10^{10}	1.74×10^{10}	1.61×10^{10}	1.68×10^{10}	2.00×10^{10}
$k_z^{f(0,0)}$	19.531	9.77	9.77	14.65	19.53
ν_z	4.02×10^{10}	2.85×10^{10}	2.85×10^{10}	3.49×10^{10}	4.02×10^{10}
$k_z^{(f)min}$	19.531	–	–	–	21.97
ν_z	4.02×10^{10}	–	–	–	4.27×10^{10}

the cutoff scheme with r_s = 3.295838Å and r_c = 4.399598Å, even though the former scheme yielded a value of only 0.7568 eV for the activation energy Q for surface migration.

The force constants k_x and k_y may also be calculated as second order derivates from the truncated Fourier series. However, since the orders are weighted quadratically in this procedure, it turns out that truncations at rather high orders are needed for convergence. It is suggested that the coefficients of the higher order terms are more adversely effected than the lower order ones by the inevitable inaccuracies in the adopted parameterized potential representation.

The force constant $k_y^{(n)}$ as calculated from the n-th order truncation is given by eqn. (2.8b). The dependence of $k_y^{(n)}$ on the order of truncation for the G, J0 and surface modified FS-AT potentials is illustrated in Figs. 3.7a, b and c. The oscillating nature of the curves in Figs. 3.7b and 3.7c reflects the fact that $k_y^{(n)}$ is defined as a second order derivative and hence that the j-th harmonic order terms are weighted as j^2. The force constant $k_x^{(n)}$ as calculated from the n-th order truncation in eqn. (2.2), is given by eqn. (2.8a). The value of $k_x^{(n)}$ at the origin (0,0) can only be determined for a model with a potential surface displaying a true minimum at the AS. The dependence of $k_x^{(n)}$ on the order of truncation for the J0 potential is illustrated in Fig. 3.7b.

Fig. 3.7a shows that, with increasing n, the force constant $k_y^{(n)}$ for the G potential tends to a constant value. The value of $k_y^{(12)}$ differs only by approximately 2.5% from $k_y^{(f)(0,0)}$ calculated using a finite difference approximation. The oscillating curve in Fig. 3.7b indicates that for the J0 model the difference between $k_y^{(10)}$ and $k_n^{(f)(0,0)}$ is a minimum, *viz.* 0.034 eV/Å^2, i.e. n = 10 seems to be an optimum truncation value; for

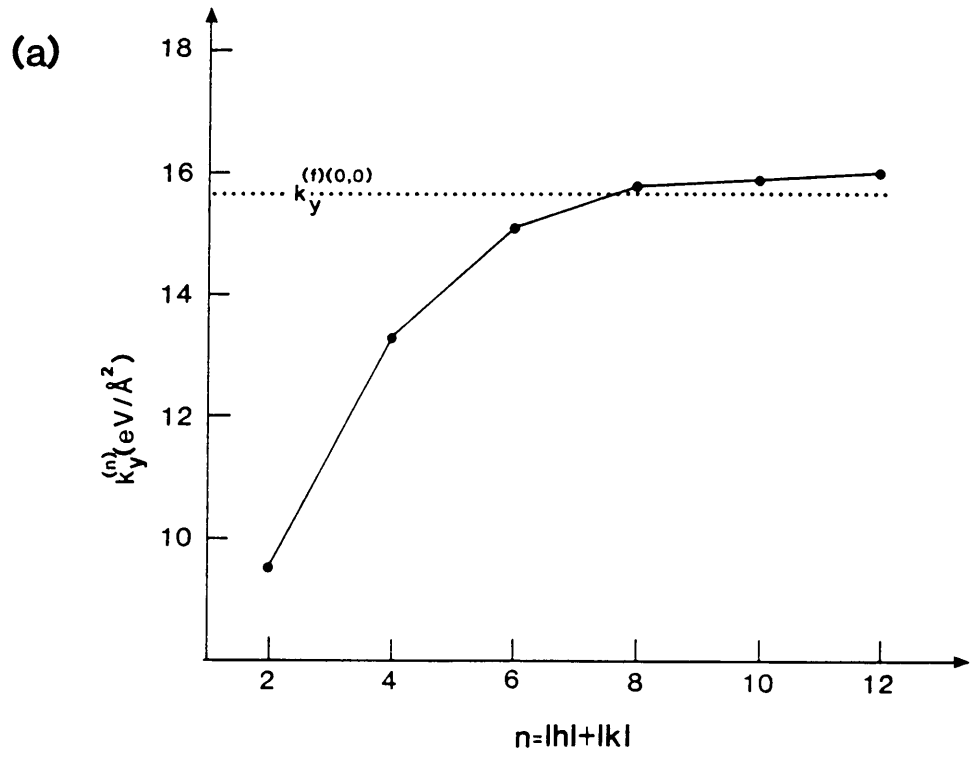

Figure 3.7 Dependence of the force constant $k_y^{(n)}$ (eqn. (2.8b)), calculated from the Fourier truncation, on the order n of truncation for (a) the Gollisch, (b) the Johnson and Oh and (c) the surface modified FS-AT potentials respectively. The superscripts (f)(0,0) and (f)(min) respectively pertain to force constants calculated at the origin with a finite difference technique and force constants calculated at the position of the absolute minimum with a finite difference technique. In Fig. 3.7c $k_y^{(f)(0,0)*}$ represents the value of a force constant calculated for the FS-AT model. The dependence of $k_x^{(n)}$ on the order of truncation for the potential of Johnson and Oh is illustrated in Fig. 3.7b.

(b)

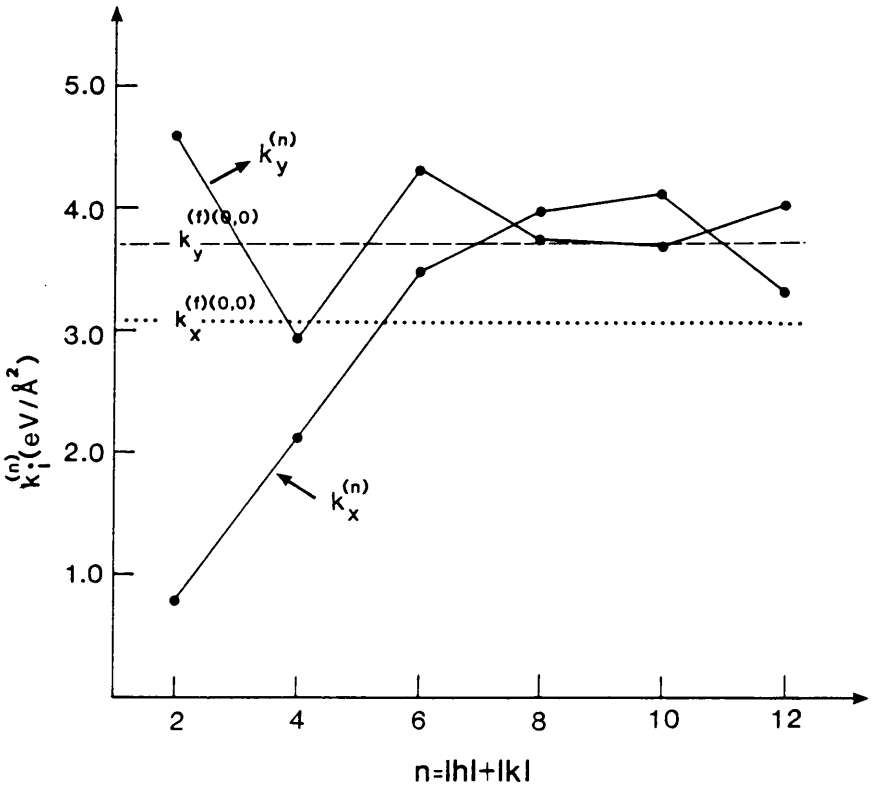

(c)

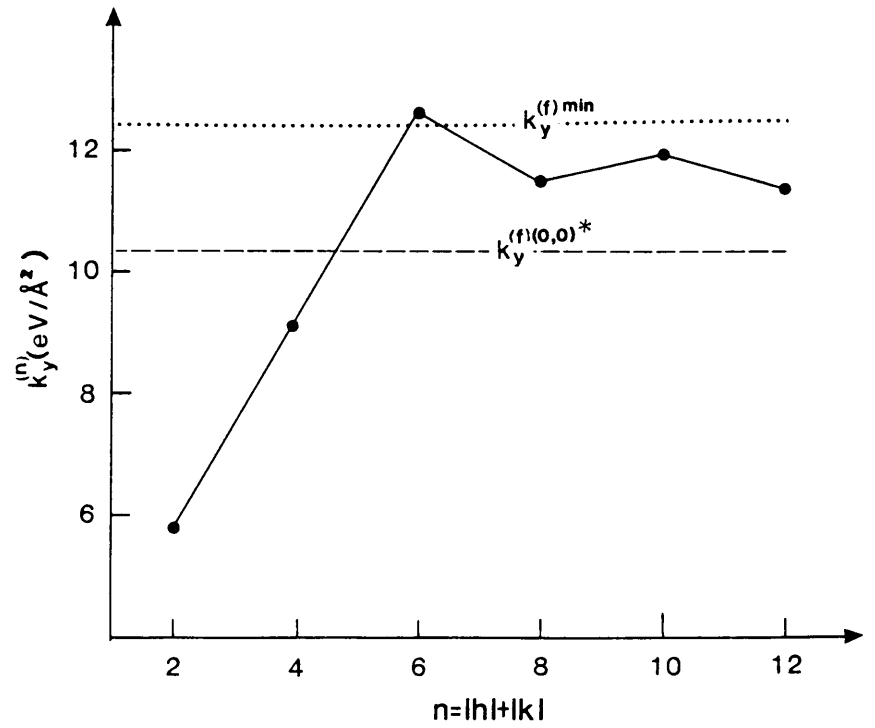

$n > 10$ the deviation increases. For the surface modified FS-AT model (Fig. 3.7c) the optimum value of n will be higher due to the ripple in the potential surface caused by the presence of the double well. Here $k_y^{(12)}$ differs by less than 11.1% from the values of $k_y^{(f)(0,0)} = 10.31$ eV/Å^2 obtained by the finite difference technique.

The calculation of the lateral force constants $k_i^{(n)}$ as second order derivatives from the Fourier series truncated at order n is not recommended, since it requires a truncation at high harmonic order and these high order coefficients are less reliable because of imperfect potential modelling.

3.5.5 Equilibrium height surface $h_e(x,y)$

Figs. 3.8a, b, c and d are contour plots of the equilibrium (height) surface h_e for the potentials under consideration. It is significant that a double minimum appears in the equilibrium height surfaces of all the models, including the FS-AT and JO models, even though their potential surfaces have single minima at the adsorption sites. At the adsorption site the equilibrium heights h_e are 1.68486Å, 2.15715Å, 2.1175Å and 2.02971Å respectively for the G, JO, FS-AT and surface modified FS-AT potentials respectively. For all potentials h_e at the adsorption site is smaller than the bulk interlayer spacing. The corresponding values of h_e at the top of a substrate surface atom is 2.22854Å, 2.53806Å, 2.50126Å and 2.44914Å respectively. Only the G potential yields a value of h_e at the top site smaller than the bulk interlayer spacing. The value of h_e at the double well minima of the G and surface modified FS-AT potential models differ by less than 0.5% and 1.6% respectively from the value at the adsorption site.

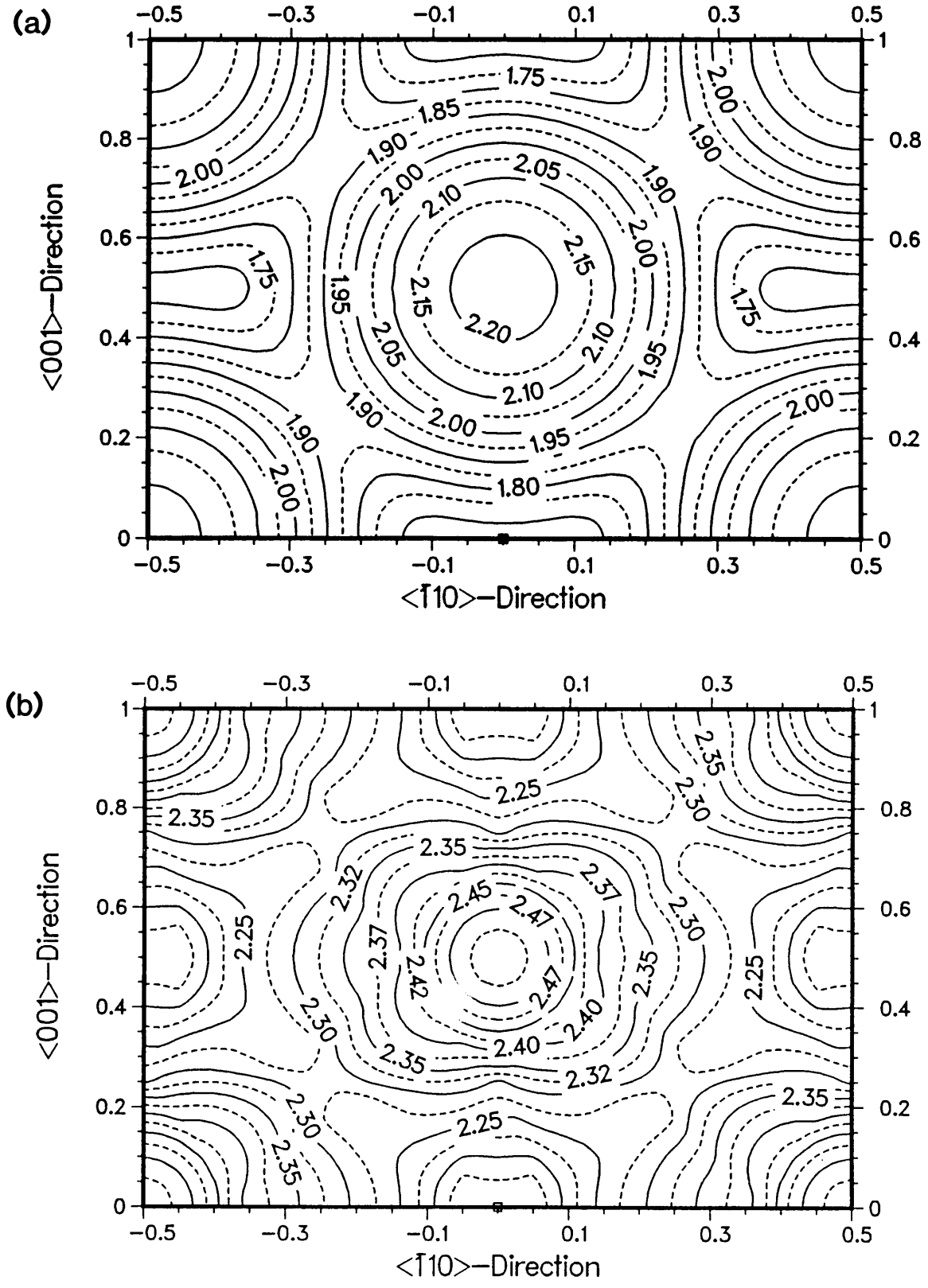

Figure 3.8 Contour plots of the equilibrium height h_e of a tungsten adatom on a W {110} surface as calculated using (a) the Gollisch, (b) the Johnson and Oh, (c) the FS-AT and (d) the surface modified FS-AT models respectively. Positions are expressed in terms of normalized rectangular unit cell sidelengths (Fig. 2.1).

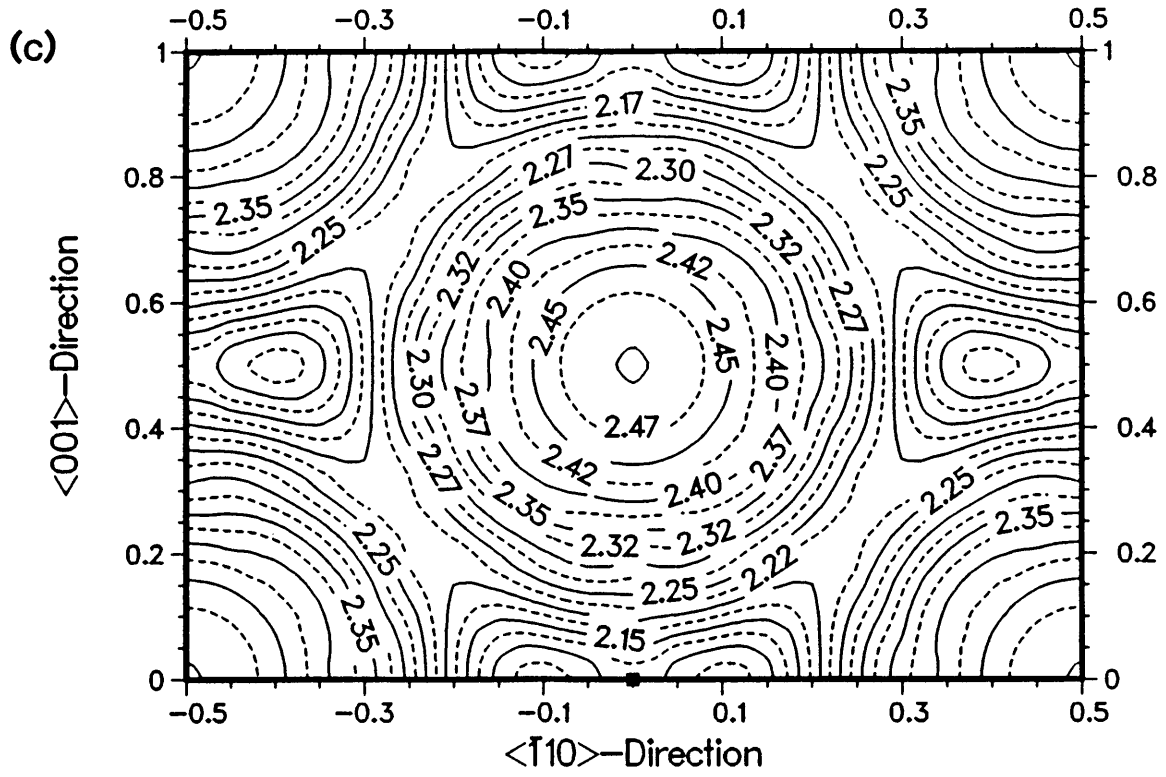

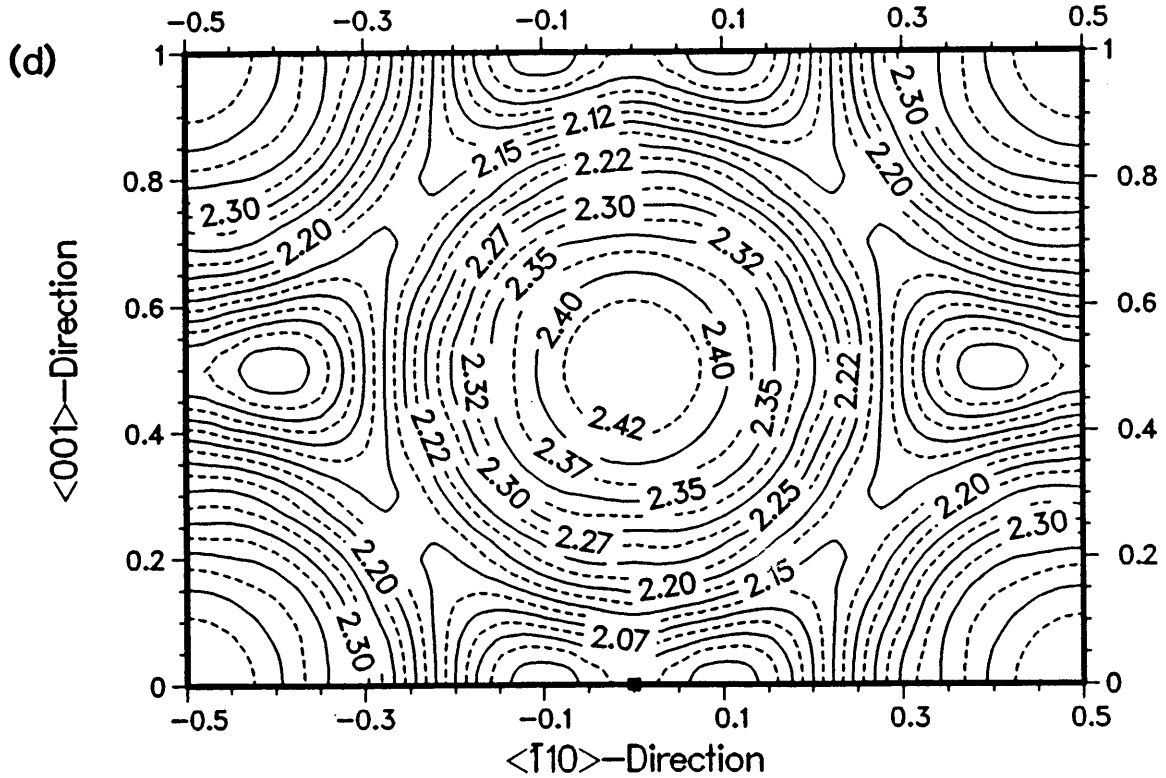

There seems to be general consensus that the outer layer of a clean W {110} surface does not reconstruct significantly (Buchholz *et al.* 1975, and Van Hove and Tong 1976) by lateral rearrangement of its atoms, despite the possibility that the uppermost tungsten atoms may settle into sites of higher coordination number. However, single adatoms and dimers do seem to settle into positions with maximum coordination, where the adsorbed atoms have three nearest neighbours instead of two, as in the lattice site. Such positions are slightly displaced from the adsorption site along the $(\bar{1}10)$ direction (Ehrlich 1977 and Bauer 1984). This tendency is reflected in the displaced minima appearing in the equilibrium height surfaces of the N-body potentials under consideration.

3.6 TUNGSTEN MONOLAYER ON W {110}

In the foregoing sections the Fourier coefficients of the interaction of an isolated adatom with a crystalline substrate have been calculated by employing N-body potentials to ensure that environmental effects are incorporated realistically. However, in epitaxial systems the adsorbed atom usually forms part of a monolayer (see Appendix C). In the case where the interatomic interaction can be approximated by a pair potential, the Fourier coefficients calculated for a single atom is just as relevant to an adatom forming part of a monolayer. If N-body potentials are used to model the interaction, the interaction energy of the adsorbed atom with the substrate, and hence also the values of the Fourier coefficients in a Fourier representation of the adatom-substrate interaction potential, are changed by the presence of the other atoms in the monolayer. It is therefore important to determine to what extent the values of the Fourier

coefficients calculated for an adatom forming part of a monolayer, deviate from that of a single adatom.

In this case the simplest possible system has been considered, *viz.* an adatom forming part of a rigid infinite monolayer, consisting of the same kind of atoms as the substrate and in complete registry with the substrate. The predictions are evidently also good approximations for finite but large monolayer islands. Due to the symmetry of the system, it is useful to employ periodic boundary conditions in order to limit the computational effort.

Calculations have thus been carried out for a tungsten monolayer on a W {110} surface. The FS-AT potential has been used to model the atomic interaction. Data for the calculation of the Fourier coefficients in a Cartesian representation (eqn. (2.1)) for the interaction energy of an adatom in the rigid monolayer with the substrate was obtained by minimizing the adatom-substrate interaction potential with respect to z for each position $(x_i^{(1)},x_j^{(2)})$ in the surface unit cell TEFG (see Fig. 2.1). The results are listed in the last column of Table 3.3.

The normalised Fourier coefficients pertaining to the truncated representation (eqn. (3.16)) suggested by van der Merwe, are listed in the first row of Table 3.4. The values of the normalized Fourier coefficients for a single adatom and an atom forming part of a monolayer (cf. last row of Table 3.4) are very similar and it can be concluded that the relative values of the Fourier coefficients are primarily determined by the symmetry of the substrate. The bonding parameter W_0, constituting an overall scale factor, is diminished by about 33% by the presence of the surrounding monolayer atoms. The desorption energy per monolayer atom E_{des} = 2.6258 eV was found to be about 3.83 eV lower than the desorption energy E_{des} of an

isolated tungsten adatom. The activation energy Q for "rigid" monolayer migration at 0.4841 eV is also lower than the corresponding adatom value of 0.6464 eV. The relaxation z_0 (defined as the deviation of the equilibrium height h_e from the bulk interlayer spacing) is only −0.0252Å, as compared to the value of −0.1206Å for an isolated adatom.

3.7 SUMMARY AND DISCUSSION

The many-body potentials introduced by Gollisch, by Johnson and Oh and by Finnis and Sinclair have been used to calculate a number of self-adsorption parameters. The Finnis and Sinclair model has been modified somewhat for application to adsorption. In the surface modified FS-AT model, an additional parameter, fitted to the experimental value of the adatom-surface migration energy Q was introduced, leaving the fitting parameters obtained from bulk properties unaltered.

It was found that all the N-body potentials under consideration yielded more realistic values of the desorption energy, activation energy for surface migration and substrate adatom equilibrium height, than the conventional Morse and Lennard-Jones pair potentials. The N-body potentials also suggest a slight contraction of the free W {110} surface in agreement with experimental data, whereas the Morse and Lennard-Jones pair potentials suggest an expansion. This confirms the superiority of N-body potentials over pair potentials for calculations at surfaces where environmental effects are important.

The models proposed by Gollisch, by Johnson and Oh and the surface modified FS-AT potential, yielded values of the activation energy for surface migration well within the experimental limits, whereas the model of Finnis and Sinclair predicts a value of Q about 0.23 eV below the lowest

empirical value of Q. The value of the desorption energy calculated with the surface modified FS-AT and G potentials deviated by less than 12% from the empirical value of this parameter.

The potential surfaces of the Gollisch and surface modified FS-AT models display the double well phenomenon in support of the observations of Bauer. This is seen as additional justification of their suitability for application to W {110} surfaces.

The optimum coefficients of the two-dimensional truncated Fourier series representations of the adatom-substrate interaction potential in skew, as well as in Cartesian axes, were calculated for the various EAM-models. In all cases the values of the coefficients decay fairly rapidly with harmonic order. While it is true that the calculated higher order Fourier coefficients have to be treated with circumspection and are normally unreliable because of the inadequacy of the potential model, it is fortunate that many important surface phenomena depend primarily on lower order terms which are believed to be sufficiently accurate.

At present the main practical application of these Fourier coefficients is in the field of epitaxy. Such systems in practice differ significantly from the simple models considered in this study; the adsorbate in the former is usually part of a monolayer or multilayer and the adsorbate and substrate materials are usually also different. In Chapter 4 the present calculations are extended to a system consisting of differing materials *viz.* a tantalum adatom adsorbed on a W {110} substrate.

With respect to the calculated force constants for normal and lateral vibrations, the potentials under consideration fall into two categories – those displaying a double well in the potential surface, *viz.* the G and surface modified FS-AT models, and those with a single minimum at the

adsorption site, *viz.* the FS, FS-AT and JO potentials. The values of the force constants calculated with the G and surface modified FS-AT models, correlate with one another. The calculated values of E_{des} are also in good agreement with experiment (8.2 eV). A similar correspondence is observed for the FS, FS-AT and JO potentials with values of E_{des} ranging between 6.4 eV and 6.7 eV. The calculated values of the force constants, relevant to low temperatures, are clearly very sensitive to the precise form of the potential energy curve in the vicinity of the minimum. The existence of a double well introduces a degeneracy into the lateral force constants and the appropriate force constant has to be selected according to the prevailing substrate temperature. The calculation of lateral force constants as second order derivatives from truncated Fourier series is not recommended since it requires truncation at high harmonic order and higher order coefficients are less reliable because of imperfect potential modelling.

Although the G and surface modified FS-AT models seem to be the most suitable surface potentials, the former predicts an unrealistically large relaxation of the W {110} surface and the latter has the disadvantage of being a hybrid model.

A desirable feature of the JO potential is that it predicts inward relaxation of less than 4% for the W {110} surface. The behavior of this potential with respect to the calculated self-desorption energy may perhaps be improved by careful adjustment of the fitting parameters.

FS-AT calculations for an adatom forming part of a monolayer show that the relative values of the coefficients in a Fourier representation of the adatom-substrate interaction potential are primarily determined by the symmetry of the substrate, but that the bonding parameter, representing an

overall scale factor, is significantly lower for an adsorbed atom forming part of a monolayer than for an isolated self-adsorbed atom.

In the following chapter the FS-AT, surface modified FS-AT, and the JO potentials will be extended for application to the tantalum on W {110} heteronuclear system.

CHAPTER 4

APPLICATION TO HETERONUCLEAR SYSTEMS: TANTALUM ON W {110} SUBSTRATES

4.1 INTRODUCTION

In this chapter the requirements for the application of embedded atom methods (EAM's) to heteronuclear systems will be discussed. An overview of existing alloy models and their application is given. The suitability of the EAM's for bcc metals introduced by Johnson and Oh (JO), and by Finnis and Sinclair (FS) for application to single tantalum adatoms adsorbed on W {110} surfaces is investigated (i) by calculating and comparing the self-adsorption parameters (*viz.* desorption energy, activation energy of adatom-surface migration and vibration frequencies of adsorbed atoms) with one another and with empirical data, and (ii) by calculating the optimum truncated Fourier series representations of the adatom-substrate interaction. In the case of the FS potential a small modification will be introduced to obtain a more realistic adsorbate-substrate interaction potential.

4.2 APPLICABILITY OF EMBEDDED ATOM METHODS TO HETERONUCLEAR SYSTEMS

The EAM provides a powerful technique for describing the properties of binary systems such as impurities in metals (Daw and Baskes 1983), alloys (Foiles *et al.* 1986 and Johnson 1989), clusters on surfaces (Gilmore *et al.* 1989), as well as adatoms adsorbed on a metal surfaces. The latter is considered to represent a simple form of alloy calculation. In the EAM

model the embedding energy is independent of the source of the background electron density. Thus the same embedding function is used to calculate the embedding energy of an atom in an alloy that would be used in the pure material (Foiles 1985). This makes the EAM particularly suitable for calculations involving atoms of different kinds.

To carry out an alloy calculation, the following is required (Johnson 1989):

(i) an embedding function $F(\rho)$ and an electron density function $f(r)$ for each atomic species;

(ii) the pair potential $\phi(r)$ for each combination of atomic species.

Since the electron density at any point is taken as the linear superposition of atomic electron densities and since the embedding energy function is assumed to be independent of the source of the background electron density, $F(\rho)$ and $f(r)$ can be taken directly from the homonuclear models.

In a system consisting of two different species, A and B, the pair interactions ϕ^{AA} and ϕ^{BB} are given by the homonuclear model. It is usually assumed that $\phi^{AB} = \phi^{BA}$, and that it is some function of the relevant homonuclear interactions, *viz.* an arithmetic (Rebonato 1989), geometric (Foiles *et al.* 1986 and Gollisch 1986b) or weighted average (Johnson 1989) of the interaction between atoms of the same species. Difficulties may be experienced with some of these averages due to certain arbitrary choices in the homonuclear models. For example, the geometric average is imaginary if one of the homonuclear two-body potentials is negative and the other positive. The weighted average

$$\phi^{AB}(r) = \frac{1}{2}\left[\frac{f^{B}(r)}{f^{A}(r)}\,\phi^{AA}(r) + \frac{f^{A}(r)}{f^{B}(r)}\,\phi^{BB}(r)\right], \qquad (4.1)$$

proposed by Johnson is only defined in the range where both $f^A \neq 0$ and $f^B \neq 0$. To further avoid singularities, the cutoff distance for the electron density function for a specific element must be equal to or greater than the cutoff distance for the two-body potential.

In a binary system with a mismatch in the lattice parameters of the constituent species, one of the species is found under conditions of expansion and the other in a state of compression. This has serious implications for the form of $F(\rho)$, which is usually determined from the properties of pure bulk materials at equilibrium. In an alloy, or at surfaces, the atoms will generally experience rather different electron densities than in the pure bulk material. The Rose equation of state (Rose *et al.* 1984) giving the sublimation energy of most metals as a function of the lattice constant, can be used to obtain information about $F(\rho)$ for electron densities well away from equilibrium.

4.3 EXISTING ALLOY MODELS

One of the first EAM alloy calculations were performed by Daw and Baskes (1983) to show that hydrogen can reduce the fracture stress in nickel. The functions $F(\rho)$ and $\phi(r)$ for Ni were determined by fitting their parameters to empirical data. The embedding function $F(\rho)$ for hydrogen was taken from electron gas computations by Puska *et al.* (1981). The electron density was assumed to be given by a linear superposition of the electron densities of the constituent atoms. The two-body potential $\phi(r)$ for Ni-H was fitted to the experimental heat of solution and the migration energy of H in Ni. ϕ_{H-Ni} was taken as the geometrical mean of ϕ_{H-H} and ϕ_{Ni-Ni}.

An investigation into the properties of H in the bulk metals Ni and Pd, as well as the binding site and adsorption energy of H on various faces of these metals, were subsequently carried out. For each of the elements Ni and Pd, the functions $F(\rho)$ and $\phi(r)$ were determined from the properties of the corresponding pure material. The unlike atom-pair interaction ϕ_{ij} was often taken as the geometric mean of ϕ_{ii} and ϕ_{jj}. Daw and Baskes found that this is equivalent to assigning the following form to ϕ_{ij}:

$$\phi_{ij}(r) = Z_i(r)Z_j(r)/r, \qquad (4.2)$$

where Z_m is considered to be the effective charge. The atomic electron densities were taken from Hartree-Fock calculations by Clementi and Roetti (1974). Due to uncertainty in the true ground state electron configuration of these metals, a parameter N_s, corresponding to the s-like content of the atomic density, was introduced. The atomic density was then given by

$$\rho^a(r) = N_s\rho_s^a(r) + (N-N_s)\rho_d^a(r), \qquad (4.3)$$

where N is the total number of outer electrons, and ρ_s^a and ρ_d^a the atomic densities of the s- and d-orbitals. N_s was fitted to the heat of solution of hydrogen in the particular metal. The embedding function $F_H(\rho)$ for hydrogen was derived from the first principle calculations of Puska *et al.* (1981). Satisfactory agreement with experiment was also found in the case of the adsorption of hydrogen on metal surfaces, as well as the calculation of surface energy and relaxation of (100), (110) and (111) faces of Ni and Pd crystals – problems which cannot be treated with pair potentials.

In his calculation of the surface segregation of Ni-Cu alloys, Foiles (1985) used the equation of state of expanded or compressed metals to determine $F(\rho)$ for electron densities substantially different from the equilibrium electron density ρ_e. The parameter N_s (eqn. (4.3)) for Cu and Ni were determined by the heats of mixing of alloys. In the pair interaction ϕ (eqn. (4.2)) the effective charge Z(r) was taken to be

$$Z(r) = Z_0 e^{-\alpha r} \tag{4.4}$$

where Z_0 was assumed to be given by the number of outer electrons of the atom. The parameter α was determined by the shear properties of the respective metals. The results obtained with this model were found to be in accordance with experimental data.

Foiles *et al.* (1986) subsequently presented a consistent set of embedding functions and short-range pair interactions suitable to describe the fcc metals Cu, Ag, Au, Ni, Pd and Pt, as well as alloy combinations of these elements. Basically the same procedure was followed as in the calculation of the surface segregation of Ni-Cu alloys, except that the effective charge Z(r) was taken to be

$$Z(r) = Z_0(1 + \beta r^{\nu})e^{-\alpha r}. \tag{4.5}$$

This involved three adjustable parameters β, α and ν. With $\nu = 1$ for Ni, Pd and Pt, and $\nu = 2$ for Cu, Ag and Au, the elastic constants of these metals were well reproduced. The parameters α, β and N_s were determined for Cu, Ag, Au, Ni, Pd and Pt so as to yield the elastic constants and vacancy formation energy of each material, as well as the dilute limits of

heats of solution of binary alloys. Here α and β were primarily determined by the shear moduli and the vacancy formation energy, and N_s was determined by the heats of alloying. Good agreement between the calculated results and the experimental data was reported.

Johnson (1989) presented an analytic nearest-neighbour EAM model for fcc metals with no adjustable parameters. The two-body potential between different species of atoms was taken as a function of the two-body potentials for the pure metals with a unique form (eqn. (4.1)) which yielded alloy models with the same invariance to electron density transformations as homonuclear models. The physical input consisted of the equilibrium lattice constant a, the cohesive energy E_c, the unrelaxed vacancy formation energy E_{UF}, the bulk modulus B and the Voigt average shear modulus G. The electron density function f(r) and the two-body potential $\phi(r)$ were both taken as exponentially decreasing functions *viz.*

$$f(r) = f_e \exp(-\beta(r/r_{1e} - 1)) \tag{4.6}$$

and

$$\phi(r) = \phi_e \exp(-\gamma(r/r_{1e} - 1)). \tag{4.7}$$

The equilibrium electron density f_e was taken as

$$f_e = S.E_c/\Omega \tag{4.8}$$

and the equilibrium two-body potential ϕ_e as

$$\phi_e = E_c/6, \tag{4.9}$$

with S, an arbitrary scaling constant taken as 1. Here Ω is the atomic volume. The embedding function $F(\rho)$ was determined by fitting the parameters to the universal equation of state (Rose *et al.* 1984) and was found to be given by

$$F(\rho) = -E_c(1 - \ell nx)x - 6\phi_e y, \qquad (4.10)$$

where $x = (\rho/\rho_e)^{\alpha/\beta}$, $y = (\rho/\rho_e)^{\gamma/\beta}$, and $\alpha = 3(\Omega B/E_c)^{1/2}$. The value of β was determined from the atomic wave functions and the resistance to shear of the model give a relationship involving all three parameters β, γ and ϕ_e. For all the fcc metals under consideration the values for β were approximately equal to 6.

Johnson (1990) extended this fcc alloy model to permit the effect of range on the results to be investigated, while retaining its analytic character. In this case f(r) was taken as a power law function

$$f(r) = f_e\left[\frac{r_{1e}}{r}\right]^{\beta} \qquad (4.11)$$

to permit the inversion of $\rho(r) \rightarrow r(\rho)$ to be carried out analytically if the range of the model extended past the first nearest neighbours. This inversion was only possible with an exponential function (eqn. (4.6)) for f(r) if the range of the model was restricted to first nearest neighbours. The heats of formation calculated with the extended model were in good agreement with the *ab initio* calculations by Terakura *et al.* (1987 and 1989).

Gollisch (1986a) developed an effective binding potential for the description of metal-metal interactions. This binding potential was then used to study the adsorption of single atoms of Cu, Ag and Au on a W {110} surface (Gollisch 1986b). The generalised form of the effective binding potential U_i is

$$U_i = \sum_{j\neq i}^{N} b_{ij}[\Phi_{ij}(r_{ij})]^{\mu S_{ij}\lambda_{ij}} - \left[\sum_{j\neq i}^{N} a_{ij}[\Phi_{ij}(r_{ij})]^{\lambda_{ij}}\right]^{\mu} \qquad (4.12)$$

with

$$\Phi_{ij}(r_{ij}) = \int \rho_i(\underline{r}-\underline{r}_i)\rho_j(\underline{r}-\underline{r}_j)d^3r \qquad (4.13)$$

where ρ_{ij} refers to the electronic charge densities for the corresponding free atoms. To simplify calculations Φ was approximated by the sum of two exponentials:

$$\Phi(r) = c_1\exp(-p_1r) + c_2\exp(-p_2r) \qquad (4.14)$$

The combination $\mu = 0.6$ and $S\mu = 2$ was applied in the calculations. For homonuclear systems the adjustable parameters b_{ij}, a_{ij} and λ_{ij} were fitted to the cohesive energy, lattice parameter and the bulk modulus of the corresponding material. In binary systems more information was required to determine a_{ij}, b_{ij} and λ_{ij}. For a heteronuclear system consisting of atoms A and B, eqn. (4.12) can be reformulated in a more specific way:

$$U_i = \sum_{j\neq i}\beta_{A(j)}\theta_{A(i)}(r_{ij})\theta_{A(j)}(r_{ij}) - \left|\sum_{j\neq i}\alpha_{A(i)}\alpha_{A(j)}\Psi_{A(i)}(r_{ij})\Psi_{A(j)}(r_{ij})\right|^{\mu} \qquad (4.15)$$

where A(i) designates the kind of atom at $\underline{r}_i$. If the definitions

$$\beta = b_{AA}^{1/2} \quad , \quad \theta_A(r_{ij}) = [\Phi_{AA}(r_{ij})]^{S\mu\lambda_{AA}/2}$$
$$\alpha = a_{AA}^{1/2} \quad , \quad \Psi_A(r_{ij}) = [\Phi_{AA}(r_{ij})]^{\lambda_{AA}/2} \qquad (4.16)$$

were applied to heteronuclear systems, it followed that

$$b_{AB} = (b_{AA}b_{BB})^{1/2},$$

$$\Phi_{AB}(r)^{\lambda_{AB}} = \Phi_{AA}(r)^{\lambda_{AA}/2}\Phi_{BB}(r)^{\lambda_{BB}/2} \qquad (4.17)$$

This implied that for application to heteronuclear systems, only the adjustable parameters and functions $\Phi(r)$ for the relevant homonuclear systems were required. Agreement between the values of the desorption energy calculated with this model and experiment was reported to be quite satisfactory.

Rebonato (1989) proposed a modification of the Finnis and Sinclair (FS) potentials for bcc metals for conditions of extension. These modified potentials were then extended for application to Mo-Nb and W-Ta alloys. In the alloy calculations the pairwise term ϕ_{AB} was taken as

$$\phi_{AB} = K_1(\phi_{AA} + \phi_{BB}) \qquad (4.18)$$

with ϕ_{AA} and ϕ_{BB} the modified FS potentials for the pure metals A and B. The n-body term was taken as

$$\Sigma\Big(\sum_{i}\sum_{j\neq i}\epsilon_{ij}^{AA}(r_{ij}-d_{AA})^2+\theta_{ij}^{BB}(r_{ij}-d_{BB})^2+\eta_{ij}^{AB}(r_{ij}-d_{AA})(r_{ij}-d_{BB})\Big)^{1/2}, \qquad (4.19)$$

where AA and BB denoted the squares of the constant A in eqn. (3.13) for the pure metals A and B, d_{AA} and d_{BB} the respective cutoff distances in eqn. (3.12) for pure metals A and B, and

$$AB = K_2(AA.BB)^{1/2}. \qquad (4.20)$$

K_1 and K_2 were adjustable parameters and the quantities ϵ_{ij}, θ_{ij} and η_{ij} were defined as follows:

$$\epsilon_{ij} = \begin{cases} 1 & , \text{ if } i = A \text{ and } j = A, \\ 0 & , \text{ otherwise,} \end{cases} \tag{4.21a}$$

$$\theta_{ij} = \begin{cases} 1 & , \text{ if } i = B \text{ and } j = B, \\ 0 & , \text{ otherwise,} \end{cases} \tag{4.21b}$$

$$\eta_{ij} = \begin{cases} 1 & , \text{ if } i = A \text{ and } j = B \text{ or } i = B \text{ and } j = A, \\ 0 & , \text{ otherwise.} \end{cases} \tag{4.21c}$$

This model yielded values of the bulk moduli of the alloys in good agreement with experiment.

4.4 EAM MODELS FOR THE TANTALUM ON W {110} HETERONUCLEAR SYSTEM

4.4.1 Model of Johnson and Oh

In the calculation of the adsorption parameters of tantalum on W {110} using the Johnson and Oh analytic bcc model, the pair potential $\phi(r)$, atomic density function $f(r)$ and the embedding function $F(\rho)$ for both tantalum and tungsten are taken from the corresponding homonuclear models. The physical input for the two elements are listed in Table 4.1. The cutoff distance r_c of $f(r)$ and $\phi(r)$ for both tungsten and tantalum was fixed at 4.4Å. Cubic equations are used to provide a smooth cutoff for both $\phi(r)$ and $f(r)$. The distance at which the cubic cutoff function joins the calculated pair potential $\phi(r)$ and the electron-density function $f(r)$ with matching value and slope is taken to be r_s. The values of r_s and r_c for both $\phi^{Ta}(r)$ and $f^{Ta}(r)$ were fixed at 4.3Å and 4.4Å respectively. For $\phi^{W}(r)$ and $f^{W}(r)$, r_s is taken as 3.29Å and 3.23Å respectively. The equilibrium electron density f_e in the expression for the atomic density

TABLE 4.1. The physical input for Johnson and Oh's monatomic bcc model*. The lattice and elastic constants are room temperature data, while the cohesive energy is for absolute zero. Ω is the atomic volume, G is the Voigt average shear modulus, A_r is the anisotropy ratio and E_{1V}^{UV} is the unrelaxed vacancy formation energy.

Metal	A(Å)	E_c(eV)	ΩB(eV)	ΩG(eV)	A_r	E_{1V}^{UF}(eV)	$E_c^{bcc}-E_c^{fcc}$
Ta	3.3026	8.089	21.66	7.91	1.57	2.95	0.24
W	3.16475	8.66	30.65	15.84	1.01	3.95	0.07

* Johnson and Oh (1989).

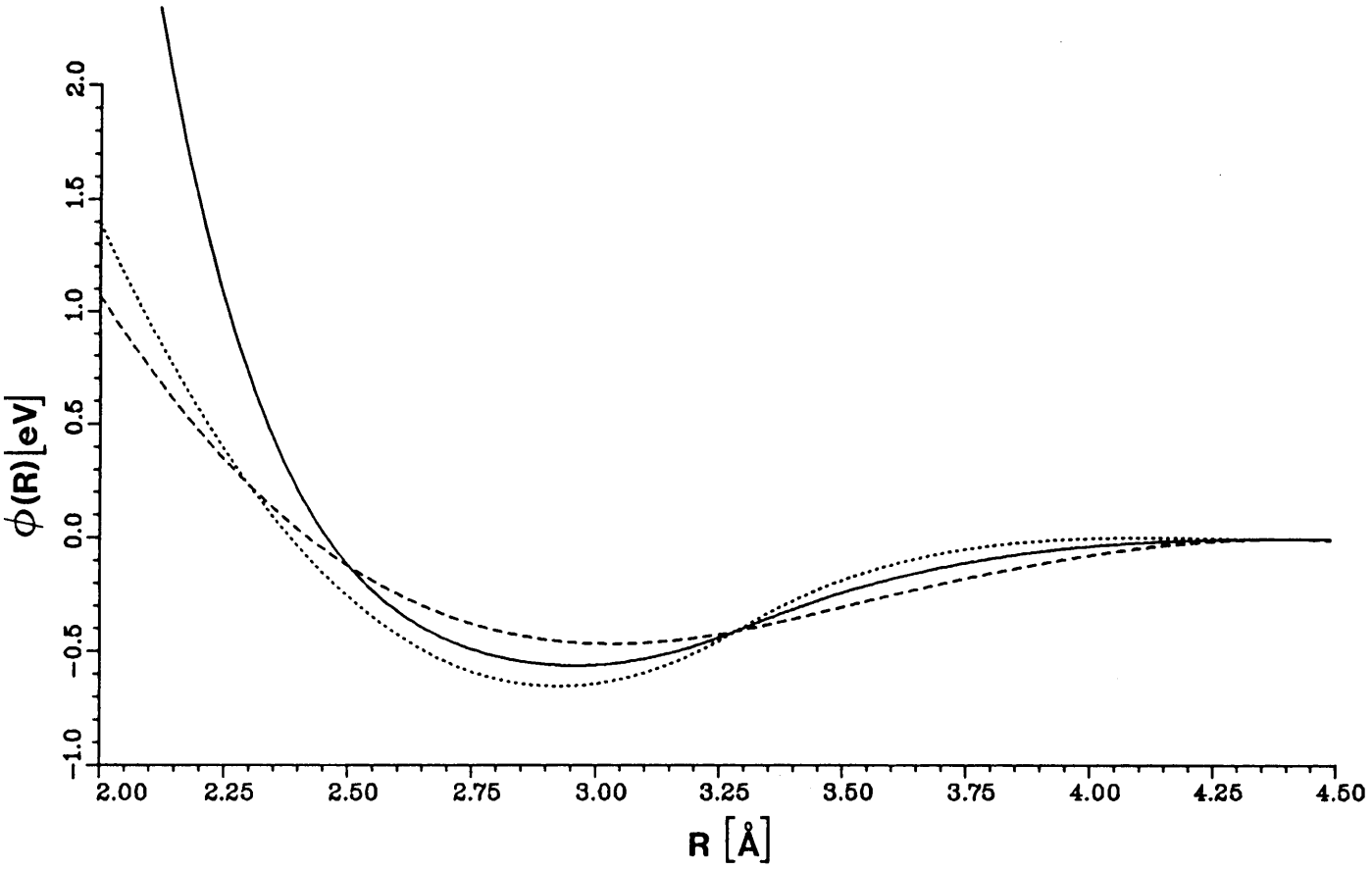

Figure 4.1 The two-body potentials in the Johnson and Oh model which contribute to the total energy for the tantalum on W {110} system. The dotted and dashed curves represent the repulsive two-body component (eqn. (2.7)) for the tungsten and tantalum homonuclear systems respectively. The solid curve represents the total unlike pair interaction (eqn. (4.22)) with hard-core modification for the tantalum on tungsten heteronuclear system.

function (eqn. (3.8)), cancels from all homonuclear calculations. For heteronuclear systems, relative values of f_e for the different elements are however required. By using eqn. (4.8), from Johnson's fcc alloy model, it is possible to show that $f_e^{Ta} = 0.449$ eV/Å^3 and $f_e^{W} = 0.546$ eV/Å^3.

The unlike-pair interaction ϕ^{Ta-W} can be described by the weighted average (eqn. (4.1)) proposed by Johnson (see Fig. 4.1). The arithmetic average yields values of the desorption energy E_{des} and the activation energy Q for surface migration which deviate further from the experimental values than with the weighted average. The geometric mean cannot be used, because for some values of r ϕ^{Ta-Ta} and ϕ^{W-W} do not have the same sign, which leads to an imaginary value for ϕ^{Ta-W}.

The modification for stiffening the two-body potential (eqn. (3.10)) has to be adjusted for the unlike-pair interaction ϕ^{Ta-W}. The modification was introduced for $r < r_o^{Ta-W} = \left[r_{1e}^{W} r_{1e}^{Ta}\right]^{1/2}$ resulting in the following expression for the total two-body potential ϕ^{Ta-W}:

$$\phi_{tot}^{Ta-W}(r) = \phi^{Ta-W}(r) + k_a^{Ta-W}\left[\phi^{Ta-W}(r) - \phi(r_o^{Ta-W})\right]\left[\frac{r}{r_o^{Ta-W}} - 1\right]^2 \qquad (4.22)$$

with

$$k_a^{Ta-W} = 4.5\left[1 + \frac{4}{A_r^{Ta-W} - 0.1}\right], \qquad (4.23)$$

A_r^{Ta-W} being the geometric mean of the anisotropy ratios of Ta and W.

4.4.2 FS-AT model

In the FS-AT calculations of the adsorption parameters for the tantalum on W {110} heteronuclear system, the parameterization of $\phi(r)$ (eqn. (3.11)), f(r) (eqn. (3.12)) and $F(\rho)$ (eqn. (3.13)) for the homonuclear model is adopted for each of the elements Ta and W. The fitting parameters for the two elements are listed in Table 4.2. For the purpose

TABLE 4.2. Fitting parameters for FS-AT monatomic models.*

FS-parameters

	d[Å]	A[eV]	c[Å]	c_0[eVÅ^{-2}]	c_1[eVÅ^{-3}]	c_2[eVÅ^{-4}]
Ta	4.076980	2.591061	4.20	1.2157373	0.0271471	−0.1217350
W	4.400224	1.896373	3.25	47.1346499	−33.7665655	6.2541999

Core-function parameters**

	B[eVÅ^{-3}]	α[Å^{-1}]	b_0[Å]
Ta	91.0	1.05	2.8629
W	90.3	1.2	2.7411

* Finnis and Sinclair (1984).

** Ackland and Thetford (1987).

of the present calculations, the alternative interpretation of ρ_i as the local electronic charge density at site i, constructed by a rigid superposition of atomic charge densities f(r), given by Finnis and Sinclair (1984), is preferred. If f(r) is interpreted as the sum of squares of overlap integrals, f^{AA}, f^{BB}, f^{AB} and f^{BA} are required for FS calculations for binary systems consisting of atoms A and B, whereas only f^{AA} and f^{BB} are required if f(r) is interpreted as an atomic charge density (Johnson 1989).

Various combinations of the relevant homonuclear interactions ϕ^{W-W} and ϕ^{Ta-Ta} were considered in describing the unlike-pair interaction ϕ^{Ta-W}. The weighted average (eqn. (4.1)) proposed by Johnson can not be applied because the electron density functions $f^{Ta}(r)$ and $f^{W}(r)$ do not have the same cutoff distance (c^{W} = 3.25Å < c^{Ta} = 4.20Å). The geometric mean can also not be used because ϕ^{Ta-Ta} has a very small negative minimum as the cutoff d^{Ta} = 4.076980Å is approached. ϕ^{W-W} remains positive while going to zero at d^{W} = 4.400224Å (see Fig. 4.2). Therefore the arithmetic average, which is defined throughout the range 0 < r < 4.400224Å, is adopted to describe the unlike-pair interaction ϕ^{Ta-W}.

The hard-core modification of Ackland and Thetford (eqn. (3.14)) also has to be adjusted for the unlike-pair interaction resulting in the following expression for ϕ_{tot}^{Ta-W}:

$$\phi_{tot}^{Ta-W}(r_{ij}) = \frac{1}{2}\left[\phi^{Ta-Ta} + \phi^{W-W}\right] + B^{Ta-W}(b_o^{Ta-W} - r_{ij})^3 \exp(-a^{Ta-W} r_{ij}), \quad \text{for } r_{ij} < b_o^{Ta-W}, \tag{4.24}$$

where B^{Ta-W} = 90.65 eVÅ^{-3} and b_o^{Ta-W} = 2.8014Å are the geometric averages of the respective values for the monatomic models, and a^{Ta-W} = 1.125Å^{-1} is the arithmetic average of the homonuclear values.

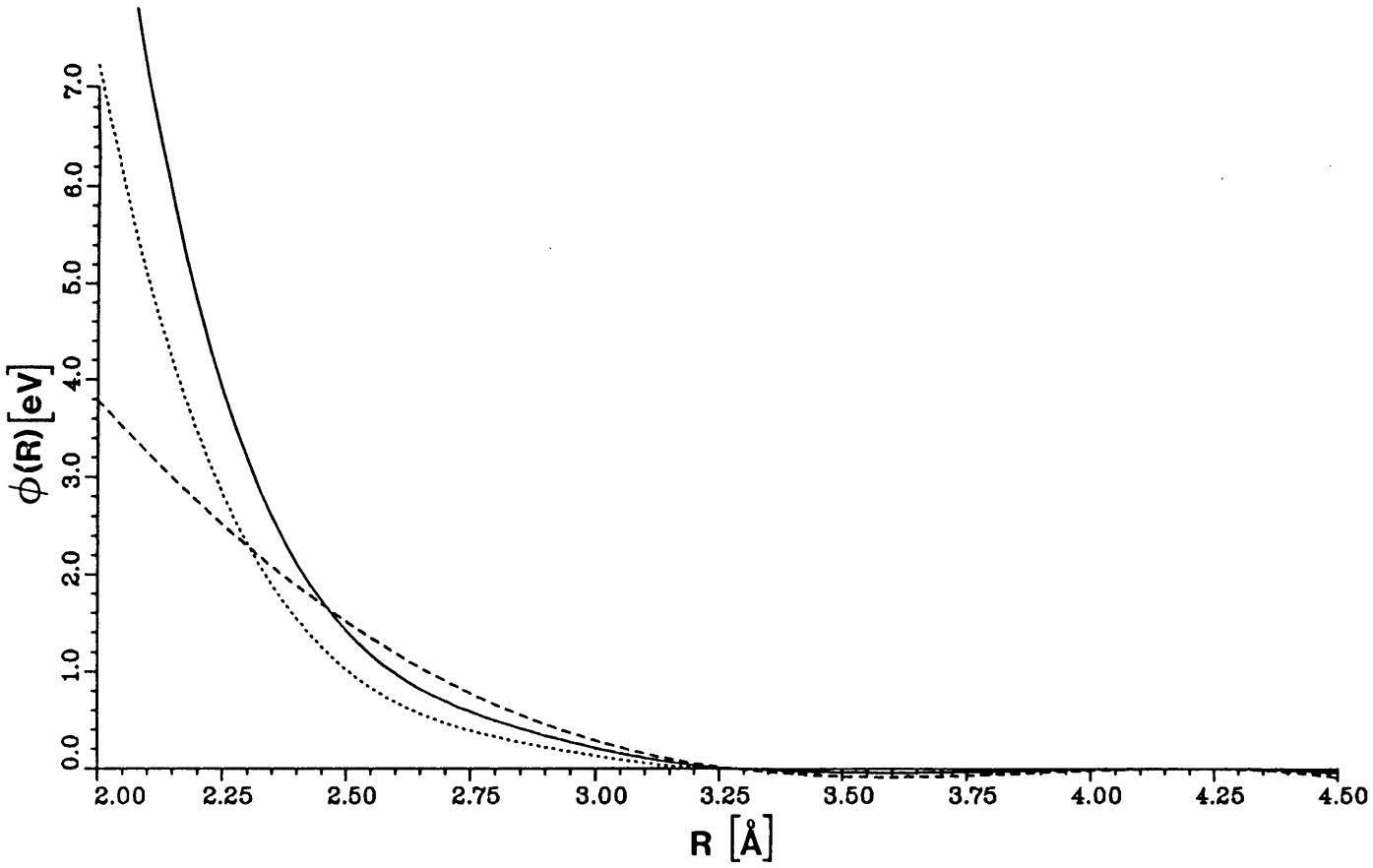

Figure 4.2 The two-body potentials in the FS-AT model which contribute to the total energy for the tantalum on W {110} system. The dotted and dashed curves represent the repulsive two-body component (eqn. (3.11)) for tungsten and tantalum homonuclear systems respectively. The solid curve represents the total unlike pair interaction (eqn. (4.24)) with hard-core modification for the tantalum on tungsten heternuclear system.

TABLE 4.3. Desorption energy E_{des}, deviation z_o and activation energy Q for surface migration of a Ta-adatom on a W {110} substrate. z_o is the deviation of the equilibrium height of the adsorbate from a W {110} bulk interlayer spacing.

Model	E_{des}[eV]	z_o[Å]	Q[eV]
FS-AT	7.3311	−0.0789	0.6006
Surf. mod. FS-AT	8.0007	−0.1304	0.7006
Johnson and Oh	6.8540	−0.0319	0.6303
Experimental	~ 7.0*	negative	0.78** 0.70+

* Plummer and Rhodin (1968).

** Basset and Parsley (1969). (Data were obtained with a few adatoms on a plane.)

\+ Tsong and Kellogg (1975). (Data were obtained for a single adatom on a perfect plane.)

4.4.3 Surface modified FS-AT model

If the FS-AT value of the desorption energy E_{des} (7.3311 eV) and the activation energy Q for surface migration (0.6006 eV) are compared to the corresponding empirical values which are of the order of 7.0 eV and 0.70 eV respectively, the activation energy is clearly too low, whereas the desorption energy lies within the experimental range (see Table 4.3). The reproduction of Q, however, is considered to be more important in the assessment of a suitable surface potential. The reproduction of E_{des} on the other hand is considered to be less important, particularly in the case of the W {110} surface where some uncertainty about the particular value of its work-function exists (Ehrlich and Kirk 1968). Assuming that the electron distribution around the tantalum adatom is distorted due to the presence of the W {110} surface, the atomic electron density function of tantalum where it interacts with tungsten atoms has been modified. An additional fitting parameter λ^{Ta} with

$$A^* = \lambda^{Ta} A, \qquad (4.25)$$

where A is the positive bonding parameter for tungsten, was introduced for the interaction of the tantalum adatom with the substrate atoms.

The corresponding values of Q and E_{des} for different values of λ^{Ta} were calculated using the FS-AT model for the Ta/W {110} system. The results are displayed in Fig. 4.3. The relationship between Q, as well as E_{des}, and λ^{Ta} is approximately linear. A value of λ^{Ta} = 1.26 yields values of 8.0007 eV and 0.7006 eV for E_{des} and Q respectively. The latter value of Q lies within the experimental range, whereas the value of E_{des} lies within 15% of the empirical value. This extended model (hereafter referred to as the surface modified FS-AT model) is also applied to the calculation of adsorption properties of a tantalum adatom on a W {110} surface.

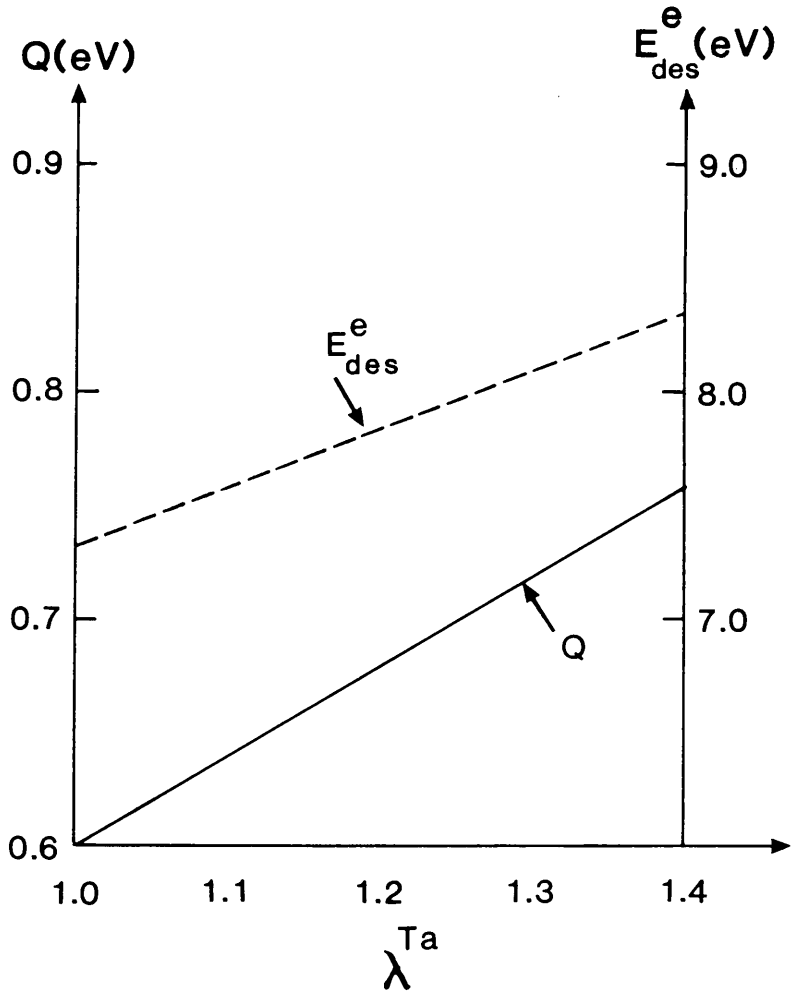

Figure 4.3 Dependences of the surface migration activation energy Q (solid line) and the desorption energy E^e_{des} (broken line) on $\lambda^{Ta} = A^*/A$, the surface modified fitting parameter adjusting the cohesive adatom-substrate interaction for the tantalum on W {110} system.

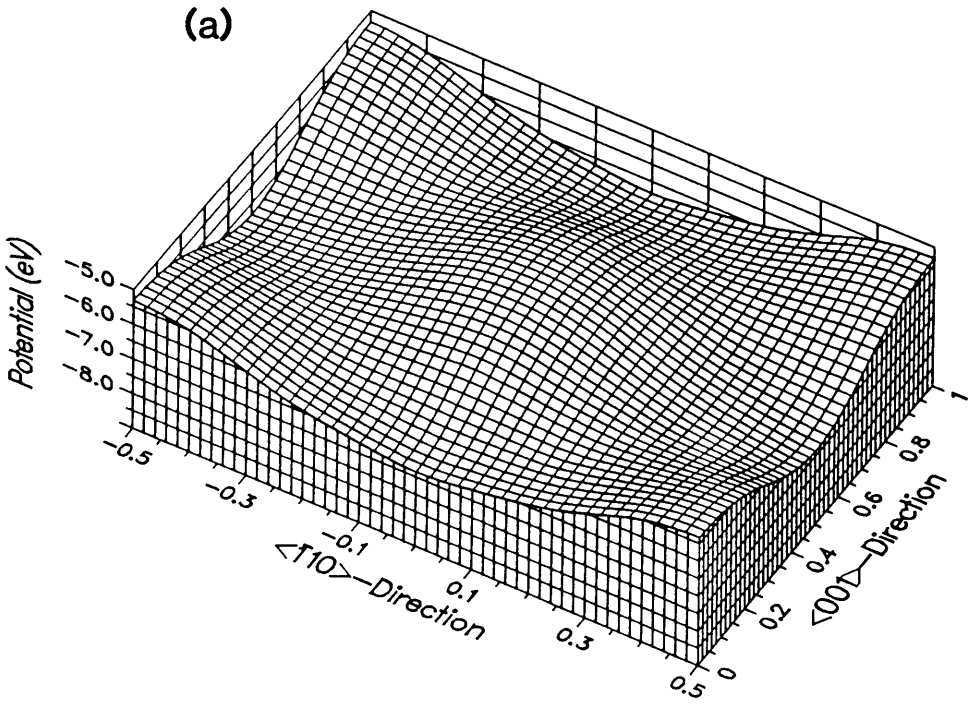

Figure 4.4 Three-dimensional representations of the potential surface E(P) in eqn. (2.5d) for migration of a tantalum adatom on a W {110} substrate: (a) the model of Johnson and Oh; (b) the FS-AT model and (c) the surface modified FS-AT model with λ^{Ta} = 1.26. Positions are expressed in terms of normalized rectangular unit cell side lengths (Fig. 2.1).

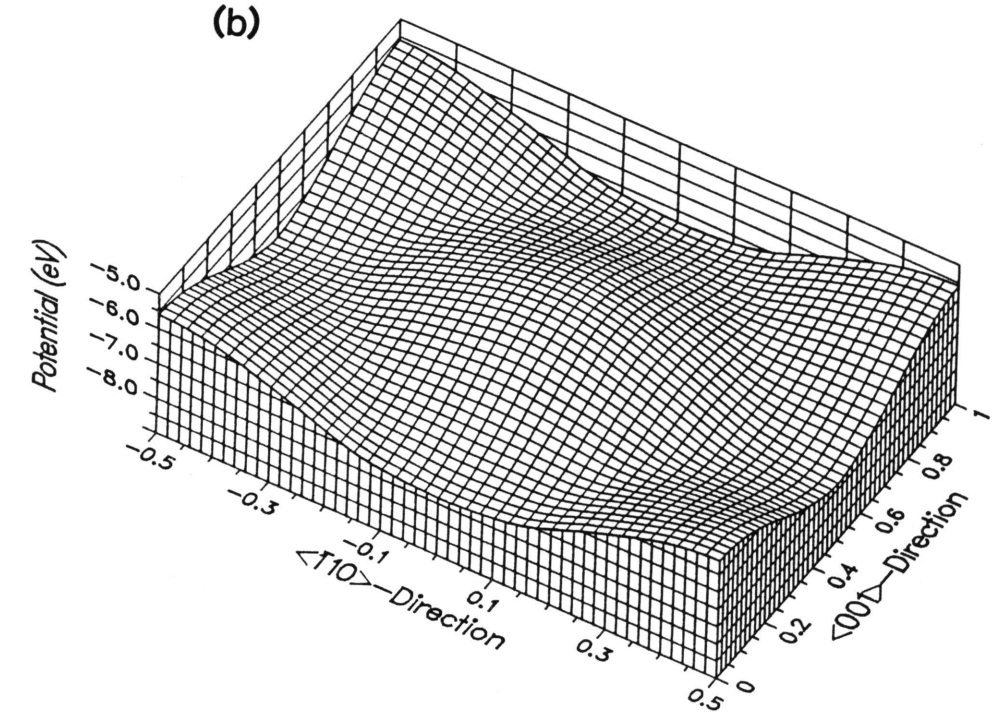

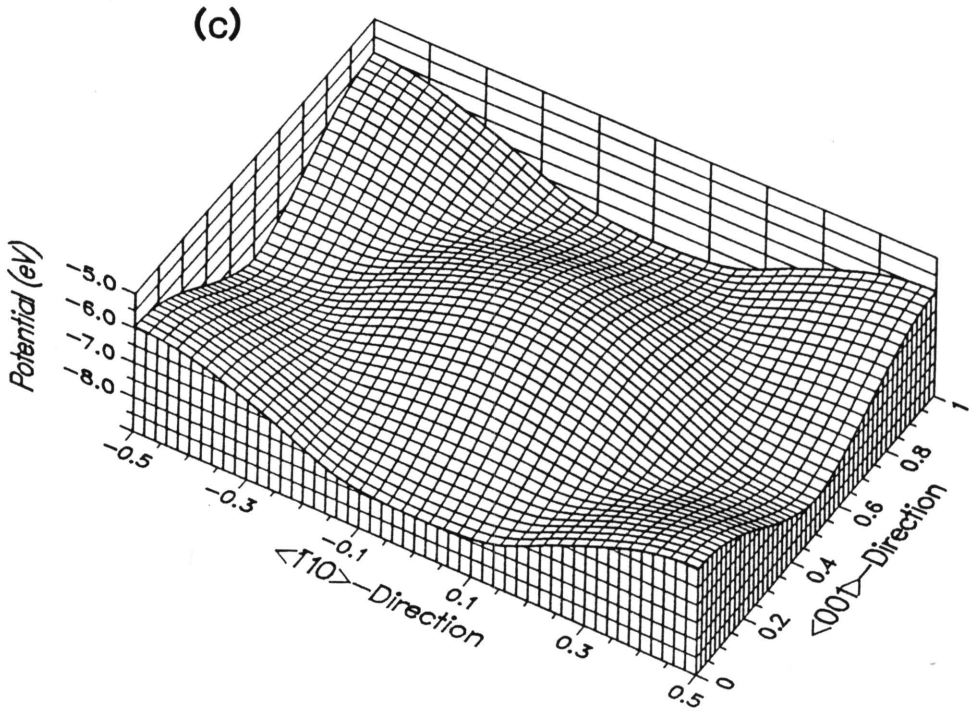

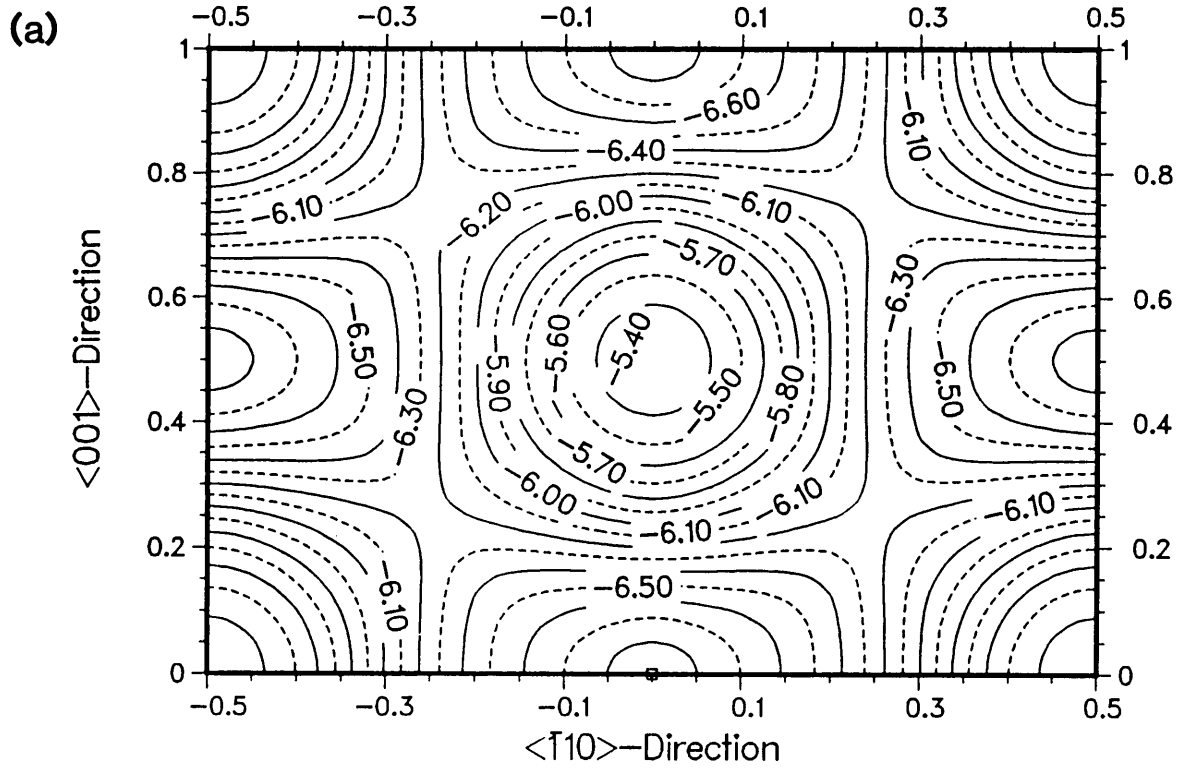

Figure 4.5 Contour plots of the self-adsorption energy E^*_{ads}(eV) (eqn. 2.5d)) of a tantalum adatom on a W {110} surface as calculated using (a) the Johnson and Oh, (b) the Finnis and Sinclair with Ackland and Thetford hard-core modification (FS-AT), and (c) the surface modified FS-AT models respectively. Positions are expressed in terms of normalized rectangular unit cell side-lengths (Fig. 2.1).

(b)

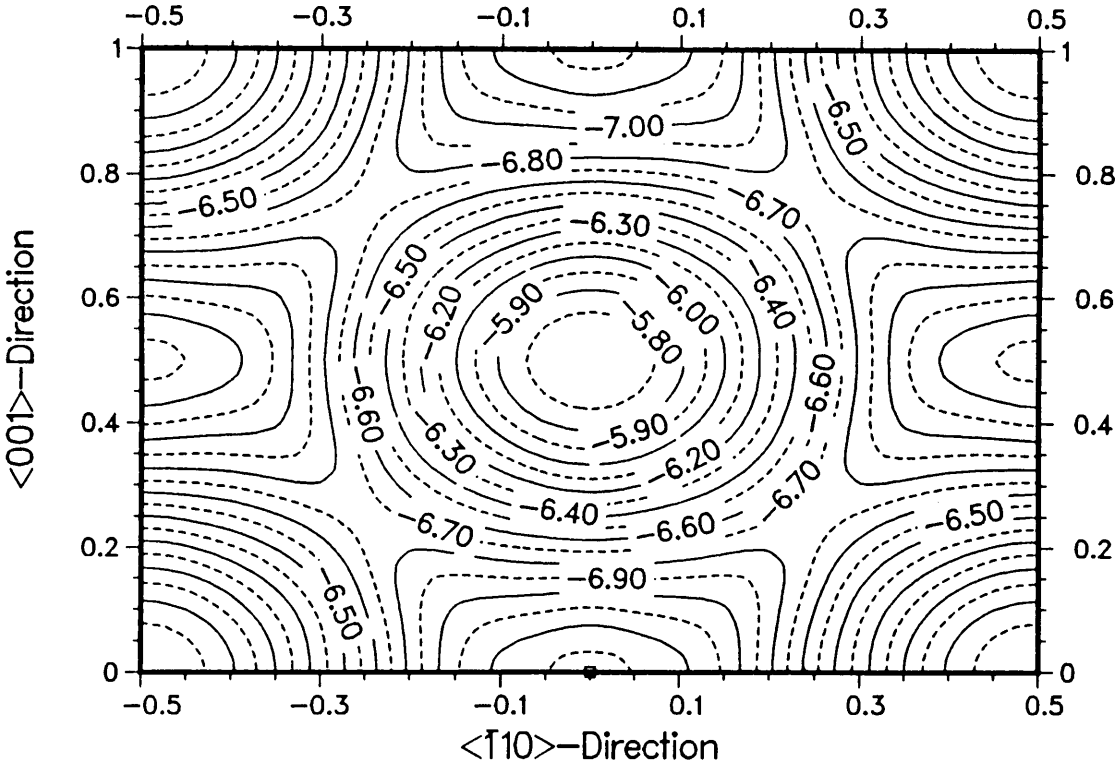

(c)

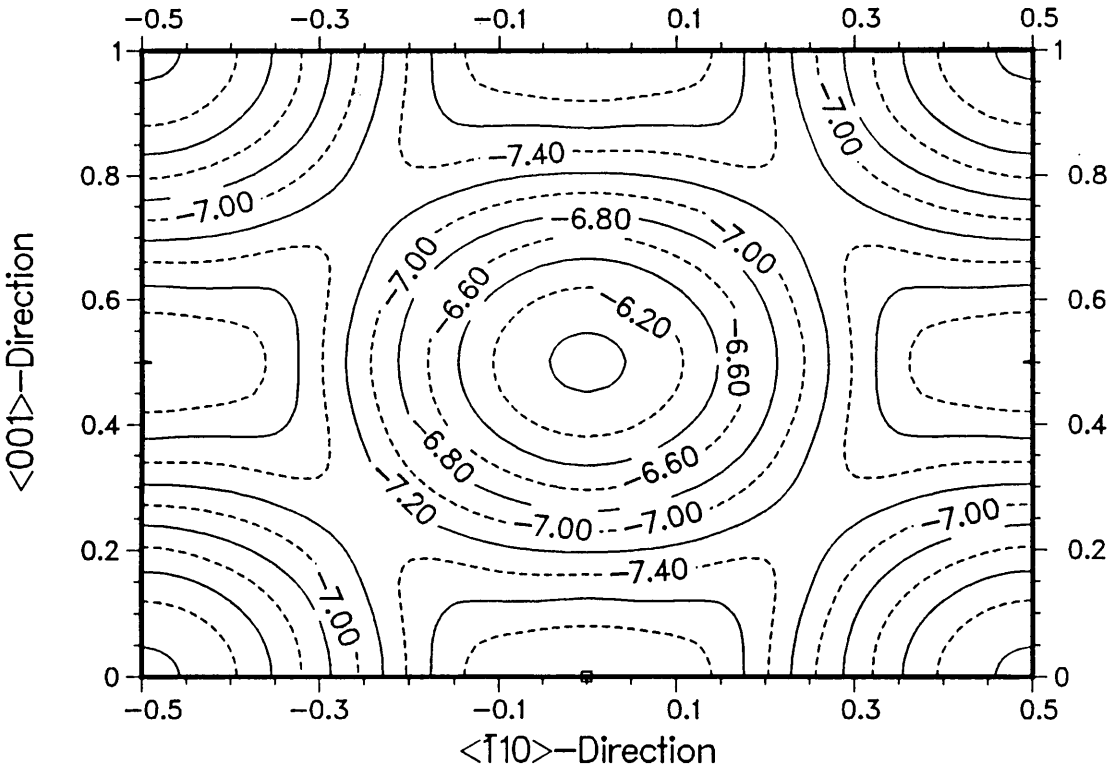

4.5 RESULTS

4.5.1 Potential surface $E(x,y,h_e)$

Three-dimensional representations of the adatom-substrate interaction potential (ASIP) (eqn. (2.5d)) within the cell KLMN of Fig. 2.1 for the JO, the FS-AT and surface modified FS-AT models respectively are displayed in Figs. 4.4 a, b and c. Contour plots (Figs. 4.5 a, b and c) of the potential surface of tantalum on the W {110} surface generated by the JO, FS-AT, as well as surface modified FS-AT models, reveal a single minimum at the adsorption site (AS). The potential surfaces for tantalum on the Ta {110} surface calculated with the JO and FS-AT models respectively also reveal a single minimum. However, the ASIP surface of a tungsten adatom on a W {110} substrate generated with the surface modified FS-AT potential, is characterized by two shallow local minima located symmetrically on either side of the adsorption site. A double well also appears in the potential surfaces of Cu, Ag and Au adatoms adsorbed on a W {110} surface generated with the binding potentials of Gollisch (1986b). The presence of the double well might be a characteristic of systems where the adatoms have about the same or a larger electronegativity than that of tungsten. The relative electronegativity of the adatom and substrate atoms is reflected in the magnitude of the surface-induced dipole moment of the adatom.

4.5.2 Desorption and activation energies

Calculated values of the desorption energy E_{des}, the surface deviation z_0 and the activation energy Q for surface migration for the potential models under consideration, are summarised in Table 4.3. The JO and FS-AT values of the desorption energy E_{des} are respectively about 2.1% lower and 4.7% higher than the approximate empirical value of 7 eV for the binding

energy of a tantalum adatom on a W {110} surface obtained by Plummer and Rhodin (1968). The surface modified FS-AT value deviates by about 14% from the experimental value.

The FS-AT and JO models yield values of the activation energy Q for surface migration of the tantalum adatom deviating by about 14% and 10% respectively from the empirical value determined by Tsong and Kellogg (1975) for a single tantalum adatom on a perfect W {110} surface. The surface modified FS-AT potential of course reproduces the empirical value of Q to which it has been fitted.

4.5.3 Truncated Fourier series representations

The adatom-substrate interaction potential data needed for finding the optimized Fourier coefficients in skew-, as well as Cartesian axes are obtained from eqn. (2.5d) with 1600 data points within the unit cell TEFG (see Fig. 2.1) for each of the JO, FS-AT and surface modified FS-AT models respectively. The truncated Fourier representation in skew axes $x^{(1)},x^{(2)}$ is given by eqn. (2.1) and the corresponding calculated coefficients A_{hk} are listed in Table 4.4. Again $A_{hk} = A_{kh}$ and $A_{h,-k} = A_{k,-h}$ in accordance with symmetry requirements. The Fourier coefficients also tend to zero with increasing harmonic order. Histograms of the standard error $\delta_s^{(n)}$ (eqn. (2.9)), providing a measure of the accuracy of the n-th order Fourier truncation, against n are shown in Figs. 4.6 a, b and c. These figures show that for a specific truncation, the JO model yields the most accurate approximation of the adatom-substrate interaction potential. When a third instead of a first order approximation is used, $\delta_s^{(n)}$ is reduced by more than 84%, 83% and 82% for the JO, FS-AT and surface modified FS-AT potentials respectively.

TABLE 4.4. Calculated Fourier coefficients A_{hk}[eV] in skew axes (eqn. (2.1)) for the interaction energy of a Ta adatom with a W {110} surface, showing the dependence on harmonic order n = |h| + |k|.

n	h,k	Johnson and Oh	FS-AT	Surface modified FS-AT
0	0,0	−6.12044	−6.53112	−7.04701
1	1,0	−0.18983	−0.21773	−0.25980
	0,1	−0.18983	−0.21773	−0.25980
2	2,0	−0.00676	−0.01480	−0.02047
	1,1	−0.01582	0.01168	0.00565
	1,−1	0.05680	0.05158	0.06820
	0,2	−0.00676	−0.01480	−0.20468
3	3,0	−0.00172	−0.00400	−0.00482
	2,1	0.00308	−0.00100	−0.00342
	1,2	0.00308	−0.00100	−0.00342
	2,−1	−0.00129	0.00949	0.01493
	1,−2	−0.00129	0.00949	0.01493
	0,3	−0.00172	−0.00400	−0.00482
4	4,0	−0.00086	−0.00045	−0.00019
	1,3	0.00015	−0.00150	−0.00229
	3,1	0.00015	−0.00150	−0.00229
	3,−1	−0.00378	0.00342	0.00639
	1,−3	−0.00378	0.00342	0.00639
	2,2	0.00278	0.00001	−0.00161
	2,−2	−0.00228	0.00124	0.00177
	0,4	−0.00086	−0.00045	−0.00019

TABLE 4.5. Calculated Fourier coefficients A_{hk}[eV] in Cartesian axes (eqn. (2.2)) for the interaction energy of a Ta adatom with a W {110} surface, showing the dependence on harmonic order n = |h| + |k|.

n	h,k	Johnson and Oh	FS-AT	Surface modified FS-AT
0	0,0	−3.06021	−3.26556	−3.52351
2	2,0	0.05680	0.05158	0.06820
	1,1	−0.37967	−0.43545	−0.51959
	0,2	−0.01582	0.01168	0.00565
4	4,0	−0.00228	0.00124	0.00177
	3,1	−0.00258	0.01898	0.02985
	2,2	−0.01353	−0.02960	−0.04093
	1,3	0.00617	−0.00200	−0.00685
	0,4	0.00298	0.00001	−0.00161
6	6,0	−0.00065	−0.00208	−0.00239
	5,1	−0.00269	−0.00585	−0.00643
	4,2	−0.00757	0.00684	0.01278
	3,3	−0.00344	−0.00800	−0.00963
	2,4	0.00031	−0.00301	−0.00458
	1,5	−0.00034	−0.00273	−0.00415
	0,6	−0.00092	−0.00117	−0.00129
8	8,0	−0.00011	−0.00005	−0.00005
	7,1	−0.00004	−0.00075	−0.00104
	6,2	−0.00209	−0.00424	−0.00489
	5,3	0.00242	0.00672	0.00863
	4,4	−0.00172	−0.00089	−0.00039
	3,5	−0.00085	−0.00062	−0.00058
	2,6	−0.00044	−0.00069	−0.00083
	1,7	−0.00023	−0.00044	−0.00042
	0,8	0.00019	0.00026	0.00026

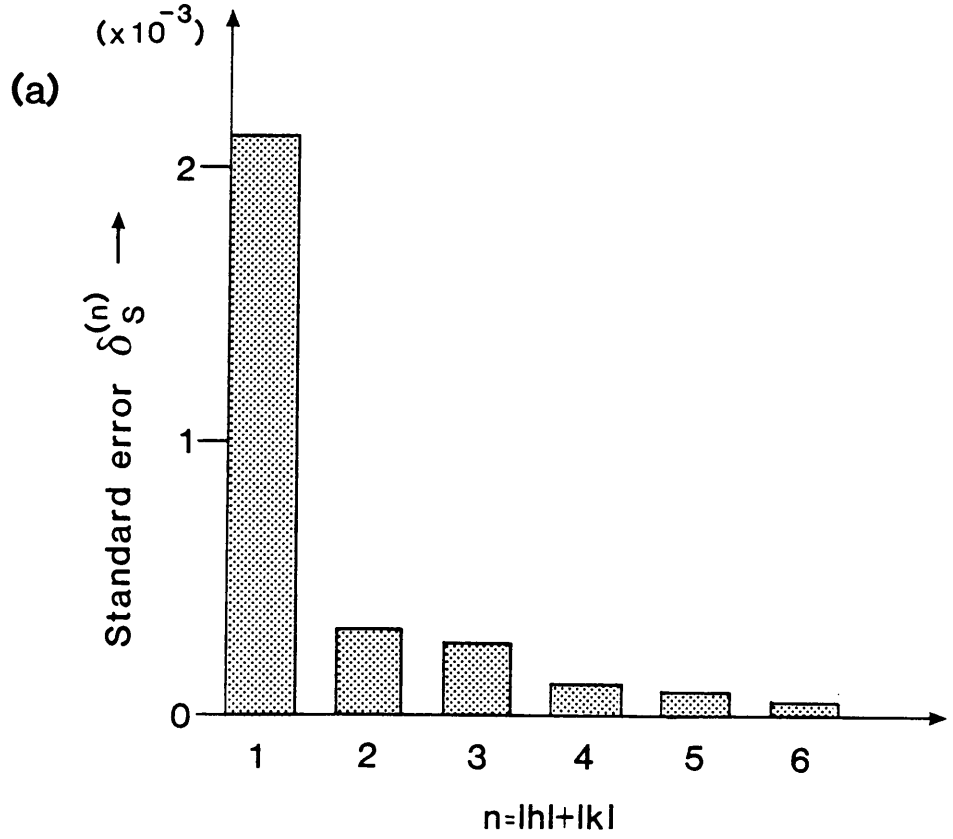

Figure 4.6 Histograms displaying the dependence of the standard error $\delta_S^{(n)}$ (eqn. (2.9)) on the order n of Fourier truncation of the adatom-substrate interaction potential expressed in skew axes for (a) the Johnson and Oh, (b) the FS-AT and (c) the surface modified FS-AT potential models as calculated for the tantalum on W {110} system.

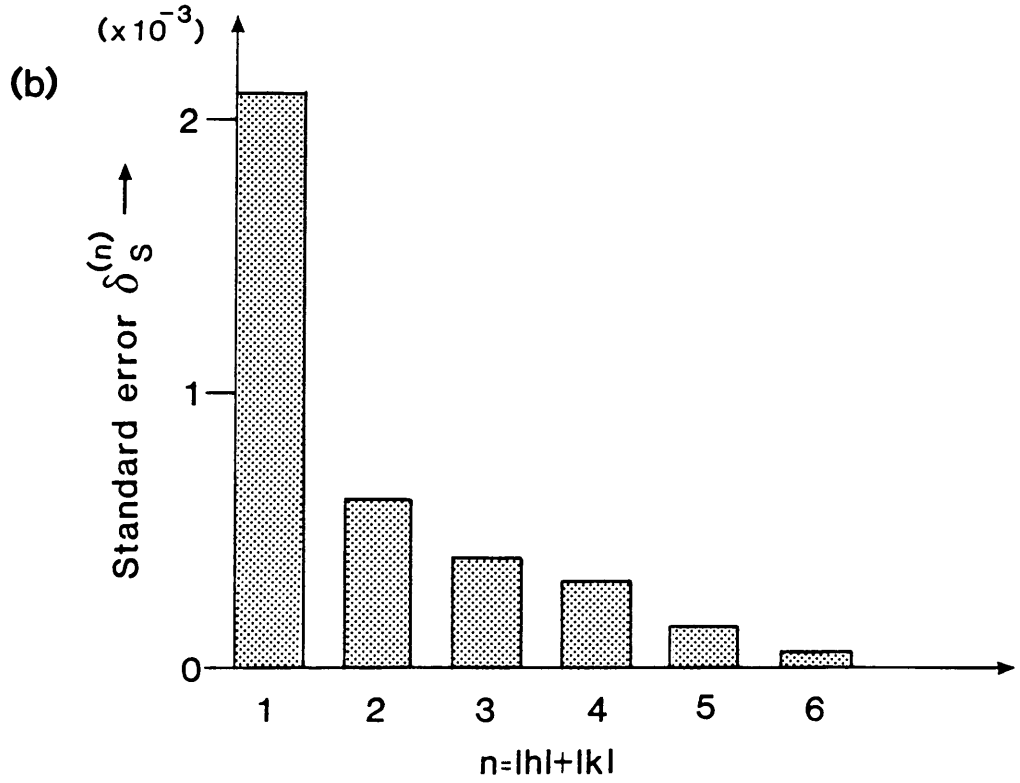

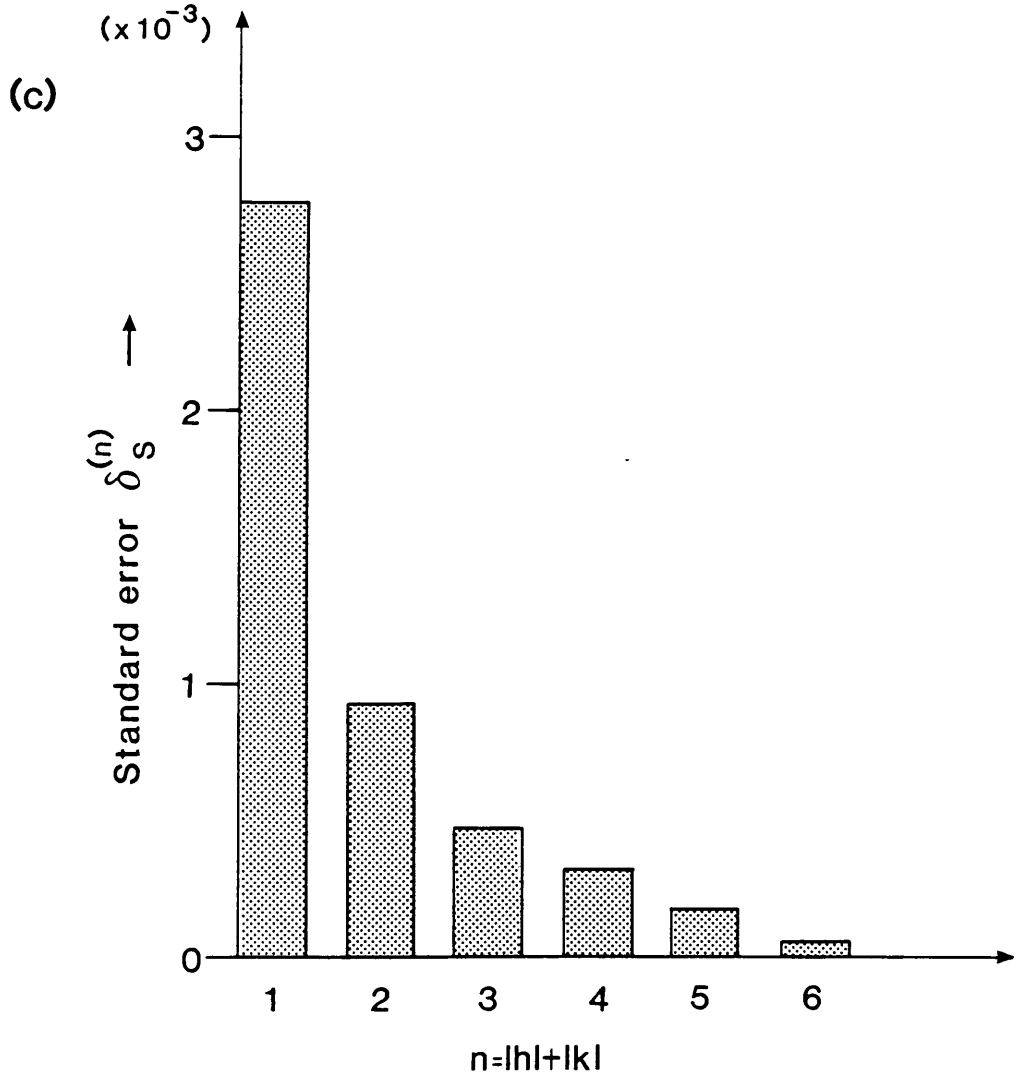

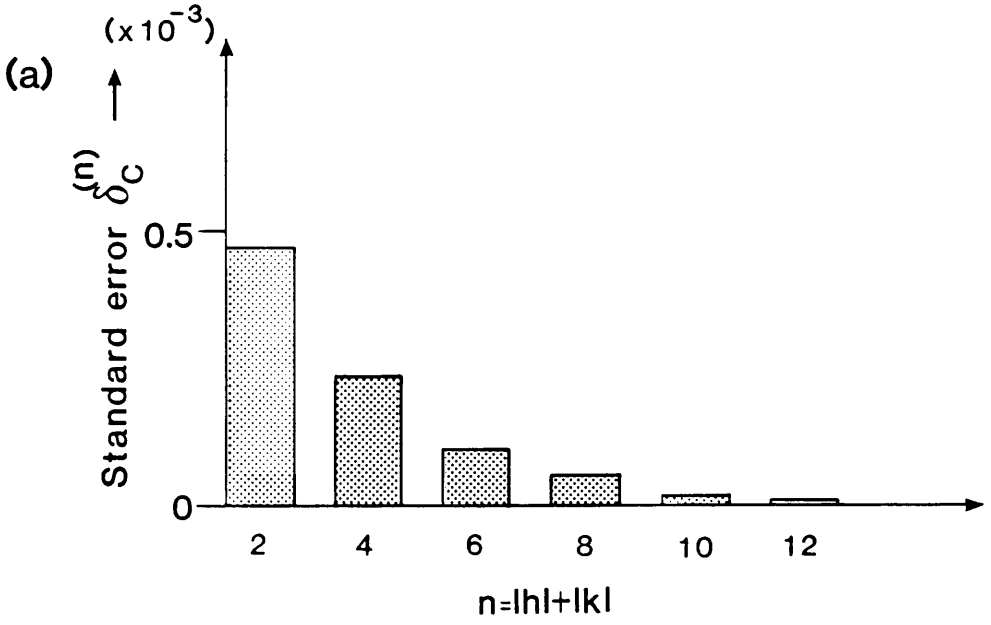

Figure 4.7 Histograms displaying the dependence of the standard error δ_C^n (eqn. (2.9)) on the order n of truncation of the Fourier series representation of the adatom-substrate interaction potential expressed in Cartesian axes for (a) the Johnson and Oh, (b) the FS-AT and (c) the surface modified FS-AT potential models as calculated for the tantalum on W {110} system.

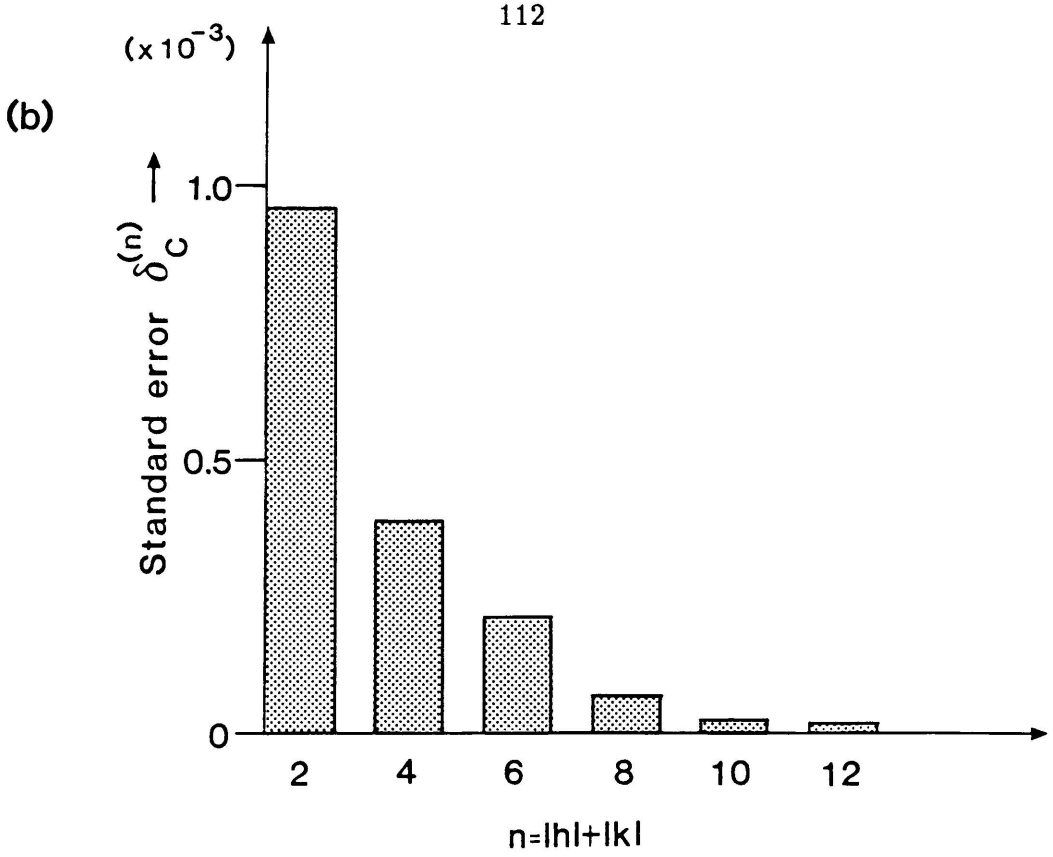

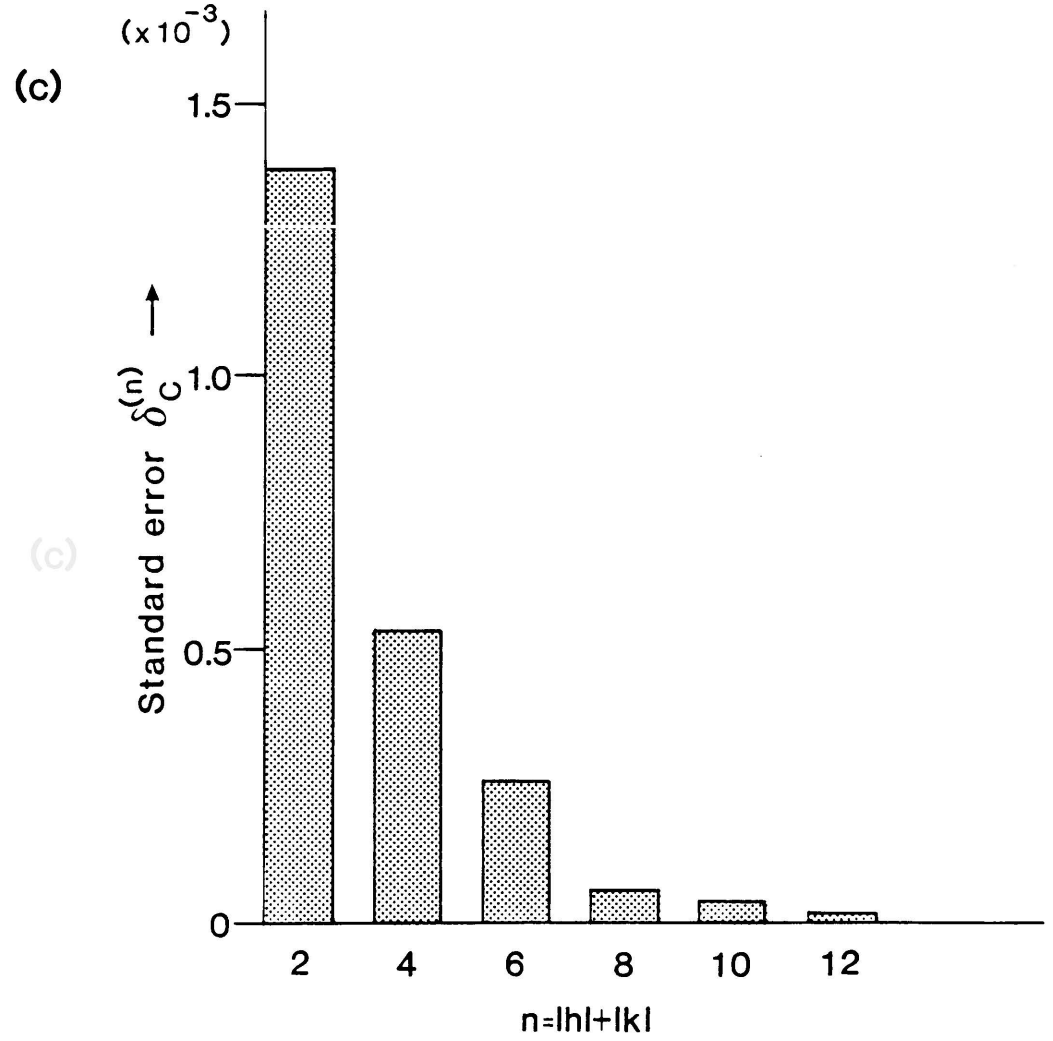

The truncated Fourier representation of the adatom-substrate interaction potential expressed in Cartesian axes x,y (see Fig. 2.1) is given by eqn. (2.2), and the corresponding Fourier coefficients A_{hk} for the models under consideration are listed in Table 4.5. The Fourier coefficients also tend to zero with increasing harmonic order. Histograms, displaying the decrease of the standard error $\delta_c^{(n)}$ with the order n of truncation, are presented in Fig. 4.7 a, b and c. A decrease of between 77% and 81% in $\delta_s^{(n)}$ is obtained by using a sixth instead of a second order truncation. This is equivalent to using a third rather than a first order truncation in skew axes. The JO potential again yields the most accurate approximation for a specific order n of truncation.

In Table 4.6 the normalized values of the coefficients previously determined by van der Merwe (1984) on a qualitative basis, are compared with those obtained using N-body potentials. In this representation (eqn. (3.16)) the potential energy at the adsorption site is taken as zero. Excellent agreement is obtained between the corresponding values of the Fourier coefficients for the tantalum on W {110} and tungsten on W {110} systems calculated with the JO, FS-AT and surface modified FS-AT models respectively (cf. Tables 4.6 and 3.4). There is also a reasonable agreement between the calculated values for the tantalum on W {110} system and the proposed values of van der Merwe, further strengthening the belief that the values of the Fourier coefficients are primarily determined by the symmetry of the substrate.

4.5.4 Force constants

All the calculated force constants and corresponding vibration frequencies are listed in Table 4.7. Since the potential surfaces of the

TABLE 4.6. Normalized Fourier coefficients A_i in a truncated representation of the interaction potential of a Ta adatom on W {110} as given by eqn. (3.16). V(0,0) is the value of the potential at the origin as calculated with eqn. (3.16). W_0 is the bonding parameter, constituting an overall scale factor in eqn. (3.16).

Model	A_1	A_2	A_3	A_4	V(0,0) [eV]	W_0 [eV]
van der Merwe	−0.4	−0.4	−0.12	−0.08	0	–
Johnson and Oh	−0.5176	−0.5176	0.1548	−0.0431	0.056	0.7336
FS-AT	−0.5443	−0.5443	0.1290	0.0292	0.056	0.8000
Surface modified FS-AT	−0.5448	−0.5448	0.1430	0.0119	0.063	0.9536

TABLE 4.7. Force constants $k_i[eV/Å^2]$ and corresponding vibration frequencies $\nu_i[s^{-1}]$ for lateral and normal vibrations of the adsorbed atom. The superscripts (f)(0,0) and (p) respectively designate force constants calculated at the origin with a finite difference technique and force constants calculated by fitting a parabola over the lower half of the potential energy curve.

	Johnson and Oh	FS-AT	Surface modified FS-AT
$k_x^{(f)(0,0)}$	2.12	1.51	0.87
ν_{x1}	1.33×10^{10}	1.12×10^{10}	0.85×10^{10}
$k_x^{(p)}$	0.92	1.30	1.56
ν_{x3}	0.87×10^{10}	1.04×10^{10}	1.14×10^{10}
$k_y^{(f)(0,0)}$	4.70	6.10	7.94
ν_{y1}	1.97×10^{10}	2.25×10^{10}	2.57×10^{10}
$k_y^{(p)}$	3.05	3.00	3.66
ν_{y3}	1.59×10^{10}	1.58×10^{10}	1.74×10^{10}
$k_z^{(f)(0,0)}$	13.43	14.65	15.87
ν_z	3.34×10^{10}	3.49×10^{10}	3.63×10^{10}

JO, FS-AT and surface modified FS-AT models all display a single minimum at the adsorption site, only the force constants $k_i^{(f)(0,0)}$ (eqn. (2.7)) and the effective force constants $k_i^{(p)}$ (i = x,y) need be calculated for lateral vibrations of the adatom. The force constants $k_x^{(f)(0,0)}$ and $k_y^{(f)(0,0)}$ are important at low substrate temperatures T_{s1} with the adatom localized at an adsorption site. The effective force constants $k_i^{(p)}$ become important at a much higher substrate temperature T_{s3} when adatom surface migration sets in. All the force constants $k_i^{(f)(0,0)}$ are determined with a finite difference approximation similar to eqn. (2.7), and the effective force constants $k_i^{(p)}$ are calculated by fitting a parabola to the lower half of the potential energy curve. In the evaluation of $k_x^{(f)(0,0)}$, $k_y^{(f)(0,0)}$ and $k_z^{(f)(0,0)}$, $\bar{\delta}$ was respectively taken as $0.0125\sqrt{2}a$ Å, $0.0125a$ Å and 0.005 Å for all three potential models under consideration. The lateral force constants yielded vibration frequencies ν (calculated with eqn. (2.6)) of between $0.85 \times 10^{10}s^{-1}$ and $2.57 \times 10^{10}s^{-1}$. The force constants $k_z^{(f)(0,0)}$ yielded values of ν lying be een $3.34 \times 10^{10}s^{-1}$ and $3.63 \times 10^{10}s^{-1}$ for vibrations normal to the substrate surface.

The force constants $k_y^{(n)}$ (eqn. (2.8b)) and $k_x^{(n)}$ (eqn. (2.8a)) obtained from the n-th order truncations of the adatom-substrate interaction potential in Cartesian axes, could be calculated for all three models. The dependence of $k_y^{(n)}$ and $k_x^{(n)}$ on the order n of truncation for the JO, FS-AT and surface modified FS-AT potentials are illustrated in Figs. 4.8 a, b and c. For all three potentials an optimum value of $k_y^{(n)}$ is obtained for truncations between the sixth and the tenth order where $k_y^{(n)}$ is relatively constant. For $k_x^{(n)}$ the best approximations to $k_x^{(f)(0,0)}$ are obtained with an eighth order truncation for the JO and FS-AT models respectively, and a sixth order truncation for the surface modified FS-AT potential.

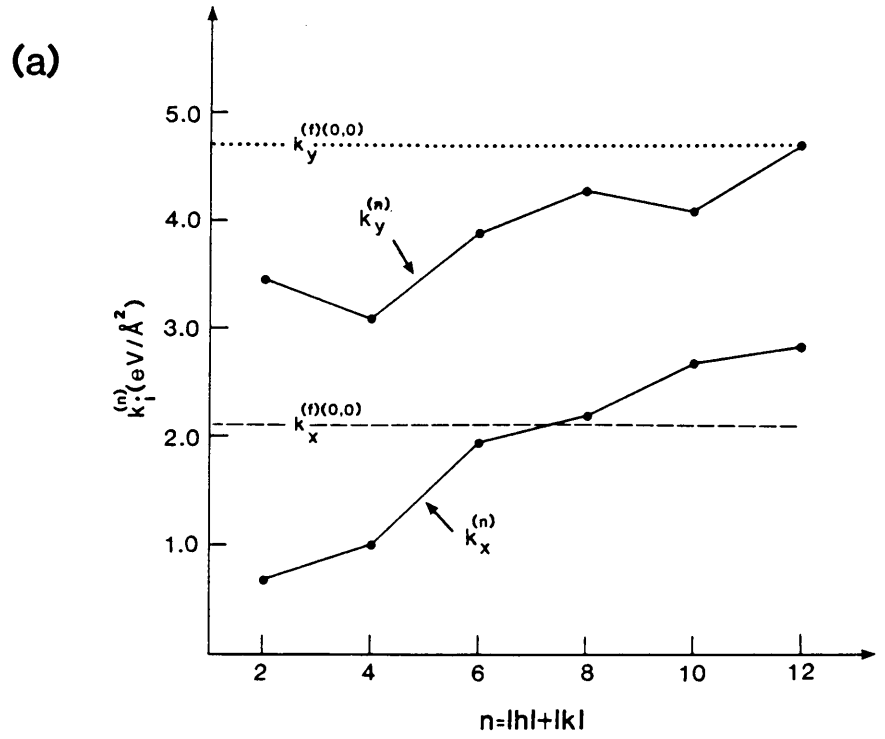

Figure 4.8 Dependence of the force constants $k_x^{(n)}$ and $k_y^{(n)}$ (eqn. (2.8a) and eqn. (2.8b)), calculated from the Fourier series truncation, on the order n of truncation for (a) the Johnson and 0h, (b) the FS-AT and (c) the surface modified FS-AT potential models as calculated for the tantalum on W {110} system. The superscripts (f)(0,0) and (f)(min) respectively pertain to force constants calculated at the origin and at the position of the absolute minimum with a finite difference technique.

(b)

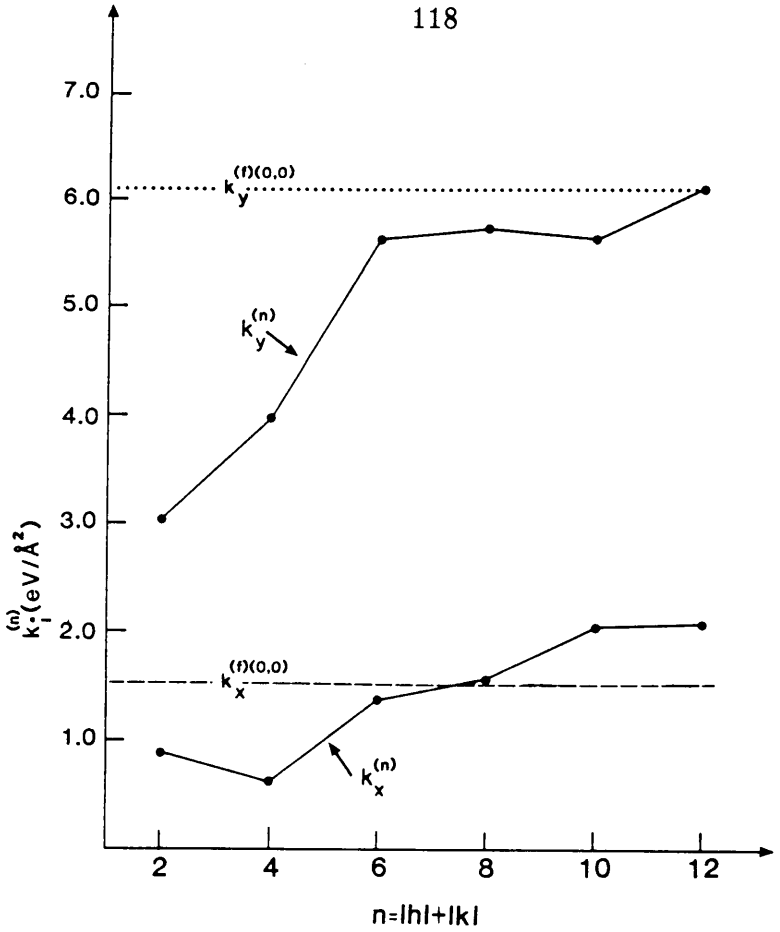

(c)

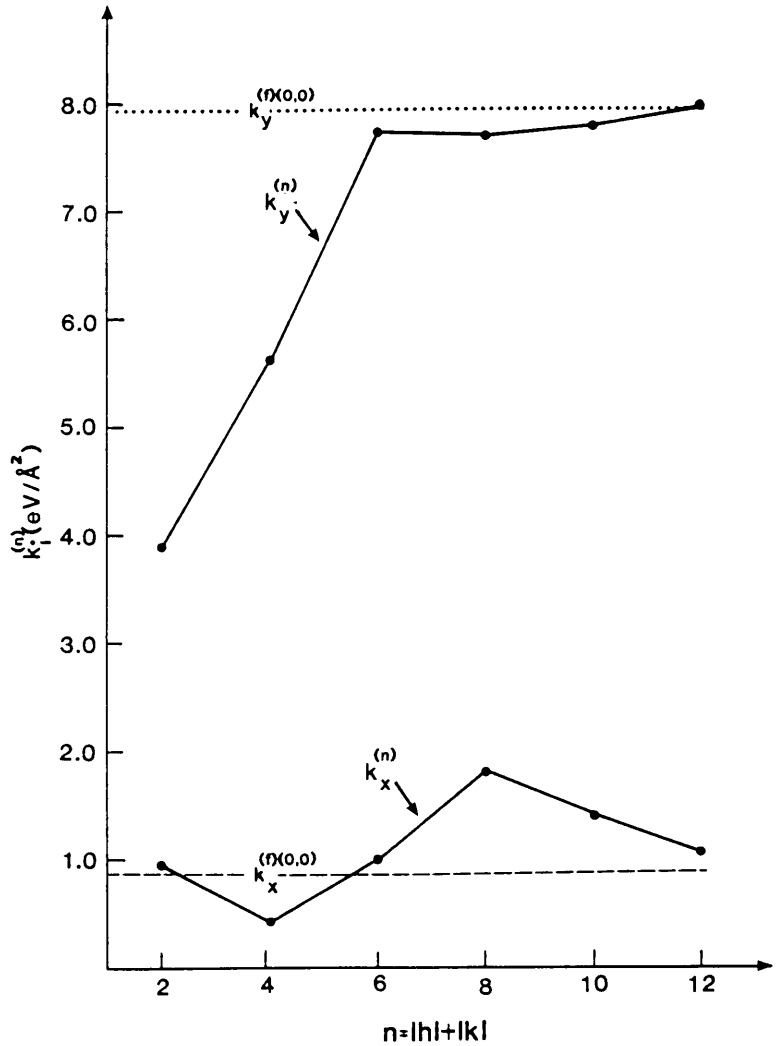

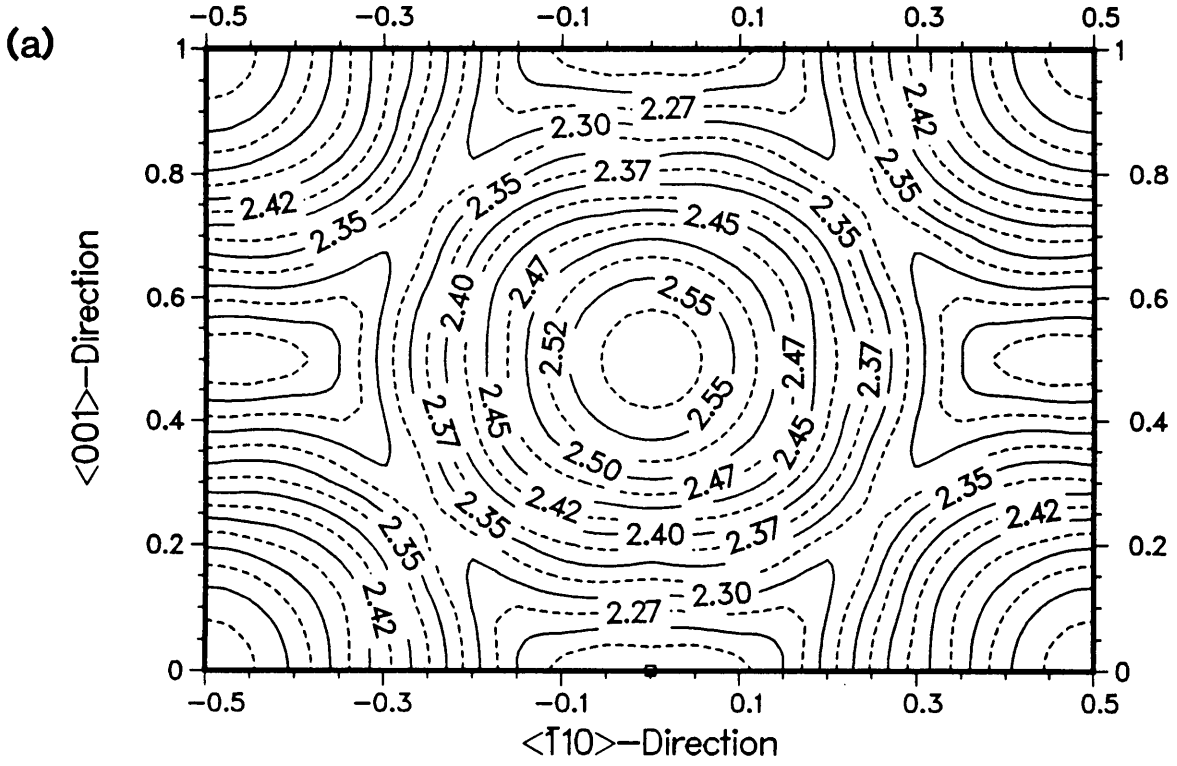

Figure 4.9 Contour plots of the equilibrium height h_e of a tantalum adatom on a {110} tungsten surface as calculated using (a) the Johnson and Oh, (b) the FS-AT and (c) the surface modified FS-AT models respectively. Positions are expressed in terms of normalized rectangular unit cell sidelengths (Fig. 2.1).

(b)

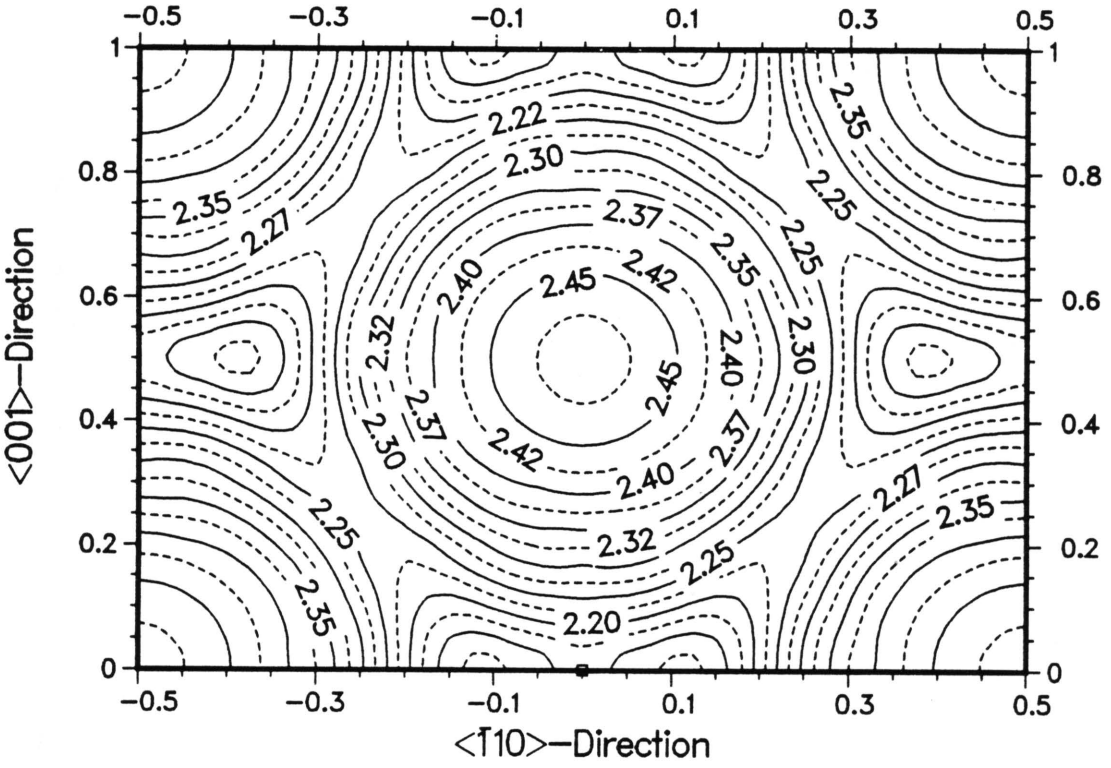

(c)

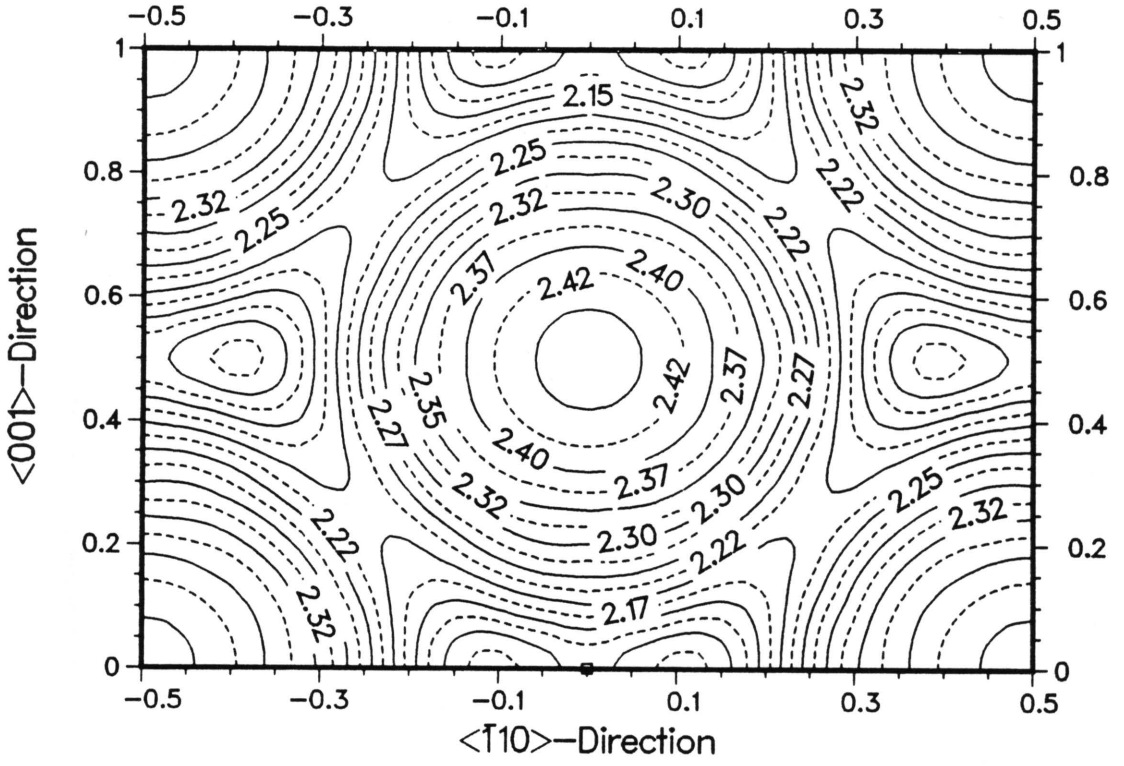

4.5.5 Equilibrium height surface $h_e(x,y)$

Figs. 4.9 a, b and c are contour plots of the equilibrium (height) surface h_e for the potentials under consideration. Double minima again appear in the equilibrium height surfaces of the FS-AT and surface modified FS-AT models even though their potential surfaces have single minima at the adsorption site. The equilibrium height surface of the JO model, however, is very flat in the vicinity of an adsorption site. This reflects the tendency of adatoms to settle into positions with maximum coordination (Ehrlich 1977).

At the adsorption site the equilibrium heights are 2.2059 Å, 2.1593 Å and 2.1077 Å for the JO, FS-AT and surface modified FS-AT models respectively. For all the models the value of h_e at the adsorption site is smaller than the bulk interlayer spacing of W, which is smaller than that of Ta. By comparing Tables 3.1 and 4.3, it follows that the deviation z_0 for the respective interaction models is consistently smaller for the tantalum on W {110} system than for the tungsten on W {110} system. This is probably due to the atomic radius of tantalum ($\approx$ 1.34 Å) being greater than that of tungsten ($\approx$ 1.30 Å).

4.6 SUMMARY AND DISCUSSION

In EAM models the embedding energy is independent of the source of the background electron density. The embedding function is characteristic for a particular kind of atom, and independent of whether it forms part of an alloy or a pure material. This makes the EAM particularly suitable for calculations pertaining to heterogeneous systems. To carry out such calculations, an embedding function $F(\rho)$ and an atomic density function $f(r)$ for each atomic species must be defined, as well as the pair potential $\phi(r)$ for

each combination of atomic species. The pair interaction for the combination of species can be taken as an arithmetic, geometric or weighted average of the interactions for each of the individual species, as appropriate to the particular mathematical form of the individual two-body potentials.

Existing alloy models have proved to be very successful in treating various bulk and surface problems, such as the calculation of the adsorption energy of H on various faces of Ni and Pd; of surface segregation of Ni-Cu alloys; calculation of the heats of formation of certain fcc metal alloys; and an analysis of the adsorption properties of single atoms of Cu, Ag and Au on a W {110} substrate. This includes problems which cannot be treated with pair potentials alone.

The many-body potentials for bcc metals introduced by Johnson and Oh, and by Finnis and Sinclair have been used to calculate a number of adsorption parameters of the tantalum on W {110} heteronuclear system. The Finnis and Sinclair model has been modified somewhat for application to adsorption problems. In the surface modified FS-AT model, an additional fitting parameter, fitted to the experimental value of the adatom-substrate migration energy Q was introduced, leaving the fitting parameters obtained from bulk properties unaltered. For both the JO and FS-AT models the hard-core modifications of the two-body component were adjusted for interaction between unlike atoms.

The potential surfaces of the JO, FS-AT and surface modified FS-AT models display a single minimum at the adsoption site when applied to the tantalum on W {110} system. It is suggested that the double well phenomenon might be a characteristic of systems with adatoms having about the same or a larger electronegativity than tungsten. Both the JO and FS-AT

models yield values of the desorption energy E_{des} within 5% of the approximate empirical value of 7 eV. However, these models yield values of the activation energy Q for surface migration which deviate by about 14% and 10% respectively from the experimental value of 0.7 eV for a single tantalum adatom on a W {110} surface. The surface modified FS-AT potential of course reproduces the empirical value of Q to which it has been fitted. Unfortunately, it yields a value of about 8 eV for the desorption energy E_{des}, which constitutes a deviation of about 14.3% from the experimental value of this quantity. In this respect the adjustment of the FS-AT potential for application to adsorption was less successful for the tantalum on W {110} system than for the tungsten on W {110} system. The reproduction of the empirical value of Q, however, is considered to be the more important requirement for a surface potential suitable for describing lateral localization of adatoms.

The optimum coefficients of the two-dimensional truncated Fourier series representations of the tantalum adatom-substrate interaction potential in skew, as well as in Cartesian axes, were calculated for the various EAM models under consideration. In all cases the values of the coefficients decay fairly rapidly with harmonic order. The JO model yields the most accurate approximation of the adatom-substrate interaction potential for a specific order n of truncation. Unfortunately the values of the calculated higher order Fourier coefficients are unreliable due mainly to the inadequacy of the potential model. However, many important surface properties depend primarily on lower order terms which are believed to be sufficiently accurate.

The lateral force constants corresponding to low substrate temperatures and the effective lateral force constants corresponding to higher

substrate temperatures, where adatom migration comes into play, were also calculated. The force constants corresponding to low temperatures are very sensitive to the precise form of the potential energy curve in the vicinity of the minimum. The calculation of the lateral force constants as second order derivatives from truncated Fourier series is again not recommended since truncation at high harmonic order, including less reliable higher order coefficients, is required. If such second order derivatives are required, the optimum order of truncation for a particular model and force constant should be selected with the necessary circumspection.

The equilibrium height surfaces of the FS-AT and surface modified FS-AT models display double minima situated symmetrically on either side of the adsorption site – the JO potential displays a single minimum. This is consistent with results obtained for the tungsten on W {110} system and could be due to a stiffer core-core repulsion in the JO model. The equilibrium heights at the adsorption site, for all three models under consideration, are smaller than the bulk interlayer spacing of tungsten. The deviation z_0, however, is consistently smaller for the tantalum on W {110} system than for the tungsten on W {110} system. It is suggested that this could be due to the atomic radius of tantalum being greater than that of tungsten.

The surface modified FS-AT model is considered to be the best surface potential for describing the tantalum on W {110} system because it reproduces the empirical value of the activation energy Q for surface migration almost exactly. However, none of the potentials investigated in Chapter 4 are totally satisfactory. The fact that reasonable agreement with adsorption parameters is obtained, even with little or no fitting to surface

properties, is very encouraging. It is expected that with finer computer tuning, the performance of the N-body potential of Finnis and Sinclair, as well as the model of Johnson and Oh, could be improved for application to heteronuclear adsorption systems.

CHAPTER 5

SUMMARY AND CONCLUSIONS

This study comprises a comparative investigation to assess the suitability of various EAM models for the calculation of adsorption properties of homo- and heteronuclear bcc metals. In the case of homonuclear systems the work was limited to the study of a tungsten adatom and an infinite tungsten monolayer adsorbed on a tungsten {110} surface. For heteronuclear systems, the case of a tantalum adatom adsorbed on a tungsten {110} surface was analysed. These two systems were selected because sufficient data are available for fitting parameters and for assessing the relative success of the models.

Appropriate definitions of the desorption energy and the activation energy for surface migration, in terms of N-body potentials, were formulated to facilitate the study. The following adsorption properties were quantified by numerical calculations employing the potential models under consideration: desorption energy, activation energy for adatom-surface migration, adatom vibration frequencies and coefficients for a truncated Fourier series representation of the adatom-substrate interaction. The reproduction of the empirical value of the activation energy for adatom-surface migration, and to a lesser degree the reproduction of the experimental value of the desorption energy, are considered adequate proof of the EAM's suitability for application to surfaces.

The following EAM models were applied to calculate the adsorption properties of a homonuclear system consisting of a tungsten adatom on a tungsten {110} surface:

(i) the binding potential of Gollisch;

(ii) the analytical model of Johnson and Oh;

(iii) the N-body potential of Finnis and Sinclair;

(iv) the Finnis and Sinclair potential with the hard-core modification of Ackland and Thetford;

and

(v) a surface modified version of the Finnis and Sinclair potential, which was fitted to the activation energy for surface migration in order to improve its performance with respect to calculating adsorption parameters.

Three of the abovementioned models were also employed in calculating the adsorption properties of a heteronuclear system consisting of a tantalum adatom on a tungsten {110} surface. These models are

(i) the analytical model of Johnson and Oh;

(ii) the Finnis and Sinclair potential with the hard-core modification of Ackland and Thetford;

and

(iii) a surface modified version of the Finnis and Sinclair potential which includes a hard-core modification and is fitted to the activation energy for surface migration of a tantalum adatom on a tungsten {110} surface.

It was found that all the N-body potentials employed in the study of the tungsten on tungsten {110} system yielded more realistic values of the desorption energy, the activation energy for adatom-surface migration and the adatom-substrate equilibrium height than conventional Morse and Lennard-Jones pair potentials. The models proposed by Gollisch, by Johnson and Oh and the surface modified FS-AT potential, yielded values of the activation energy for surface migration of a tungsten adatom on a tungsten {110} surface well within the experimental limits, whereas the basic model of Finnis and Sinclair predicts a value more than 26% below the lowest empirical value. The value of the self-desorption energy calculated with the potential of Gollisch and the surface modified FS-AT model deviated by less than 12% and 0.5% respectively from the corresponding empirical value. Both models also display a double well in their respective potential energy surfaces. This is in agreement with the observations of Bauer that a tungsten adatom on a tungsten {110} surface is slightly displaced from the lattice site along the $\langle\bar{1}10\rangle$ direction. The prediction of a double well thus supports the applicability of EAM's to adsorption phenomena. These considerations suggest that the surface modified FS-AT model is the most suitable surface potential for application to self adsorption on tungsten {110}.

The models proposed by Johnson and Oh, and by Finnis and Sinclair (with the hard-core modification of Ackland and Thetford) yield values of the activation energy for surface migration of a tantalum adatom on a tungsten {110} surface which are respectively about 14% and 10% lower than the experimental value. The surface modified FS-AT potential naturally reproduces the empirical value to which it has been fitted. The potential of Johnson and Oh, and the Finnis and Sinclair model with the Ackland and

Thetford hard-core modification yield values which are respectively about 5% lower and 5% higher than the experimental value of the desorption energy of the heteronuclear system tantalum on tungsten {110}. The surface modified FS-AT model is less successful for the heteronuclear system and yields a value of the desorption energy deviating by about 14.3% from the experimental value. However, the heteronuclear system is evidently more complicated than the homonuclear one, and it is to be expected that a simple modification such as the one proposed in this study, would not be able to fully cope with these complexities. The double well phenomenon is absent from the potential surfaces predicted by all the models. It is therefore not possible to identify a specific model as being more appropriate than all others.

With respect to the calculation of the truncated Fourier series representations of the adatom-substrate interaction potential for both the tungsten on tungsten {110} and tantalum on tungsten {110} systems, it was found that the Fourier coefficients tend to zero with increasing harmonic order. A comparison, for different systems, of the normalized Fourier coefficients, previously introduced by van der Merwe on a qualitative basis, indicated that the relative values of the Fourier coefficients are largely determined by the symmetry of the substrate. This belief is further strengthened by the fact that the normalized coefficients determined for an adatom forming part of a monolayer are very similar to those for an isolated atom. The bonding parameter constituting the overall scale factor, is however substantially lower for an adatom forming part of a monolayer and confirms that adatom-substrate interaction is significantly influenced by lateral adatom-adatom interaction due to many-body effects.

The calculation of the lateral force constants for vibrations parallel to the surface as second order derivatives from Fourier series truncated at order n, is not recommended, since accuracy requires a truncation at high harmonic order, whereas high order coefficients are less reliable. Force constants which are determined as a second order difference at the potential minimum, are evidently very sensitive to the calculated form of the potential energy curve in the vicinity of the minimum. The detailed form of the adatom-substrate interaction potential energy curve is determined by the interatomic interaction model used in the calculation. This is reflected by the rather large variation in the values of a specific force constant calculated using different potential models.

All the N-body potential models considered in this study, with the exception of the model of Johnson and Oh, yield equilibrium height surfaces which have double wells located symmetrically on either side of the adsorption site for both the homonuclear and heteronuclear systems. For the tungsten on tungsten {110} system the double well phenomenon is also present in the adatom-substrate interaction potential surfaces calculated with the Gollisch and surface modified FS-AT potentials. The mathematical condition for the existence of the double well in the potential energy surface is clearly that the first derivative of the total adatom-substrate interaction potential at the lattice site with respect to the coordinate defining the $\langle\bar{1}10\rangle$ direction is zero, while the second derivative is negative. However, due to the complex and varied mathematical forms of the N-body potentials under consideration, it is extremely difficult to deduce from these conditions which potential model will give rise to the double well phenomenon. It is also not clear why the double well phenomenon appears in the equilibrium height surfaces of certain potentials, but not

in the corresponding potential surfaces. This could be related to the fact that the potential is not a monotonic function of the height parameter. Unfortunately the scope of this study is not wide enough to determine for which combinations of metals and under what conditions the double well phenomenon will be present. Future studies of the adsorption properties of other bcc elements, as well as fcc elements, adsorbed on the {110} and other faces of a tungsten substrate, might throw more light on this phenomenon.

The extension of the foregoing considerations of the adsorption properties of adatoms to other combinations of metals and other substrate surfaces is envisaged. The formidable task of calculating the optimum truncated Fourier series representations of the adsorbate-substrate interaction potential for real epitaxial systems consisting of small, as well as extended islands, employing EAM methods will also be attempted. The performance of the various EAM models with respect to the calculation of adsorption parameters may perhaps be improved still further by careful adjustment of the fitting parameters.

This study represents the first attempt to calculate adsorption parameters with EAM models for the systems under consideration. Results in good agreement with experiment were obtained. The study also demonstrated that simple modifications to already versitile N-body models yield potentials which are admirably suited in the description of adsorption phenomena.

REFERENCES

Ackland, G.J., Finnis, M.W., and Vitek, V., 1988, *J. Phys.* F, **18**, L153.

Ackland, G.J., and Thetford, R., 1987, *Phil. Mag.* A, **56**, 15.

Ackland, G.J., Tichy, G., Vitek, V., and Finnis, M.W., 1987, *Phil. Mag.* A, **56**, 735.

Al-Rawi, O.Z., and Jones, J.P., 1983, *Surf. Sci.*, **124**, 220.

Banerjea, A., and Smith, J.R., 1988, *Phys. Rev.* B, **37**, 6632.

Baskes, M.I., 1987, *Phys. Rev. Lett.*, **59**, 2666.

Basset, D.W., and Parsley, M.J., 1969, *Br. J. Appl. Phys.*, **2**, 13.

Bauer, E., 1984, *The Chemical Physics of Solid Surfaces and Heterogneous Catalysis*, eds. D.A. King and D.P. Woodruff (Amsterdam: Elsevier) pp. 3-57.

Braun, M.W.H., 1987, *Epitaxy on substrates with hexagonal symmetry*, DSc dissertation, University of Pretoria.

Brent, R.P., 1973, *Algorithms for Minimization without Derivatives* (Englewood Cliffs: Prentice Hall), Chapter 5.

Broughton, J.Q., and Gilmer, G.H., 1983, *J. Chem. Phys.*, **79**, 5105.

Bruch, L.W., and Venables, J.A., 1984, *Surf. Sci.*, **148**, 167.

Buchholz, J.C., Wang, G.-C., Lagally, M.G., 1975, *Surf. Sci.*, **49**, 508.

Carnevali, P., Ercolessi, F., and Tosatti, E., 1987, *Surf. Sci.*, **189**, 645.

Clementi, E., and Roetti, C., *Atomic Data and Nuclear Data Tables* (Academic, New York 1974) Vol. 14. Nos. 3 and 4.

Coppersmith, S.N., Fisher, D.S., Halperin, B.I., Lee, P.A., and Brinkman, W.F., 1982, *Phys. Rev.* B, **25**, 349.

Daw, M.S., and Baskes, M.I., 1983, *Phys. Rev. Lett.*, **50**, 1285.

Daw, M.S., and Baskes, M.I., 1984, *Phys. Rev.* B, **29**, 6443.

Ehrlich, G., and Kirk, C.F., 1968, *J. Chem. Phys.*, **48**, 1465.

Ehrlich, G., 1977, *Surf. Sci.*, **63**, 422.

Ercolessi, F., Parrinello, M., and Tosatti, E., 1986a, *Surf. Sci.*, **177**, 314.

Ercolessi, F., Tosatti, E., and Parrinello, M., 1986b, *Phys. Rev. Lett.*, **57**, 719.

Eridon, J.M., and Rao, S., 1988, preprint. (Paper at Materials Research Society Meeting Boston.)

Eridon, J., and Rao, S., 1989, *Phil, Mag. Lett.*, **59**, 31.

Finnis, M.W., and Heine, V., 1974, *J. Phys.* F, **4**, L37.

Finnis, M.W., and Sinclair, J.E., 1984, *Phil. Mag.* A, **50**, 45.

Foiles, S.M., 1985, *Phys. Rev.* B, **32**, 7685.

Foiles, S.M., Baskes, M.I., and Daw, M.S., 1986, *Phys. Rev.* B, **33**, 7983.

Friedel, F., 1969, in *Electrons*, Vol. I of *Physics of Metals*, ed. J.M. Ziman (London: Cambridge University Press).

Garofalo, M., Tosatti, E., and Ercolessi, F., 1987, *Surf. Sci.*, **188**, 321.

Gollisch, H., 1986a, *Surf. Sci.*, **166**, 87.

Gollisch, H., 1986b, *Surf. Sci.*, **175**, 249.

Gilmore, C.M., Sprague, J.A., Eridon, J.M., and Provenzano, V., 1989, *Surf. Sci.*, **218**, 26.

Gomer, R., 1983, *Surface Mobilities on Solid Materials*, ed. Vu Thien Binh (New York: Plenum Press), pp. 1-6.

Gupta, R.P., 1981, *Phys. Rev.* B, **23**, 6265.

Hohenberg, P., and Kohn, W., 1964, *Phys. Rev.* B, **136**, 864.

Jiang, P., Marcus, P.M., and Jona, F., 1986, *Solid State Commun.*, **59**, 275.

Johnson, R.A., 1972, *Phys. Rev.* B, **6**, 2094.

Johnson, R.A., 1973, *J. Phys.* F, **3**, 295.

Johnson, R.A., 1988a, *Phys. Rev.* B, **37**, 3924.

Johnson, R.A. 1988b, *Phys. Rev.* B, **37**, 6121.

Johnson, R.A., 1989, *Phys. Rev.* B, **39**, 12554.

Johnson, R.A., 1990, *Phys. Rev.* B, to be published.

Johnson, R.A., and Oh, D.J., 1989, *J. Mater. Res.*, **4**, 1195.

Jona, F., 1978, *J. Phys.* C, **11**, 4271.

Jones, J.P., and Roberts, E.W., 1977, *Surf. Sci.*, **62**, 415.

Knowles, T.R., and Suhl, H., 1977, *Phys. Rev. Lett.*, **39**, 1417.

Meada, K., Vitek, V., and Sutton, A.P., 1982, *Acta. Metall.*, **30**, 2001.

Neustadter, H.E., and Bacigalupi, R.J., 1967, *Surf. Sci.*, **6**, 246.

Nørskov, J.K., 1982, *Phys. Rev.* B, **26**, 2875.

Oh, D.J., and Johnson, R.A., 1988, *J. Mater. Res.*, **3**, 471.

Plummer, E.W., and Rhodin, T.N., 1968, *J. Chem. Phys.*, **49**, 3479.

Prutton, M., 1975, *Surface Physics*, (Oxford: Clarendon Press), pp. 90-111.

Puska, M.J., Nieminen, R.M., and Manninen, M., 1981, *Phys. Rev.* B, **24**, 3037.

Rebonato, R., 1989, *Phil. Mag.* B, **60**, 325.

Rose, J.H., Smith, J.R., Guinea, F., and Ferranté, J., 1984, *Phys. Rev.* B, **29**, 2963.

Steele, W.A., 1973, *Surf. Sci.*, **36**, 317.

Stoop, L.C.A., 1977a, *Proc. 7th Intern. Vac. Congr. and 3rd Intern. Conf. Solid Surfaces*, Vienna, 1977 (Horn: F. Berger & Söhne), pp. 1121-1124.

Stoop, L.C.A., 1977b, *Thin Solid Films*, **42**, 33.

Stoop, L.C.A., 1983, *Thin Solid Films*, **103**, 375.

Stoop, P.M., Braun, M.W.H., and van der Merwe, J.H., 1988, *S. Afr. J. Sci.*, **84**, 655.

Stoop, P.M., and Snyman, J.A., 1988, *Thin Solid Films*, **158**, 151.

Stott, M.J., and Zaremba, E., 1980, *Phys. Rev.* B, **22**, 1564.

Sutton, A.P., Finnis, M.W., Pettifor, D.G., and Ohta, Y., 1988, *J. Phys.* C, **21**, 35.

Terakura, K., Mohri, T., and Oguchi, T., 1989, *Materials Sci. Forum*, 3739.

Terakura, K., Oguchi, T., Mohri, T., and Watanabe, K., 1987, *Phys. Rev.* B, **35**, 2169.

Tománek, D., and Bennemann, K.H., 1985, *Surf. Sci*, **163**, 503.

Tománek, D., Mukherjee, S., and Bennemann, K.H., 1983, *Phys. Rev.* B, **28**, 665.

Tsong, T.T., and Cowan, P.L., 1979, *Chemistry and Physics of Solid Surfaces* II, ed. R. Vanselow, (Boca Raton: CRC Press), pp. 209-236.

Tsong, T.T., and Kellogg, G., 1975, *Phys. Rev.* B, **12**, 1343.

van der Merwe, J.H., 1982, *Phil. Mag.* A, **45**, 145.

van der Merwe, J.H., 1984, *Chemistry and Physics of Solid Surfaces V*, eds. R. Vanselow and R. Howe (Berlin: Springer Verlang), pp. 365-400.

van der Merwe, J.H., and Braun, M.W.H., 1985, *Appl. Surf. Sci*, **22/23**, 545.

Van Hove, M.A., and Tong, S.Y., 1976, *Surf. Sci.*, **54**, 91.

APPENDIX A

ANALYTIC EXPRESSIONS FOR THE OPTIMUM FOURIER COEFFICIENTS IN A TRUNCATED FOURIER SERIES REPRESENTATION IN SKEW AXES

The Fourier series representation in skew axes $x^{(1)},x^{(2)}$ for the adatom-substrate interaction potential (ASIP) of a bcc {110} surface, with the origin at an adsorption site, and truncated at the n-th harmonic order, is

$$F_s^n(\xi,\eta) = A_{oo} + \sum_{h=1}^{n} 2A_{ho}\cos 2\pi h\xi + \sum_{k=1}^{n} 2A_{ok}\cos 2\pi k\eta$$

$$+ \sum_{h,k=1}^{n=h+k} [2A_{hk}\cos 2\pi(h\xi+k\eta) + 2A_{h,-k}\cos 2\pi(h\xi-k\eta)], \qquad (A.1)$$

where $\xi = x^{(1)}/b$, $\eta = x^{(2)}/b$; b being the nearest neighbour distance. Now let

$$F(A_{oo},A_{ho},A_{ok},A_{hk},A_{h,-k}) = \sum_{i,j=1}^{m} [F_s^n(\xi_i,\eta_j) - E_{ij}]^2, \qquad (A.2)$$

where $F_s^n(\xi_i,\eta_j)$ is the Fourier series approximation of the ASIP at a point $P(\xi_i,\eta_j)$ in the unit cell TEFG (Fig. 2.1) and E_{ij} (DATA) is the energy in eqn. (2.5d) calculated at $P(\xi_i,\eta_j)$ using a given model of the interaction potential. (In this study various N-body potential models were employed.) Here m >> n,h,k as the number of data points will in general greatly exceed the order of truncation. Applying the least squares criterion, the

coefficients $A_{oo}, A_{ho}, A_{ok}, A_{hk}$ and $A_{h,-k}$ must now be selected in such a way that

$$\frac{\partial F}{\partial A_{oo}} = 0, \tag{A.3}$$

$$\frac{\partial F}{\partial A_{ho}} = 0, \tag{A.4}$$

$$\frac{\partial F}{\partial A_{ok}} = 0, \tag{A.5}$$

$$\frac{\partial F}{\partial A_{hk}} = 0, \tag{A.6}$$

$$\frac{\partial F}{\partial A_{h,-k}} = 0, \tag{A.7}$$

for $h,k = 1,\ldots,r$, with $r \leq n$. Eqn. (A.3) implies that

$$0 = \sum_{i,j=1}^{m} 2[F_s^n(\xi_i,\eta_j) - E_{ij}]$$

yielding

$$\sum_{i,j=1}^{m} [A_{oo} + \sum_{h=1}^{n} 2A_{ho}\cos 2\pi h\xi_i + \sum_{k=1}^{n} 2A_{ok}\cos 2\pi k\eta_j$$

$$+ \sum_{h,k=1}^{n=h+k} [2A_{hk}\cos 2\pi(h\xi_i + k\eta_j) + 2A_{h,-k}\cos 2\pi(h\xi_i - k\eta_j)]]$$

$$= \sum_{i,j=1}^{m} E_{ij}. \tag{A.8}$$

By interchanging the order of summation, we obtain:

$$A_{oo}m^2 + \sum_{h=1}^{n}\sum_{i,j=1}^{m} 2A_{ho}\cos 2\pi h\xi_i + \sum_{k=1}^{n}\sum_{i,j=1}^{m} 2A_{ok}\cos 2\pi k\eta_j$$

$$+ \sum_{h,k=1}^{n=h+k}\sum_{i,j=1}^{m} [2A_{hk}\cos 2\pi(h\xi_i + k\eta_j) + 2A_{h,-k}\cos(h\xi_i - k\eta_j)]$$

$$= \sum_{i,j=1}^{m} E_{ij}. \qquad (A.9)$$

However the summation over i and j is actually a summation over a set of points D_m where

$$D_m = \{\xi_i = i\delta,\ \eta_j = j\delta \mid i,j = 1,\ldots,m \text{ and } \delta = \frac{1}{m} = \xi_{i+1} - \xi_i$$

$$= \eta_{j+1} - \eta_j\} \qquad (A.10)$$

Eqn. (A.9) can be rewritten as follows:

$$A_{oo}m^2 + \sum_{h=1}^{n}\sum_{i,j=1}^{m} 2A_{ho}\cos 2\pi h\xi_i + \sum_{k=1}^{n}\sum_{i,j=1}^{m} 2A_{ok}\cos 2\pi k\eta_j$$

$$+ \sum_{h,k=1}^{n=h+k}\sum_{i,j=1}^{m} [2A_{hk}(\cos 2\pi h\xi_i\cos 2\pi k\eta_j - \sin 2\pi h\xi_i\sin 2\pi k\eta_j)$$

$$+ 2A_{h,-k}(\cos 2\pi h\xi_i\cos 2\pi k\eta_j + \sin 2\pi h\xi_i\sin 2\pi k\eta_j)]$$

$$= \sum_{i,j=1}^{m} E_{ij}. \qquad (A.11)$$

Consider the sum $\sum_{i=1}^{m} \cos 2\pi h\xi_i$:

$$\sum_{i=1}^{m} \cos 2\pi h\xi_i = R_e \sum_{i=1}^{m} e^{\pm i2\pi hi\delta}$$

$$= R_e \left[\frac{e^{\pm i2\pi h\delta}(1 - e^{\pm i2\pi h\delta m})}{(1 - e^{\pm i2\pi h\delta})} \right]$$

$$= R_e \frac{e^{\pm i2\pi h\delta}(1 - \cos 2\pi h - \pm i \sin 2\pi h)}{(1 - e^{\pm i2\pi h\delta})}$$

$$= 0 \quad \text{for} \quad h \neq m = \frac{1}{\delta}, \text{ where } \pm i = \sqrt{-1}. \tag{A.12}$$

Similarly it follows that

$$\sum_{i=1}^{m} \sin 2\pi h\xi_i = 0 \quad \text{for} \quad h \neq m. \tag{A.13}$$

From eqns. (A.11), (A.12) and (A.13) it follows that

$$A_{oo} = \frac{1}{m^2} \sum_{i,j}^{m} E_{ij}. \tag{A.14}$$

Eqn. (A.4) implies that

$$0 = \sum_{i,j=1}^{m} 2[F_s^n(\xi_i, \eta_j) - E_{ij}] \cos 2\pi h\xi_i. \tag{A.15}$$

From the results in eqns. (A.12) and (A.13) and the fact that

$$\sum_{i,j=1}^{m} (\cos 2\pi h\xi_i)^2 = \sum_{i,j=1}^{m} \left[\frac{1}{2} + \frac{1}{2} \cos 2\pi h 2\xi_i\right]$$

$$= \frac{m^2}{2} \qquad (A.16)$$

it follows that

$$A_{ho} = \frac{1}{m^2} \sum_{i,j=1}^{m} E_{ij} \cos 2\pi h\xi_i. \qquad (A.17)$$

By similar arguments it can be shown that eqns. (A.5), (A.6) and (A.7) imply that

$$A_{ok} = \frac{1}{m^2} \sum_{i,j=1}^{m} E_{ij} \cos 2\pi k\eta_j, \qquad (A.18)$$

$$A_{hk} = \frac{1}{m^2} \sum_{i,j=1}^{m} E_{ij} \cos 2\pi (h\xi_i + k\eta_j), \qquad (A.19)$$

and

$$A_{h,-k} = \frac{1}{m^2} \sum_{i,j=1}^{m} E_{ij} \cos 2\pi (h\xi_i - k\eta_j). \qquad (A.20)$$

APPENDIX B

ANALYTIC EXPRESSIONS FOR THE OPTIMUM FOURIER COEFFICIENTS IN A TRUNCATED FOURIER SERIES REPRESENTATION IN CARTESIAN AXES

The n-th order Fourier truncation for the adatom-substrate interaction potential (ASIP) on a bcc {110} surface expressed in Cartesian axes, may be written as

$$F_c^n(X,Y) = \sum_{\substack{h,k=0 \\ (h+k)\text{even}}}^{n} A_{hk}\{\cos[2\pi(hX + kY)] + \cos[2\pi(hX - kY)]\}, \qquad (B.1)$$

where $X = x/a_x$, $Y = y/a_y$ (see Fig. 2.1). Consider the sum of the squared differences over a set of m^2 data points D_m:

$$F(A_{oo},A_{ho},A_{ok},A_{hk}) = \sum_{i,j=1}^{m} [F_c^n(X_i,Y_j) - E_{ij}]^2, \qquad (B.2)$$

where E_{ij} are the calculated values of the ASIP (eqn. (2.5d)) and

$$D_m = \{(X_i,Y_j) | X_i = i\delta \quad \text{and} \quad Y_j = j\delta;\ \ i,j = 1,\ldots,m = 1/\delta\}. \qquad (B.3)$$

For an optimum value of the Fourier coefficient A_{hk}

$$0 = \frac{\partial F}{\partial A_{hk}}$$

$$= 2 \sum_{i,j=1}^{m} [F_c^n(X_i,Y_j) - E_{ij}][\cos\{2\pi(hX_i + kY_j)\} + \cos\{2\pi(hX_i - kY_j)\}]. \qquad (B.4)$$

It follows that

$$\sum_{i,j=1}^{m} E_{ij}[\cos\{2\pi(hX_i + kY_j)\} + \cos\{2\pi(hX_i - kY_j)\}]$$

$$= A_{hk} \sum_{i,j=1}^{m} [\cos\{2\pi(h'X_i + k'Y_j)\} + \cos\{2\pi(h'X_i - k'Y_j)\}]$$
$$[\cos\{2\pi(hX_i + kY_j)\} + \cos\{2\pi(hX_i - kY_j)\}]. \qquad (B.5)$$

The right hand side consists of four terms of which the following is a typical one:

$$S = \sum_{i,j=1}^{m} \cos\{2\pi(h'X_i + k'Y_j)\}\cos\{2\pi(hX_i + kY_j)\}$$

$$= \frac{1}{2} \sum_{i,j=1}^{m} [\cos\{2\pi(h'+h)i\delta + 2\pi(k'+k)j\delta\} + \cos\{2\pi(h'-h)i\delta + 2\pi(k'-k)j\delta\}]$$

$$= \frac{1}{2} R_e \sum_{i,j=1}^{m} [e^{2\pi\underline{i}[(h'+h)i + (k'+k)j]\delta} + e^{2\pi\underline{i}[(h'-h)i + (k'-k)j]\delta}]$$

$$= \frac{1}{2} R_e \left[\frac{e^{\pi\underline{i}[(h'+h)](m+2)\delta}}{e^{\pi\underline{i}(h'+h)\delta}} \cdot \frac{e^{\pi\underline{i}(h'+h)(m+2)\delta} - e^{-\pi\underline{i}(h'+h)(m+2)\delta}}{e^{\pi\underline{i}(h'+h)\delta} - e^{-\pi i(h'+h)\delta}} \cdot G(k'+k)\right.$$
$$\left. + H(h'-h)\cdot K(k'-k)\right]$$

$$= \frac{1}{2}\{\cos[\pi(h'+h)\delta(m-1)] \frac{\sin[\pi(h'+h)m\delta]}{\sin[\pi(h'+h)\delta]} \cdot \cos[\pi(k'+k)\delta(m+1)] \frac{\sin\pi(k'+k)m\delta}{\sin\pi(k'+k)\delta}$$
$$+ H(h'-h)\cdot K(k'-k)\}, \qquad (B.6)$$

where $H(h'-h)\cdot K(k'-k)$ is a trigonometric expression similar to the first term on the right hand side of eqn. (B.6), but with $h'+h$ and $k'+k$ respec-

tively replaced by h'−h and k'−k. Because $m\delta = 1$ and $k,h',k,k' \ll m$, it follows that

$$S = \begin{cases} \frac{m^2}{2} & \text{for } h' = h \text{ and } k' = k, \\ \frac{m^2}{2} & \text{for } h' = -h \text{ and } k' = -k, \\ 0 & \text{otherwise.} \end{cases} \qquad (B.7)$$

In the remaining three terms in eqn. (B.5), the product of the two terms in $h'X_i - k'Y_j$ and $hX_i - kY_j$ will also yield a sum $m^2/2$, whereas the other two terms vanish for the conditions defined in eqn. (B.7) because one of the two factors in each term will contain h'+h and the other h'−h, etc. Hence

$$A_{hk} = \frac{1}{m^2} \sum_{i,j=1}^{m} [\cos\{2\pi(hX_i + kY_j)\} + \cos\{2\pi(hX_i - kY_j)\}]. \qquad (B.8)$$

With k = 0, eqn. (B.5) becomes

$$\sum_{i,j=1}^{m} E_{ij}\cos 2\pi hX_i = A_{ho} \sum_{i,j=1}^{m} [\cos\{2\pi(h'X_i + k'Y_j)\} + \cos\{2\pi(h'X_i - kY_j)\}]\cos 2\pi hX_i$$

$$= \frac{A_{ho}}{2} [\cos\{\pi(h'+h)\delta(m+1)\} \frac{\sin[\pi(h'+h)m\delta}{\sin[\pi(h'+h)\delta]} \cdot \cos[\pi k'\delta(m+1)] \frac{\sin\pi k'm\delta}{\sin\pi k'\delta}$$
$$+ H(h'-h)\cdot K(k') + H(h'+h)\cdot K(-k') + H(h'-h)\cdot K(-k')]$$

$$= A_{ho}[H(h'+h)\cdot K(k') + H(h'-h)\cdot K(k')]$$

$$= A_{ho}\begin{cases} m^2 & \text{for } h' = h \text{ en } k' = 0, \\ m^2 & \text{for } h' = -h \text{ en } k' = 0, \\ 0 & \text{otherwise.} \end{cases} \qquad (B.9)$$

Hence

$$A_{ho} = \frac{1}{m^2} \sum_{i,j=1}^{m} E_{ij} \cos 2\pi h\delta i. \tag{B.10}$$

Similarly

$$A_{ok} = \frac{1}{m^2} \sum_{i,j=1}^{m} E_{ij} \cos 2\pi k\delta j. \tag{B.11}$$

With $h = k = 0$, eqn. (B.5) becomes

$$2 \sum_{i,j=1}^{m} E_{ij} = 2A_{oo} \sum_{i,j=1}^{m} [\cos\{2\pi(h'X_i + k'Y_j)\} + \cos\{2\pi(h'X_i - k'X_j)\}]$$

$$= 2A_{oo}[\cos\{\pi h'\delta(m+1)\} \frac{\sin\pi h'n\delta}{\sin\pi h'\delta} \cos\{\pi k'\delta(m+1)\} \frac{\sin\pi k'\delta m}{\sin\pi k'\delta} + H(h')\cdot K(-k')]$$

$$= \begin{cases} 4A_{oo}m^2 & \text{for } h' = k' = 0, \\ 0 & \text{otherwise.} \end{cases} \tag{B.12}$$

Hence

$$A_{oo} = \frac{1}{2m^2} \sum_{i,j=1}^{m} E_{ij}. \tag{B.13}$$

Eqns. (B.8), (B.10), (B.11) and (B.13) define the optimum coefficients for the Fourier truncation defined by $F_c^n(X,Y)$.

APPENDIX C

FOURIER COEFFICIENTS: EPITAXY

Reliable quantitative knowledge of the Fourier coefficients in a two-dimensional Fourier series representation of the adsorbate-substrate interaction potential for an atom which forms part of an overlayer, is of vital importance for the prediction of epitaxial orientations, particularly when the interfacial symmetries are different as in (111)fcc/(110)bcc epitaxy (van der Merwe 1982, and van der Merwe and Braun 1985). Whereas a non-zero Fourier coefficient identifies a possible epitaxial configuration, the magnitude of the coefficient constitutes a measure of the tendency towards the realization of such an orientation.

The results of van der Merwe and Braun have been derived for a "rigid" model (rigid overlayer and substrate). The conditions for ideal epitaxial configurations, derived by adopting the conventional assumption that epitaxy is likely when the interfacial potential energy is a minimum, are also applicable, though only semi-quantatively, to real crystals.

In the analysis (Braun 1987) it is assumed that the adsorbate-substrate interaction potential $V(\xi,\eta)$ has the periodicity and symmetry of the substrate surface lattice and may thus be represented by a Fourier series

$$V(\xi,\eta) = \sum_{h,k=-\infty}^{\infty} A_{hk}\exp[(2\pi i(h\xi + k\eta)], \qquad (C.1)$$

where $\vec{r} = \xi\vec{a}_1 + \eta\vec{a}_2$ is a substrate surface vector in real space and $\vec{q}_{hk} = h\vec{a}_1^* + k\vec{a}_2^*$ a substrate reciprocal lattice translation vector. The total interaction energy V_G of an overgrowth island is obtained by summing over all $G[=(2M+1)(2N+1)]$ adatoms, obtaining

$$V_G(p,q) = \sum_{h,k=-\infty}^{\infty} A_{hk}\exp(i2\pi\gamma_o)\,\frac{\sin\pi(2M+1)p(h,k)}{\sin\pi p(h,k)}\,\frac{\sin\pi(2N+1)q(h,k)}{\sin\pi q(h,k)} \qquad (C.2)$$

where $\gamma_o = h\xi_o + k\eta_o$; ξ_o,η_o being the position of the overgrowth origin in the substrate coordinate system. Also p(h,k) and q(h,k) are components of the wave vector $\vec{q}_{hk}$ expressed in the overgrowth reciprocal lattice. It follows from (C.2) that V_G has minima where p and q are simultaneously integers. Thus ideal epitaxial configurations may be realized if the lattice translation vector in the substrate reciprocal lattice is also a lattice translation vector in the overgrowth reciprocal lattice. The normalized depths of the minima as measures of the expitaxial "strengths" (tendencies) for the realization of ideal epitaxial configurations are defined by the Fourier coefficients (amplitudes)

$$v_{hk} = |A_{hk}|, \qquad (C.3)$$

where each pair of h and k is associated with a particular choice of p and q, p and q being integers.

It must be pointed out that in the above analysis the assumption was made that the total interaction energy V_G of the overgrowth island is obtained by simply adding together the interaction energy of each individual overgrowth atom with the crystal substrate, independent of the

presence of the other overgrowth atoms. Although the interfacial energy as calculated by properly taking into account the influence of monolayer atom-atom interaction on the monolayer-substrate interaction will differ from that as calculated by van der Merwe and Braun (1985), the latter will nevertheless constitute a practical general approximation as is confirmed by epitaxial data.